Aus der Klinik für Neurochirurgie
Geschäftsführender Direktor: Prof. Dr. med. Christopher Nimsky

des Fachbereichs Medizin der Philipps-Universität Marburg

Analysis of ADAM8 in the tumor microenvironment of Pancreatic Ductal Adenocarcinoma

Inaugural-Dissertation
zur Erlangung des Doktorgrades
der gesamten Naturwissenschaften
(Dr. rer. nat.)

dem Fachbereich Medizin der Philipps-Universität Marburg vorgelegt

von

Lena Cook
aus Bad Windsheim
Marburg, 2022

Angenommen vom Fachbereich Medizin der Philipps-Universität Marburg am: 13.04.2022

Gedruckt mit Genehmigung des Fachbereichs Medizin:

Dekanin: Frau Prof. Dr. Denise Hilfiker-Kleiner
Referent: Herr Prof. Dr. Jörg-Walter Bartsch
Korreferent: Herr Prof. Dr. Oliver Schilling

In loving memory of my mother

Table of Content

List of abbreviations

ADAM	A disintegrin and metalloproteinase
AKT	Protein kinase B
ARDS	Acute respiratory distress syndrome
BRCA2	breast cancer gene 2
CA 19-9	Carbohydrate antigen 19-9
CAB39	Calcium binding protein 39
CCL	Chemokine C-C motif ligand
CD	Cluster of differentiation
CDKN2A	Cyclin dependent kinase inhibitor 2A
COPD	Chronic obstructive pulmonary disease
CP	Chronic pancreatitis
CREB	Cyclic adenosine monophosphate responsive element-binding protein
CRISPR	Clustered regularly interspaced short palindromic repeats
CT	Computed tomography
CXCL	Chemokine C-X-C motif ligand
DAB	3,3'-Diaminobenzidine
ECM	Extracellular matrix
EGF	Epidermal growth factor
EGFR	Epidermal growth factor receptor
EMT	Epithelial-mesenchymal transition
EphB4	Ephrin type-B receptor 4
ERCP	Endoscopic retrograde cholangiopancreatography
ERK1/2	Extracellular signal-regulated 1/2 kinases
ESCRT	Endosomal sorting complexes required for transport
EUS	Endoscopic ultrasonography
EV	Extracellular vesicles
FACS	Fluorescence activated cell sorting
FAK	Focal adhesion kinase
Flk-1	Vascular endothelial growth factor-2
Flt-1	Vascular endothelial growth factor-1

FRET	Förster resonance energy transfer
GBM	Glioblastoma
GM-CSF	Granulocyte-macrophage colony-stimulating factor
hA8	Human ADAM8
HUVEC	Human umbilical vein endothelial cells
IFN	Interferon
IHC	Immunohistochemistry
IL	Interleukin
JAK	Janus kinase
KPC	$Kras^{LSL\text{-}G12D}$, $Trp53^{R172H/+}$, $Pdx^{Cre/+}$
KRAS	Kirsten rat sarcoma virus
LCN2	Lipocalin 2
LPS	Lipopolysaccharides
MAPK	Mitogen-activated kinase
M-CSF	Macrophage colony-stimulating factor
miRNA	MicroRNA
MMP	Matrix metalloprotease
MPO	Myeloperoxidase
MRI	Magnet resonance imaging
MT1	Membrane-type 1
MVB	Multivesicular bodies
NF-κB	Nuclear factor kappa-light-chain-enhancer of activated B cells
NK	Natural killer
NLR	Neutrophil-to-leukocyte ratio
NSCLC	Non-small-cell lung cancer
OPN	Osteopontin
OS	Overall survival
PanIN	Pancreatic intraepithelial neoplasia
PAR1	Protease-activated receptor 1
PDAC	Pancreatic Ductal Adenocarcinoma
Pdx	Pancreatic and duodenal homeobox 1
PET	Positron emission tomography

PI3K	Phosphoinositide 3-kinase
PMA	Phorbol 12-myristate 13-acetate
PPAR	Proliferator-activated receptor
qPCR	Quantitative polymerase chain reaction
Rho GTPase	Src kinase and ras homolog guanosine triphosphate hydrolyzing enzyme
sEV	Serum EV
SH3	Src homology 3
SMA	Smooth-muscle actin
SMAD4	Small mothers against decapentaplegic family member 4
Src	Sarcoma
STAT3	Signal transducer and activator of transcription 3
TAM	Tumor-associated macrophage
TGF-α	Transforming growth factor alpha
Tie-2	Angiopoietin-1 receptor
TM	Transmembrane
TME	Tumor microenvironment
TMZ	Temozolomide
TNBC	Triple-negative breast cancer
TNF	Tumor necrosis factor
TNF-R	Tumor necrosis factor receptor
TP53	Transformation related protein 53
TSG101	Tumor susceptibility gene 101
UTR	Untranslated region
VEGF	Vascular endothelial growth factor

List of figures

1 Introduction

1.1 Pancreatic Ductal Adenocarcinoma

People diagnosed with pancreatic cancer have a poor prognosis and 5-year overall survival (OS) rate of only 10% (Siegel *et al.*, 2021). Carcinomas that originate from the exocrine part of the pancreas have been described to account for more than 90% of all pancreatic cancer cases. Among these malignancies, Pancreatic Ductal Adenocarcinoma (PDAC) is the most frequent tumor disease (Orth *et al.*, 2019). In particular, the absence of early symptoms, a late diagnosis, early metastasis, and tumor marker deficiency contribute to one of the most aggressive and lethal cancer phenotypes (Miquel *et al.*, 2021). Surgical removal of the primary tumor and adjuvant chemotherapy, such as Gemcitabine monotherapy, is currently the only curative treatment that exists. Due to the lack of early symptoms and a resulting late diagnosis, only 15-20% of tumors are resectable (Vincent *et al.*, 2011; Hessmann *et al.*, 2020). In contrast, patients with inoperable tumors and distant metastases, especially to the liver, peritoneum, and lungs, undergo systemic chemotherapy (Yachida and Iacobuzio-Donahue, 2009). Depending on the patient's health status, two different standards of care combinations are administered to increase median overall survival. Besides Gemcitabine combined with nab-Paclitaxel (Hoff *et al.*, 2013), FOLFIRINOX consisting of leucovorin, fluorouracil, irinotecan, and oxaliplatin is the more promising chemotherapeutic regime, even if there is only a slight improvement in health for patients with pancreatic cancer (Conroy *et al.*, 2011; Conroy *et al.*, 2018). The emergence of PDAC is a stepwise process. Before the actual tumor develops, so-called precursor lesions arise. The latter existing in three different types, pancreatic intraepithelial neoplasias (PanIN) is the most common precursor form that occurs. With an increase in the number of lesions and molecular alterations, PanINs can be graded in low- to high-grade dysplasia, also known as PanIN 1-3. Furthermore, during PanIN to PDAC progression, key mutations in onco- and tumor suppressor genes drive the development of tumorigenesis (Hruban *et al.*, 2000; Hezel *et al.*, 2006). In more than 90% of all PDAC patients, an oncogenic activation of the kirsten rat sarcoma virus (KRAS) has been detected – this was especially evident at the beginning of carcinogenesis (Almoguera *et al.*, 1988; Hruban *et al.*, 1993). In addition, mutations in tumor suppressor genes of cyclin-dependent kinase inhibitor 2A (CDKN2A) and transformation related protein 53 (TP53) are visible in higher frequencies while, breast cancer gene 2 (BRCA2) and small mothers against decapentaplegic (SMAD) family member 4 (SMAD4) are apparent in lower frequencies (Caldas *et al.*, 1994; Redston *et al.*, 1994; Goggins *et al.*, 1996; Bardeesy *et al.*, 2006).

1.1.1 The tumor microenvironment and tumor-associated macrophages in PDAC

An essential feature of PDAC is the strong desmoplastic reaction, also called the tumor microenvironment (TME), that accounts for approximately 90% of the actual tumor mass. Tumor cells initiate the tumor cross-talk of the TME by secreting various proinflammatory cytokines and growth factors. As a result, a complex network of several cell types, mainly consisting of activated fibroblasts, immune cells, blood vessels, and neural cells, accumulate into the tumor stroma (Figure 1; Feig *et al.*, 2012; Neesse *et al.*, 2015; Huber *et al.*, 2020). The interaction within the TME leads to the intense production of extracellular matrix (ECM) components such as growth factors, matrix metalloproteases (MMP), cytokines, and structural proteins, mainly collagen I (Figure 1; Hessmann *et al.*, 2020). Until today, many studies have demonstrated that tumor stroma in PDAC is significantly involved in tumor progression, vascularization, metastasis, and chemoresistance (Matsuo *et al.*, 2009; Xu *et al.*, 2010b; Griesmann *et al.*, 2017; Nywening *et al.*, 2018).

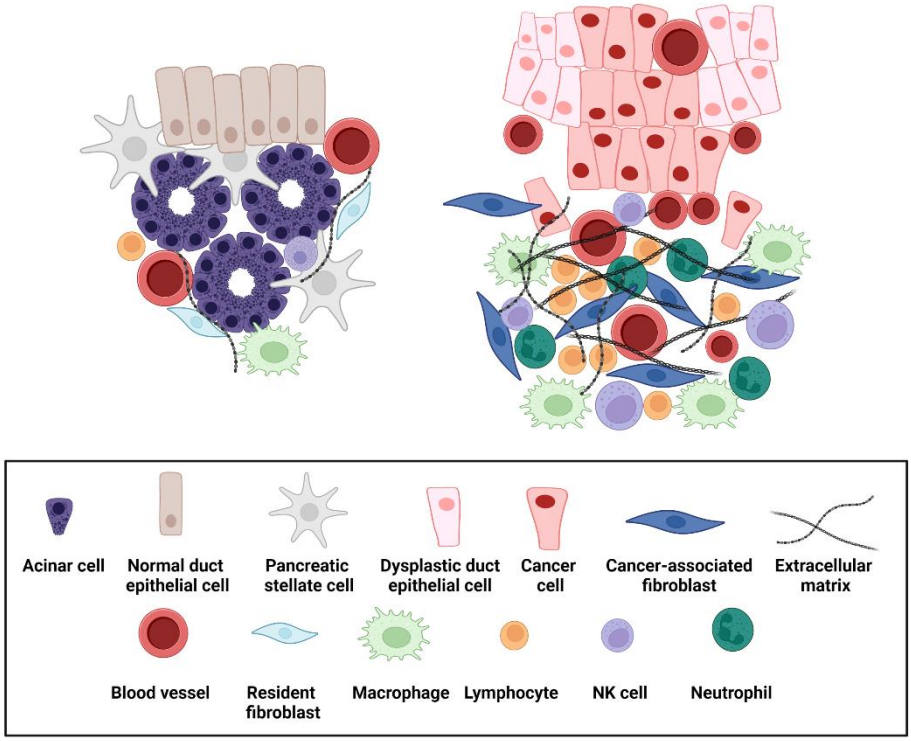

Figure 1. The tumor microenvironment in PDAC. The comparison of the cellular composition of normal pancreatic tissue (upper left) and the dense desmoplastic stroma of the PDAC tumor microenvironment (upper right). Created with Biorender.com (adapted and modified from Orth *et al.*, 2019)

As a result, the tumor stroma and its associated components are of great interest as a drug target and the associated desired cure of the disease. Furthermore, cells of the innate immune system, mainly granulocytes, monocytes, macrophages, and dendritic cells, have an essential role in the TME of PDAC. Infiltrating macrophages are the most

abundant immune cells in the tumor stroma and negatively correlate with patient survival (Ino *et al.*, 2013; Zhu *et al.*, 2017; Yang *et al.*, 2020).

In response to tumorigenesis, chemokines and cytokines such as chemokine C-X-C motif ligand 12 (CXCL12), chemokine C-C motif ligand 2 (CCL2), granulocyte-macrophage colony-stimulating factor (GM-CSF), macrophage colony-stimulating factor (M-CSF), and interleukin 3 (IL-3) are secreted, thus resulting in the recruitment of circulating monocytes to the tumor stroma. In situ, either the recruited monocytes develop into tumor-associated macrophages (TAMs), or elsewhere postulated tissue-resident macrophages become TAMs (Gordon and Taylor, 2005; Santoni *et al.*, 2014; Zhu *et al.*, 2017; Huber *et al.*, 2020). The emergence of TAMs is described as a dynamic process between different functional and phenotypic polarization states. A distinction is mainly made between the subtypes M1 and M2. Polarized M1 macrophages predominantly secrete pro-inflammatory cytokines such as IL-12, IL-23, and tumor necrosis factor (TNF), reactive nitrogen intermediates, and reactive oxygen intermediates. M2 macrophages, on the other hand, produce anti-inflammatory signals, increase the expression of vascular endothelial growth factor (VEGF) or epidermal growth factor (EGF), and reduce antigen presentation upon polarization (Mosser and Edwards, 2008; Biswas and Mantovani, 2010). Due to the complex signaling network described above, the role of TAMs has been widely and extensively discussed. Various studies attribute an immunosuppressive part to TAMs, promoting angiogenesis, tumor progression, and metastasis in PDAC (Griesmann *et al.*, 2017; Nywening *et al.*, 2018).

1.2 A disintegrin and metalloproteinase 8

The proteolytically active protease termed “a disintegrin and metalloproteinase 8” (ADAM8) is associated with several diseases such as respiratory diseases, bone destruction, liver injury, neurodegeneration, neuroinflammation, and neoplasias (Schlomann *et al.*, 2000; Ainola *et al.*, 2009; Mahoney *et al.*, 2009; Chen *et al.*, 2016; Conrad *et al.*, 2019; Awan *et al.*, 2021b). The chromosomal localization of the *ADAM8* gene is mapped to chromosome 10q26.3 and comprises 23 exons. The translated protein product consists of 824 amino acids and was first isolated from monocytic immune cells by Yoshida *et al.* in 1990 (Yoshida *et al.*, 1990; Yoshiyama *et al.*, 1997). As a type I transmembrane (TM) glycoprotein, ADAM8 can be assigned to the metzincin superfamily and is therefore structurally composed of a prodomain, followed by a catalytically active metalloprotease domain, disintegrin domain, cystein-rich/EGF-like structure, and a cytoplasmic tail (Figure 2). ADAM8 possesses a typically conserved zinc-binding site (HEXGHXXGXXHD) as part of its metalloprotease domain for enzyme

function (Figure 2; Bode *et al.*, 1996). To exert its proteolytic activity, removing the pro-domain of the 120 kilodaltons (kDa) heavy protein is a critical step and is achieved by autocatalysis in the *trans*-Golgi network. In contrast, other members of the ADAM family, except ADAM28, are dependent on a different mechanism and are activated by furin-like convertases (Howard *et al.*, 2000; Schlomann *et al.*, 2002).

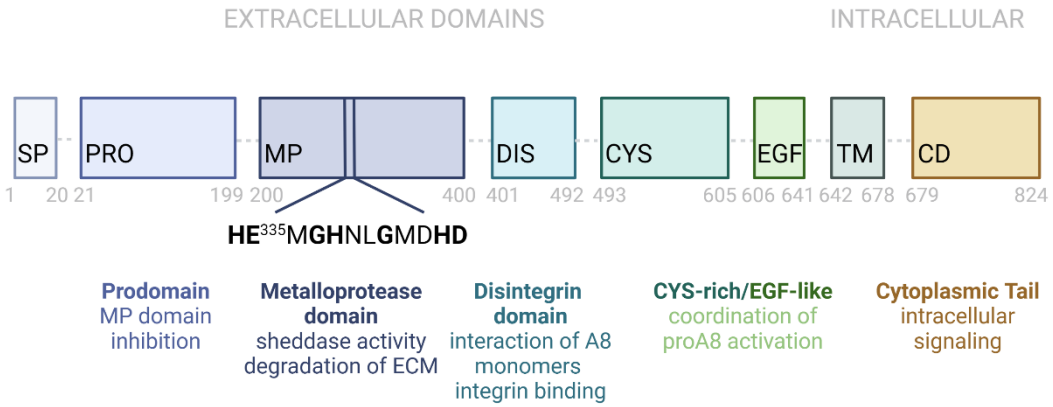

Figure 2. The functional domain structure of ADAM8. ADAM8 can be subdivided into a prodomain, metalloprotease domain, disintegrin domain, CYS-rich/EGF-like domain, and the cytoplasmic tail. Created with Biorender.com (adapted and modified from Conrad *et al.*, 2019)

The autocatalytic cleavage of the prodomain occurs in a two-step reaction and depends on the assembly of at least two ADAM8 monomers. The disintegrin and cystein-rich/EGF-like domains enable multimerization and facilitate intermolecular cleavage, resulting in a 90-kDa mature ADAM8. In addition, various isoforms such as the remnant form (60 kDa) or soluble ADAM8 (~30 kDa) that result from further processing are known as well (Schlomann *et al.*, 2002; Hall *et al.*, 2009; Schlomann *et al.*, 2015). Unlike other ADAM family members, ADAM8 is not ubiquitously but selectively expressed at low levels in cell types of the immune system, central nervous system, bone, and lung epithelial (Schlomann *et al.*, 2000; Choi *et al.*, 2001; King *et al.*, 2004; Kelly *et al.*, 2005). Furthermore, ADAM8 seems to be dispensable for normal development and homeostasis, as Adam8-deficient mice show no impairment in embryonic development and are viable (Kelly *et al.*, 2005). Specific stimuli such as bacterial lipopolysaccharide (LPS), interferon-γ (IFN-γ), TNF-α, interleukin 1β (IL-1β), IL-4, IL-13, or peroxisome proliferator-activated receptor-γ (PPAR-γ) during pathophysiological processes like inflammation or neoplasia upregulate ADAM8 expression (Yoshiyama *et al.*, 1997; Schlomann *et al.*, 2000; Hodgkinson and Ye, 2003; King *et al.*, 2004; Ainola *et al.*, 2009). In contrast to inflammatory processes, in which the occurrence of growth factors and cytokines control the upregulation of ADAM8, its expression is found to be constitutive in tumor contexts (Conrad *et al.*, 2019). The increased expression of ADAM8 leads to

proteolytic shedding of adhesion molecules, cytokine receptors, and ECM components, demonstrating a broad spectrum of substrates. Due to the lack of a specific substrate, there is an overlap in the substrate range of ADAM8 with ADAM10 and ADAM17 (Schlomann *et al.*, 2002). Above all, these include proteins with an immune function, such as the low-affinity IgE receptor (CD23), tumor necrosis factor receptor 1 (TNF-R1), and L-Selectin (Fourie *et al.*, 2003; Naus *et al.*, 2006; Gómez-Gaviro *et al.*, 2007; Bartsch *et al.*, 2010). Other examples are proteins that play a role in tumor-associated processes such as angiopoietin-1 receptor (Tie-2), vascular endothelial growth factor receptor-1 (Flt-1), vascular endothelial cadherin (VE-cadherin), vascular endothelial growth factor receptor 2 (Flk-1), ephrin type-B receptor 4 (EphB4), platelet endothelial cell adhesion molecule (CD31), E-selectin, and fibronectin (Zack *et al.*, 2009; Guaiquil *et al.*, 2010). Although ADAM8 is proteolytically active, it is also involved in specific signaling pathways independent of its catalytical domain. The *C*-terminal region of ADAM8 harbors two potential phosphorylation sites (Serine 758, Tyrosine 766) and five different sarcoma (Src) homology 3 (SH3) motifs that allow the interaction with adaptor proteins that in turn can execute downstream effects (Kleino *et al.*, 2015). Another example is the binding of ADAM8 to β1-Integrin and the subsequent phosphorylation of focal adhesion kinase (FAK), mitogen-activated kinase (MAPK), and protein kinase B/phosphoinositide 3-kinase (AKT/PI3K), leading to increased invasive behavior of tumor cells (Schlomann *et al.*, 2015; Dong *et al.*, 2015; Conrad *et al.*, 2018). The following section will give more details on the role of ADAM8 in cancer.

1.2.1 ADAM8 in cancer

The development of malignant cells is a complex process, where specific key events, in conjunction with the interplay of various regulators, drive cancerogenesis. In this context, overexpression of ADAM8 has been demonstrated in several cancer types and is associated with poor patient outcomes (Valkovskaya *et al.*, 2007; He *et al.*, 2012; Romagnoli *et al.*, 2014; Yang *et al.*, 2014; Conrad *et al.*, 2019). In 2006, Wildeboer *et al*. demonstrated that ADAM8 expression is upregulated to significant levels in brain tumors such as glioblastoma (GBM) and astrocytoma. Here, essential mechanisms of metastasis such as tumor cell migration and invasion were described to be mediated by the proteolytic activity of ADAM8. Furthermore, ADAM8 seems crucial to temozolomide (TMZ) resistance, the standard chemotherapy of GBM, since treating GBM cells with TMZ induced ADAM8 expression (Dong *et al.*, 2015). The upregulation of ADAM8 in gliomas was confirmed by another study published by Li *et al.* in 2021, demonstrating the positive staining for ADAM8 in GBM tissue samples of 50 patients. In addition, TAMs,

tumor-associated neutrophils, and tumor-associated natural killer (NK) cells of these tissue samples exhibited marked ADAM8 expressions, suggesting a role for ADAM8 in TME communication and, therefore, tumor progression. In this context, ADAM8 also seems to be involved in promoting angiogenesis by regulating osteopontin (OPN) levels in TAMs in GBM (Li *et al.*, 2021). In line with GBM, ADAM8 was also shown to be linked to cancerogenesis in triple-negative breast cancer (TNBC), as overexpression of the protease leads to the increased release of VEGF-A, promoting neovascularization in the tumor micro milieu. Further, an additional elevation of ADAM8 levels in breast cancer was shown to be induced by hypoxia and to facilitate the migration of tumors through endothelial monolayer, the detachment of tumor cells, and the formation of metastases (Romagnoli *et al.*, 2014). Additionally, another study verified the increased ADAM8 expression in primary tumors and metastases derived from breast cancer patients. This was further investigated using a mouse model in which high ADAM8 expression in circulating tumor cells correlated with a higher incidence of brain metastases. Moreover, ADAM8 expression was found to regulate MMP-9 expression levels in breast cancer, a metalloprotease involved in potentiating a migratory and invasive phenotype of tumor cells underlining the suggested role for ADAM8 in tumor progression and metastases formation (Park, 2009; Conrad *et al.*, 2018). In non-small-cell lung cancer (NSCLC), high ADAM8 levels in patient-derived tissue microarrays and serum were correlated with advanced tumor progression and related dissemination to distant organs proposing ADAM8 as a potential diagnostic marker (Ishikawa *et al.*, 2004). In 2010, Hernández *et al.* discovered two spliced and truncated isoforms of ADAM8 with distinct functions only detectable in lung cancer cell lines. One of these isoforms was put into context to facilitate bone metastasis and induce a higher tumor burden. Furthermore, ADAM8 upregulation was described to mediate chemoresistance. NSCLC cells overexpressing ADAM8 were less sensitive to cisplatin-induced apoptosis. Only the silencing of ADAM8 promoted the response to chemotherapy (Zhang *et al.*, 2013).

1.2.2 ADAM8 in PDAC

In 2007, Valkovskaya *et al.* examined the occurrence of ADAM8 messenger ribonucleic acid (mRNA) and protein in PDAC patient-derived and normal pancreas-derived tissue. This investigation detected a significant elevation of ADAM8 expression in the plasma membrane of tumor cells, mainly in degenerating acinar cells and tubular complexes. It was the first study to report an association between high ADAM8 expression levels with poor overall survival of PDAC patients (Valkovskaya *et al.*, 2007). Based on these findings, several pancreatic cancer cell lines were tested for ADAM8 mRNA and protein

expression in a normoxic or hypoxic experimental setting *in vitro*. The results revealed that ADAM8 expression is enhanced upon hypoxia, displaying the potentially important role of ADAM8 during tumor progression and metastasis since oxygen tension in tumors is a critical event in cancerogenesis (Valkovskaya, 2008). Experiments under hypoxic conditions were also conducted by Puolakkainen *et al.* in 2014. Unlike previously described, nonmetastatic and metastatic PDAC cell lines were first co-cultivated with primary macrophages and then exposed to a hypoxic environment. Co-culture alone already consistently increased the expression of ADAM8 and MMP-9, and the invasive behavior of all pancreatic cancer cell lines was upregulated. The observed effect of macrophages on PDAC cells was intensified by applying hypoxic conditions and seemed to be ADAM8-dependent since silencing of ADAM8 reduced macrophage- or hypoxia-induced invasion of PDAC cells *in vitro* (Puolakkainen *et al.*, 2014). Supplementary to the *in vitro* data described before, another study collected mechanistic and *in vivo* data in the context of ADAM8 and PDAC (Schlomann *et al.*, 2015). PDAC cell lines were generated with a stable knockout or overexpression to examine the gain or loss of function of ADAM8. Both migration and invasion were increased in cells with a strong ADAM8 expression, whereas in knockout cells, migrative and invasive behavior was downregulated dosage-dependently. Furthermore, to assess the regulation of other MMPs involved in tumor-associated processes, a proteolytic activity matrix assay was performed and subsequently revealed an increase in MMP-2 and MMP-14 activity upon ADAM8 overexpression, whereas cells lacking ADAM8 were less active. Due to its localization in the membrane of tumor cells and MAPK signaling being crucial to PDAC development, the interaction of ADAM8 with β1-Integrin and downstream signaling was investigated (Hayes *et al.*, 2016; Principe *et al.*, 2017). The activation of β1-Integrin by ADAM8 led to the phosphorylation of FAK and MAPK, suggesting that ADAM8 may regulate MMP-2 and MMP-14 activities via MAPK signaling to promote the dissemination of tumor cells in PDAC (Schlomann *et al.*, 2015). In accordance with *in vitro* data, this study also exhibited the ability of ADAM8 to increase tumor burden and invasion in a xenograft model. Tumors that evolved from implanted cells overexpressing ADAM8 had larger volumes. Additionally, infiltration to adjacent organs such as the spleen, diaphragm, and peritoneum and metastasis to the liver was reported to occur more frequently than in tumors lacking ADAM8 expression (Schlomann *et al.*, 2015). Another experimental setup demonstrated that ADAM8 inhibition in a genetically engineered PDAC mouse model (*Kras*$^{LSL\text{-}G12D}$, *Trp53*$^{R172H/+}$, *Pdx*$^{Cre/+}$; KPC) improved overall survival by the occurrence of fewer metastases (Schlomann *et al.*, 2015). These results suggest that ADAM8 is involved in many tumor-associated and -promoting processes and might be a potential therapeutic target or diagnostic tool.

1.3 Extracellular Vesicles

During homeostasis or pathological processes such as inflammation or tumorigenesis, intercellular communication is enabled by direct cell-cell contact, secretory proteins, and extracellular vesicles (EV; Chang and Pauklin, 2021). EVs are secreted particles enclosed in a lipid bilayer and can be classified into three groups according to their size and origin: exosomes (diameter 30 – 150 nm), microvesicles or so-called ectosomes (diameter 100 – 1000 nm), and apoptotic bodies (diameter 500 – 1000 nm). In contrast to apoptotic bodies and microvesicles described to budd from the cell membrane, exosomes are secreted by fusion of multivesicular bodies (MVB) with the cell membrane, more precisely exocytosis (Osaki and Okada, 2019). Exosome biogenesis is associated with the endosomal network, in which specific components are directed to either lysosomal degradation or cell surface membrane for exocytosis. In particular, endosomes are described to occur in three different forms: early endosome, late endosome, and recycling endosome. After sorting out the components to be recycled or degraded, exosomes form by constricting the late endosomal membrane resulting in intraluminal vesicles within the late endosome, termed MVB (Akers *et al.*, 2013). Different mechanisms for EV cargo loading have been reported in the literature so far. Among these, endosomal sorting complexes required for transport (ESCRT) machinery for internalizing biomolecules in EVs is the most extensively described form (Mir and Goettsch, 2020). Nevertheless, ESCRT-independent mechanisms such as lipid raft-, tetraspanin-, and ceramide-mediated processes were published (Wei *et al.*, 2021). However, the exact mechanism for exosome packaging is still the subject of intensive research. Nearly all cell types release EVs or specific exosomes to exchange proteins, lipids, or nucleic acids, thereby inducing particular signaling pathways or biological functions. For instance, cell-cell communication, immune response modulation, and cancerogenesis were reported in several studies (Robbins and Morelli, 2014; Maia *et al.*, 2018).

1.3.1 ADAMs in Exosomes

The content of EVs has been the subject of recent proteomics research and has thus revealed the exosomal existence of proteolytically active enzymes such as MMPs and ADAMs (Shimoda and Khokha, 2017; Das *et al.*, 2019). In 2006, Keller *et al.* postulated that exosome release and ectodomain-shedding by ADAM proteases are linked processes since ADAM proteases and exosome secretion are stimulated by similar molecules (Stoeck *et al.*, 2006). Another study supported this suggestion, showing that inhibition of ADAM-mediated processes prevented exosome release (Hawari *et al.*,

2004). One of the most studied ADAM proteases, ADAM10, was reported to be predominantly secreted as a mature form in exosomes derived from different cell types. In a human B-cell line, ADAM10 was described to execute binding and cleavage of CD23 L1 neural adhesion molecule inside both MVB and released exosomes, proofing ADAM-mediated activity in vesicles (Mathews *et al.*, 2010). Upon phorbol 12-myristate 13-acetate (PMA) or LPS stimulation, ADAM17 has also been demonstrated to be secreted as an active form by exosomes derived from a lung cancer cell line (Groth *et al.*, 2016). Concurrent with ADAM17, ADAM15 was demonstrated to be packed in EVs in a breast cancer cell line; further, the occurrence was increased after PMA stimulation emphasizing the potential role of ADAMs in the tumor microenvironment (Lee *et al.*, 2012).

1.4 Aim of this thesis

ADAM8 is a proteolytically active transmembrane metalloprotease with multiple functions such as the extracellular release of proteins and receptors from the cell membrane, degradation of the extracellular matrix, and the induction of intracellular signaling (Conrad *et al.*, 2019). In PDAC, ADAM8 was found to be highly expressed and to promote tumor progression by increasing the invasion and dissemination of tumor cells proposing ADAM8 as a potential therapeutic target (Valkovskaya *et al.*, 2007; Schlomann *et al.*, 2015). Since the PDAC tumor microenvironment is a complex network of tumor-associated cells that secrete extracellular matrix, cytokines, and metalloproteases, treatment of pancreatic cancer is not only limited to the tumor cells themselves but must also include the tumor stroma (Hessmann *et al.*, 2020). This work aims to elucidate the critical role of ADAM8, especially in the tumor microenvironment, to verify its potential as a diagnostic tool and therapeutic target.

2 Summary of the publications

2.1 Cohort Analysis of ADAM8 Expression in the PDAC Tumor Stroma

Christian Jaworek*, Yesim Verel-Yilmaz*, Sarah Driesch, Sarah Ostgathe, **Lena Cook**, Steffen Wagner, Detlef K. Bartsch, Emily P. Slater*, Jörg W. Bartsch*
*These authors have contributed equally to this work

(2021) Journal of Personalized Medicine, 11 (113): DOI: 10.3390/jpm11020113

2.1.1 Scientific summary

The most characteristic feature of PDAC disease is its activated desmoplastic nature with a high extracellular matrix content and numerous tumor-associated cells. Thus, immune cells are recruited during carcinogenesis by inflammatory signals secreted by tumor cells (Huber *et al.*, 2020). In this context, ADAM enzymes such as ADAM8 were reported to modulate cell migration and invasion, promoting PDAC tumor progression and metastasis in an *in vitro* and *in vivo* experimental setting (Schlomann *et al.*, 2015). Following a glioblastoma study, in which ADAM8 was detectable in tumor-associated immune cells at high levels, we examined the ADAM8 expression in the stroma of PDAC tumor sections from a cohort of 72 patients (Gjorgjevski *et al.*, 2019).

Prior to the experiments, all tumor tissue samples of PDAC patients, surgically resected in the Department of Visceral Surgery at the University Hospital Marburg, were histologically evaluated and classified according to Union for International Cancer Control; tumor, node, metastasis classification (UICC-TNM; Brierley *et al.*, 2017). 50 PDAC patients of our cohort were assigned to two different groups depending on their median survival times. The boundary between the two groups was set at 18 months, resulting in n = 16 patients surviving less than 18 months and n = 34 patients surviving longer than 18 months. Obtained tissue sections were then 3,3'-diaminobenzidine (DAB)-stained for ADAM8, resulting in different positive signal intensities and immunohistochemistry (IHC) scores ranging from 0 to 3 (representative images, Figure 1A-D; detailed description of IHC scoring, (Conrad *et al.*, 2018). Except for two PDAC sections that showed minor to none ADAM8 expression, all tumor tissues were positively stained for ADAM8. However, comparing the evaluated IHC scores for both groups, we detected no significant difference in ADAM8 expression between both survival groups (Figure 1E). To investigate the presence of ADAM8 in specific tumor-associated cells, sections of n = 10 representative PDAC patients were double-stained for ADAM8 and stromal cell marker and subsequently quantified (Figure 3). Co-localization of ADAM8

was observed with macrophage marker cluster of differentiation (CD68; Figure 2B) for 0-17%, NK-cell marker neural cell adhesion molecule (CD56; Figure 2F) for 18-75%, and neutrophil marker myeloperoxidase (MPO; Figure 2H) for 30-90%. No significant match was visible for T-cell marker CD3 (Figure 2C), CD4 (Figure 2D), CD8 (Figure 2E), and stellate cell marker smooth-muscle actin (SMA; Figure 2G). In addition, ADAM8-positive neutrophils were particularly abundant in post-capillary veins, from where neutrophils usually infiltrate tissues (Figure 4). For quantification and further comparison, ADAM8-positive neutrophil density (n/μm^2) was determined by counting neutrophils in at least three independent post-capillary veins with an area of >2000 μm^2 within the tumor tissue. Pearson correlation of neutrophil density and patient survival data showed significant results (r = -0.463, p = 0.0006; Figure 5A). Further, neutrophil density was significantly higher in patients with a median survival of fewer than 18 months (p = 0.0128; Figure 5B). In contrast, neutrophils present in peripheral blood (p = 0.2797) and the neutrophil-to-leukocyte ratio (NLR, p = 0.5143) did not correlate with PDAC patient survival.

2.1.2 Description of own contribution

The personal contribution to the preparation of this publication includes participation in the experimental design, supervision of the experiments, and curation of data shown in Figures 1-4.

2.2 Extracellular Vesicle-Based Detection of Pancreatic Cancer

Yesim Verel-Yilmaz*, Juan Pablo Fernández*, Agnes Schäfer, Sheila Nevermann, **Lena Cook**, Norman Gercke, Frederik Helmprobst, Christian Jaworek, Elke Pogge von Strandmann, Axel Pagenstecher, Detlef K. Bartsch, Jörg W. Bartsch*, Emily P. Slater*
* These authors have contributed equally to this work

(2021) Frontiers in Cell and Developmental Biology, 9:
DOI: 10.3389/fcell.2021.697939

2.2.1 Scientific summary

The lack of specific biomarkers and the resulting late detection of PDAC disease contributes to a short overall survival and a grim prognosis for PDAC patients (Zhang *et al.*, 2018). In this context, exosomes isolated from body fluids of diseased patients and their molecular content are current research subjects since cargo molecules were described to differ from healthy to tumor patients (Sumrin *et al.*, 2018). MicroRNAs (miRNAs) are small non-coding RNAs consisting of 18-22 nucleotides. Malignant

processes such as proliferation, migration, and invasion of tumor cells have been reported to be caused by miRNA-mediated dysregulation of specific genes (Peng and Croce, 2016). Therefore, several studies examined the role of exosomal miRNAs in the tumor cross-talk, potentially providing novel diagnostic markers for the early detection of PDAC (Soung *et al.*, 2017). Further, the alteration of miRNA expression levels is associated with ADAM8 in TNBC, particularly miR-720 (Das *et al.*, 2016). Based on these findings, this study intended to investigate the occurrence of ADAM8 and associated miRNAs in exosomes of PDAC patients and their potential as biomarkers for the early detection of PDAC.

Exosomes were isolated by sequential ultracentrifugation and filtration from the blood serum of 20 healthy donors, 7 patients with precursor lesions, and 72 PDAC patients. Afterwards they were examined regarding their characteristic properties. Electron microscopy of a representative exosome preparation revealed the typical bilayer structure (Figure 1A). Independent of their health status, exosomes derived from control or diseased patients had the appropriate size of < 120 nm (Figure 1B-D) and showed the same distribution in blood sera (Figure 1E). The only difference noted was the presence of CD9 in vesicles from healthy subjects compared to PDAC patients. Different CD9 levels were found in exosomes from diseased patients (Figure 1F), whereas in healthy donors, CD9 levels were relatively consistent (Figure 1G). For the detection of ADAM8 in the described exosomes, a bead-coupled fluorescence activated cell sorting (FACS) analysis (Figure 2A) was performed, and positive counts were found in all preparations (Figure 2B-G). Moreover, ADAM8 abundance increased upon disease status: exosomes derived from pancreatic precursor lesion patients ($p = 0.0139$) and PDAC patients ($p < 0.0001$) had significantly more positive ADAM8 beads than healthy individuals (Figure 2H). Additionally, the proteolytic activity of exosomes derived from PDAC patients on a förster resonance energy transfer (FRET)-based CD23 substrate (Figure 3B) was higher than in healthy controls (Figure 3A). However, to further investigate the content of pancreatic cancer-derived exosomes, 7 oncomiRNA were found to be dysregulated in PDAC patient-derived exosomes (Figure 3C). Among these, miR-451 showed the strongest upregulation and miR-720 downregulation compared to healthy donor vesicles (Figure 3C). Subsequent quantitative polymerase chain reaction (qPCR) analysis of the complete patient cohort verified the observed results. Additionally, the data of 10 chronic pancreatitis (CP) and 7 precursor lesion patients derived exosomes were supplemented to this analysis. The upregulation of miR-451 was detectable in precursor lesions and even more so in exosomes isolated from PDAC patients. Exosomes of CP patients had comparable levels of miR-451 as in healthy control samples (Figure 3 D,E). MiR-720 levels in exosomes from CP and PDAC patients were lower than in healthy control

samples, whereas exosomes derived from precursor lesion patients had similar levels as the control samples (Figure 3F,G). In another experimental setup, isolated exosomes of Panc89 with a knockout of the *ADAM8* gene served to validate the described miRNA-ADAM8 association. Exosomal miR-451 expression was 11-fold down ($p = 0.0102$), and miR-720 3.2-fold upregulated ($p = 0.0032$) in Panc89 ADAM8 knockout cells compared to exosomes derived from Panc89 cells expressing wildtype ADAM8.

2.2.2 Description of own contribution

The personal contribution to the preparation of this publication includes participation in the experimental design, the execution and data analysis of Figures 3A,B and S1, and the isolation of exosomes derived from Panc89 cells for Figure 3H.

2.3 ADAM8-Dependent Extracellular Signaling in the Tumor Microenvironment Involves Regulated Release of Lipocalin 2 and MMP-9

Lena Cook, Marie Sengelmann, Birte Winkler, Constanze Nagl, Sarah Koch, Uwe Schlomann, Emily P. Slater, Miles A. Miller, Elke Pogge von Strandmann, Bastian Dörsam, Christian Preußer, Jörg W. Bartsch

(2022) International Journal of Molecular Sciences, 23 (4): DOI: 10.3390/ijms23041976

2.3.1 Scientific summary

Within the TME, communication between several cell types is obligatory for regulating various complex tumor-associated processes such as tumor immunity, stroma remodeling, metastasis, angiogenesis, and drug resistance. In this context, the interaction of tumor and immune cells is either mediated by direct cell-to-cell contact or indirectly through secretion of soluble factors such as cytokines, growth factors, or in forms of EVs (Dominiak *et al.*, 2020). Moreover, EVs can harbor remodeling enzymes such as MMPs and ADAMs executing communication via cleavage of receptors, cytokines, inflammatory or ECM proteins in the TME (Das *et al.*, 2019). Neutrophil gelatinase-associated lipocalin, also known as lipocalin 2 (LCN2), has been frequently linked to pancreatic inflammation, tumorigenesis, and tumor progression (Gomez-Chou *et al.*, 2017; Gumpper *et al.*, 2020). As a secreted glycoprotein, LCN2 can dimerize with MMP-9, thereby modulating its proteolytic activity (Yan *et al.*, 2001; Tschesche *et al.*, 2001). In this context, the knockdown of ADAM8 in TNBC cells led to a downregulation of MMP-9 expression and reduced invasiveness (Conrad *et al.*, 2018). It was also

reported that upon co-cultivation of PDAC cells with macrophages, MMP-9 expression was increased and accompanied by enhanced migration and invasion (Puolakkainen *et al.*, 2014). The subject of this study was to examine the role of ADAM8 in macrophage-tumor cell communication and the regulation of MMP-9 and LCN2.

To investigate the role of ADAM8 in the tumor cross-talk, we initially conducted a knockout of the *ADAM8* gene in two PDAC and one TNBC cell line. For this, we used a clustered regularly interspaced short palindromic repeats/CRISPR-associated 9 (CRISPR/Cas 9) system to induce a genomic *ADAM8* knockout in Panc89 (Figure 1A-D), AsPC1 (Figure S1A,B), and MB-231 cells (Figure 2E, Figure S2,G). Since only Panc89 cells were used in the main experiments, we first investigated their functional properties. ADAM8 deficiency in Panc89 cells resulted, as expected, in reduced migrative and invasive behavior, whereas proliferation was unimpaired (Figure 1E-H). Based on the metalloprotease domain of ADAM8, we examined the impact of ADAM8-absence on activities of particular proteases by a FRET-based peptide cleavage assay, revealing decreased MMP-9 and ADAM8 activities (Figure 1P,Q; Miller *et al.*, 2011). Although activity was measured, MMP-9 expression was barely detectable at the mRNA level, as Ct values exceeded 30 (Figure 1N). Despite high mRNA expression of ADAM17, we assessed low cleavage rates for ADAM17. Only MMP-2 expression showed significant differences at mRNA level; however, MMP-2 activity, which had low values, was not affected (Figure 1N-Q). As a next step, we sought to determine whether ADAM8 influences MMP-9 activity levels indirectly by regulating LCN2 expression. Previous experiments made us aware of LCN2 using a protease/inhibitory array of supernatants derived from MB-231 cells, indicating that LCN2 and MMP-9 expression is downregulated in cells lacking ADAM8 expression (Figure 2A-C). These results could be confirmed for both MB-231 and Panc89 cells on mRNA and protein levels (Figure 2D-G). Moreover, the regulation of extracellular proteolysis in tumorigenesis has been a complicated network based on the interaction of enzymes and inhibitors; thus, we examined the potential effect of LCN2 on ADAM8 activity using the same FRET-base peptide cleavage assay as described above. Regardless of the applied concentration, recombinant LCN2 did not affect the proteolytic functionality of recombinant ADAM8 *in vitro* (Figure 2H).

Communication within the TME can be mediated by extracellular vesicles, thereby modifying and affecting signaling or metabolic processes in recipient cells (Dominiak *et al.*, 2020). Therefore, exosomes were isolated from Panc89 cells by sequential ultracentrifugation and subsequently analyzed regarding their typical properties. The successful exosome preparation was confirmed by both NanoFCM analysis and electron microscopy, displaying the appropriate size of 30-150 nm (Figure 3A,B) followed by the

antibody-based detection of exosome-associated proteins such as tumor susceptibility gene 101 (TSG101), CD81, and flotillin-1 (Figure 3C,F). Interestingly, exosomal ADAM8 was found to be secreted as an active protease, whereas whole-cell lysates of Panc89 showed both the mature and pro-forms of ADAM8 (Figure 3C). In accordance with these findings, exosomes derived from Panc89 control cells had significantly higher protease activities than exosomes isolated from ADAM8-deficient Panc89 cells (Figure 3D). The membranes of the applied exosomes were not disrupted, so protease activity could only be measured on the outside of the exosomal bilayer. Next, we were interested in investigating the mechanism underlying the sorting of ADAM8 into extracellular vesicles. As part of the ESCRT machinery, TSG101-dependent cargo-loading is mediated by recognizing a PS/TAP motif at targeted proteins, found at the *C*-terminal end of ADAM8 (Nabhan *et al.*, 2012). No specific evidence for the presumed interaction was detected since immunofluorescence staining of TSG101 and ADAM8 revealed little to no co-localization (Figure 3E). Supplementary to these results, we aimed to find out if cells lacking the *C*-terminal domain of ADAM8 are still being loaded into extracellular vesicles. For this purpose, ADAM8-deficient Panc89 cells were used to knock in either full-length ADAM8 or ADAM8 lacking the C-terminal structure ("hA8ΔCD rescue"). After exosomes were isolated, the subsequent immunoblot revealed the detection of ADAM8 in both preparations (Figure 3F). Next, we wanted to ascertain whether LCN2 and MMP-9 were sorted into exosomes and included MB-231 cells in this experimental part. The immunodetection of LCN2 displayed a positive signal for exosomes derived from Panc89 and MB-231 control cells. Interestingly, lower levels of LCN2 were present in exosomes from Panc89 cells lacking ADAM8 expression (Figure 4A), whereas LCN2 in exosomes from MB-231 ADAM8 knockout cells could not be detected (Figure 4B). However, MMP-9 was only secreted in exosomes from MB-231 cells (Figure 4B) and not in Panc89 cell-derived exosomes at all (Figure 4A).

Considering the possible important role of ADAM8-dependent LCN2 expression in PDAC, we read up on another study that reported the effect of LCN2 on the cell surface maintenance of EGF-receptor (EGFR), therefore regulating EGFR signaling (Yammine *et al.*, 2019). In this context, we examined EGFR and downstream signaling in Panc89 ADAM8 knockout cells, and interestingly, EGFR phosphorylation was not affected (Figure 5A,C). Nevertheless, activation of MAPK was lower in ADAM8-deficient Panc89 cells. The treatment of Panc89 ADAM8 knockout cells with transforming growth factor-alpha (TGF-α) further downregulated MAPK phosphorylation significantly (Figure 5A,D), whereas LCN2 expression was elevated to Panc89 control cell levels (Figure 5A,B). Additionally, we did not observe any protein expression changes upon treatment with recombinant LCN2 (Figure 5).

Based on the results so far, we were interested in how ADAM8-dependent regulation of LCN2 is affected by cells of the TME, particularly macrophages. For the experimental setup, the THP-1 cell line derived from acute monocytic leukemia was differentiated into M0 macrophages and then co-cultured with Panc89 cells. As a result, LCN2 expression significantly increased upon co-culture on mRNA and protein levels. The observed effect was even more pronounced in Panc89 control cells than in Panc89 cells lacking ADAM8 expression (Figure 6C,E). Surprisingly, the analysis of MMP-9 expression revealed an upregulation after co-culture, not only at the mRNA but especially at the protein level. However, no differences in MMP-9 expression were detected in both Pan89 cell lines (Figure 6D,E). Although MMP-9 expression was not affected by the absence of ADAM8 in Panc89 cells after co-culture, we noted significant differences in MMP-9 activity when we used conditioned supernatants for zymography (Figure 6F,G). In addition, the cell structure and morphology of the pancreatic cancer cell lines changed to a more mesenchymal appearance after co-culture (Figure 6H). In the last part of our experiments, we wanted to verify to what extent the ADAM8-dependent regulation of LCN2 and MMP9 is affected by the polarization status of the macrophages employed. Firstly, Panc89 control cells had approximately 2.5-fold higher ADAM8 levels after co-culture with M2 macrophages than with M0, M1, or without co-culture (Figure 7A,C). Besides, we observed the highest ADAM8-independent induction of MMP-9 expression in tumor cells co-cultured with M0 macrophages from non-detectable levels to ~65,000 pg/mL; however, both M1 and M2 increased MMP-9 levels to about 40,000 pg/mL (Figure 7A,B). In contrast, two macrophage types induced LCN2 expression and associated secretion of Panc89 control cells upon co-culture dependent on ADAM8. Interestingly, ADAM8-deficient Panc89 cells that were co-cultivated with M1 macrophages showed similar LCN2 levels compared to the co-cultured Panc89 control cells (Figure 7A,D). Finally, we treated both Panc89 control and Panc89 ADAM8 knockout cells with macrophage-conditioned supernatants to establish the link between co-culture and exosome-based communication as a preliminary experiment. The therefore mimicked co-culture had no effects on LCN2 expression, whereas the MMP-9 protein level was elevated in an ADAM8-dependent manner (Figure S9).

2.3.2 Description of own contribution

The personal contribution to the preparation of this publication includes participation in writing the manuscript, as well as the experimental setup, execution, and data analysis of Figure 1A-H,N,O, Figure 2D-H, Figure 3C-F, Figure 4A, Figure 6A,E, Figure 7, Figure S1, Figure S2, Figure S6, Figure S8C,D and Figure S9. The contributing authors, Marie

Sengelmann, Birte Winkler, and Constanze Nagl worked in their Master's thesis (M.S.) and their Bachelor's thesis (B.W. and C.N.) under my supervision.

3 Discussion

3.1 Cohort Analysis of ADAM8 Expression in the PDAC Tumor Stroma

The correlation of verifiable ADAM8 expression with increased tumor cell migration, invasion, or dissemination in PDAC was the subject of several research studies (Valkovskaya *et al.*, 2007; Puolakkainen *et al.*, 2014; Schlomann *et al.*, 2015). In this context, an earlier study demonstrated that qPCR analysis of healthy pancreatic and PDAC derived tissue revealed significantly elevated levels of ADAM8 in tumor samples. The observed results were then correlated with survival data of PDAC patients. Patients with higher ADAM8 mRNA expression had shorter overall survival times than patients with lower ADAM8 mRNA levels (Valkovskaya *et al.*, 2007). Consistent with these results, ADAM8 protein expression was detected in all PDAC tissue sections of the Marburg patient cohort using immunohistochemistry. In our cohort, however, we could not detect a significant correlation of ADAM8 expression in tumor cells with patient survival. Since different methods were used to assess ADAM8 levels in tumor tissue of PDAC patients, the comparability of these two studies must be viewed critically. On the one hand, there is no distinction possible between tumor and stromal cells when using tumor tissue for RNA extraction. On the other hand, RNA isolation from tissue samples and subsequent qPCR analysis is independent of semi-quantitative assessments and scoring of parameters like staining intensities, as previously applied for correlation analyses of ADAM8 and survival of tumor patients (Li *et al.*, 2012; Romagnoli *et al.*, 2014; Conrad *et al.*, 2018). However, immunohistochemical staining of tumor-tissue sections offers the possibility to distinguish between positive signals either in tumor or in stromal cells. The critical function of tumor-associated cells in the diagnosis, prognosis, and treatment of PDAC is widely discussed. In the case of TAMs, various studies used different markers, and the number of patients included varied, emphasizing the need for more specific markers (Kurahara *et al.*, 2011; Ino *et al.*, 2013; Knudsen *et al.*, 2017).

Given the presence of ADAM8 in various immune cells and its inducibility by inflammatory stimuli, we were interested in the expression profile of ADAM8 in tumor-associated cells (Yoshida *et al.*, 1990; Yoshiyama *et al.*, 1997; Schlomann *et al.*, 2000; Gómez-Gaviro *et al.*, 2007; Valkovskaya *et al.*, 2007). The conducted double-staining revealed a co-localization of ADAM8 with macrophages, NK cells, and neutrophils. Contrary to what was shown by Li *et al.* in GBM patients, we detected ADAM8 most frequently in neutrophils and NK cells and to a lesser extent in macrophages (Li *et al.*, 2021). However, the role of ADAM8 in immune cells is the subject of current research and discussed in the context of various diseases. For instance, a recent study postulated

that the lack of ADAM8 in macrophages promotes chronic obstructive pulmonary disease (COPD) by increasing the numbers of infiltrating macrophages and upregulating EGFR-mediated mucus cell metaplasia, a hallmark of COPD (Polverino *et al.*, 2018). In compliance with Polverino *et al.*, another study showed that the absence of ADAM8 in leukocytes had a pro-inflammatory effect on allergic airway inflammation in mice by inducing apoptotic signaling pathways in those cells. Since an infiltration of leukocytes, particularly eosinophils and macrophages, into the airways during asthma inflammation and COPD promotes disease progression, these studies suggested that the improvement of leukocyte-derived ADAM8 may be a potential therapy for asthma and COPD disease relief (Knolle *et al.*, 2013; Polverino *et al.*, 2018).

As a completely opposite result, Dreymueller *et al.* demonstrated that mRNA knockdown, enzyme inhibition, or gene knockout of ADAM8 impaired transendothelial and transepithelial migration of macrophages in acute lung inflammation *in vitro*. Unlike described by Knolle *et al.*, no effects of ADAM8-deficiency on leukocyte proliferation or survival were observed *in vitro*. However, the absence of ADAM8 reduced the number of infiltrating leukocytes into the lung (Dreymueller *et al.*, 2017). Contrary results on the role of ADAM8 were also described for allergic asthma, leaving a dispute whether ADAM8 is a “friend or foe” in allergic asthma (Naus *et al.*, 2010; Chen *et al.*, 2013; Knolle *et al.*, 2013). These contrary results concluded that ADAM8 can act either stage-specific or strain-specific in mice. Given the competence of ADAM8-positive immune cells to inflammation sites, its impact might be due to the recruitment of relevant immune cells (macrophages, neutrophils, NK cells) during disease development and their impact on disease progression.

On the protective site of ADAM8, it was shown that both neutrophils and macrophages are recruited during skeletal muscle regeneration to clear the remnants of destroyed muscle fibers. *In vivo* data from skeletal muscle of dystrophin-null mice crossed with Adam8 knockout mice confirmed the assumption that infiltration of neutrophils and macrophages into the tissue is ADAM8 dependent. Consequently, ADAM8-positive neutrophils and macrophages have been shown to dispose of injured muscle fibers that contribute to skeletal muscles' successful regeneration (Nishimura *et al.*, 2015).

As a demonstration of detrimental effects of ADAM8, a current study by Conrad *et al.* using intravital microscopy in *Adam8*-deficient mice again confirmed that neutrophil recruitment and transepithelial migration is ADAM8 dependent *in vivo*. The pulmonary infection of *Adam8* knockout mice with *Pseudomonas aeruginosa,* a commonly used method to induce acute respiratory distress syndrome (ARDS) in animals, was followed by fewer neutrophil counts, reduced morbidity, limited lung injury, and decreased bacterial burden. Moreover, ADAM8 expression and proteolytic activity in ARDS patients

are associated with higher mortality, clearly demonstrating that ADAM8-inhibition is a therapeutic option (Conrad *et al.*, 2022).

In contrast to the disputable role of ADAM8 in lung diseases, ongoing studies in oncology strongly suggest that ADAM8 is involved in tumor progression so that inhibition of ADAM8 seems an attractive option. For instance, studies in GBM suggested that ADAM8 expression in tumor cells and TAMs regulates angiogenesis-associated processes in cancer disease. More detailed, the experiments conducted by Li *et al.* showed that ADAM8 can regulate a protein involved in angiogenesis termed osteopontin (OPN) in both, cancer cells and macrophages. Supernatants of macrophages derived from *Adam8* deficient mice showed decreased tube formation capacity in a human umbilical vein endothelial cells (HUVEC)-based angiogenesis assay, postulating that ADAM8 regulates OPN levels in macrophages while promoting angiogenesis and thus tumor progression (Li *et al.*, 2021).

Because both disease-promoting and improving roles have been described for ADAM8, it is essential to elucidate the function of ADAM8 in tumor-associated macrophages, NK cells, and neutrophils of PDAC. In this regard, our study identified the most frequent co-localization of ADAM8 with neutrophils mainly found in post-capillary venules within the tumor area. More interestingly, after quantifying the ADAM8-positive neutrophil density for all tumor tissue sections of our patient cohort, we could show that the abundance of ADAM8-positive neutrophils negatively correlated with patient survival. These results indicate that ADAM8-positive neutrophils in tumor tissue may provide a measure of disease progression and thus serve as a prognostic factor. Therefore, we concluded that ADAM8 is essential for neutrophil mobility and transmigration through the endothelium in PDAC. Interestingly, we recently demonstrated for ARDS that ADAM8 was significant for neutrophil recruitment in lung tissue by the interaction of its cytoplasmic domain with the unconventional myosin1f (myo1f; Conrad *et al.*, 2022). In contrast to this, we achieved to convey that both the NLR and neutrophil counts in peripheral blood of PDAC patients did not correlate with patient survival. Comparing this data with the existing literature, we found that using a NLR ratio as well as scoring of general neutrophil infiltration for correlation analyses is still under debate (Stotz *et al.*, 2013; Piciucchi *et al.*, 2017; Wikberg *et al.*, 2017; Iwai *et al.*, 2020; Naso *et al.*, 2021).

Overall, our study detected ADAM8 in the Marburg PDAC patient cohort, supporting its presumed essential role in tumorigenesis and dissemination of PDAC. In addition, there is evidence for ADAM8 expression in tumor-associated cells such as macrophages, NK cells, and neutrophils. The role of ADAM8 in NK cells and macrophages is still uncertain and should be further investigated. Nevertheless, based on the literature and the findings of our study, it can be argued that ADAM8 tends to exert tumor-promoting rather than

tumor-suppressing functions by either improving the general “fitness” of tumor cells (invasion, proliferation) or recruiting tumor-associated cells such as macrophages and neutrophils. The detection of ADAM8 in neutrophils of tissue sections could aid in the diagnosis and prognosis of PDAC patients to improve disease progression and treatment.

3.2 Extracellular Vesicle-Based Detection of Pancreatic Cancer

Detection of ADAM8 in tumor-associated neutrophils in post-capillary venules and the subsequent quantification allowed us to identify a potential prognostic method for patients at risk for PDAC (Jaworek *et al.*, 2021). The health outcome, as well as the pathological diagnosis of diseased patients, are essential for the appropriate treatment. Nevertheless, one of the biggest challenges in PDAC is the early detection of the disease. The lack of specific symptoms during the development of PDAC makes early diagnosis and thus curative treatment difficult, if not almost impossible (Vincent *et al.*, 2011; Hessmann *et al.*, 2020). Despite commonly used medical imaging methods such as computed tomography (CT), endoscopic retrograde cholangiopancreatography (ERCP), upper endoscopic ultrasonography (EUS), magnet resonance imaging (MRI), and positron emission tomography (PET), tumors are usually detected in a more advanced state and therefore have little to no treatability (Yee *et al.*, 2018). Carbohydrate antigen 19-9 (CA 19-9) has gained acceptance as a biomarker in sera from PDAC patients and is still used today. However, elevated CA 19-9 levels can mislead diagnostics since biliary obstruction, endocrinal, gynecological, hepatic, pulmonary, spleen, and malignancies apart from pancreatic cancer can increase the amount of serum CA 19-9 (Ballehaninna and Chamberlain, 2012; Kim *et al.*, 2020).

The search for more specific and suitable biomarkers is the subject of current research. It has turned out that the content of EVs, in particular, exosomes, derived from patients’ blood appeared to serve as a potential diagnostic tool for the detection of early-stage PDAC tumors (Yee *et al.*, 2020). To obtain a better insight into the molecular content of serum EVs (sEVs), we isolated and characterized exosomes from 72 PDAC patients and compared them with exosomes derived from 20 healthy individuals and 7 patients with precursor lesions. Electron microscopy and ZetaView® analyses of the EV samples confirmed the size and shape prescribed for exosomes (Fuhrmann *et al.*, 2015; Théry *et al.*, 2018).

Given the prognostic value of ADAM8, we wanted to investigate the diagnostic potential of ADAM8 in exosomes of PDAC patients (Jaworek *et al.*, 2021). In lung cancer, as well as gastric and breast cancer, significantly increased ADAM8 levels were found in blood

from diseased patients compared to healthy control groups (Ishikawa *et al.*, 2004; Romagnoli *et al.*, 2014; Chung *et al.*, 2019). However, no differences were observed in detecting soluble ADAM8 in sera from PDAC patients and healthy individuals (Valkovskaya *et al.*, 2007). Considering EVs as a powerful diagnostic tool, we applied a bead-coupled FACS analysis of the isolated sEVS from our control group and our patient cohorts. Apart from the fact that ADAM8 was present in all sEVs, the data analysis revealed a positive correlation of high exosomal ADAM8 secretion with disease progression, demonstrating that ADAM8 is a tumor-dependent cargo of EVs. In agreement with the membrane localization in EVs, we identified a correlating proteolytic activity of sEVs derived from PDAC patients using a FRET-based CD23 substrate, whereas ADAM8 activity of sEVs isolated from healthy individuals was hardly detectable. Although this peptide substrate is not ADAM8-specific, the high amount of detectable ADAM8 levels in sEVs of diseased patients suggests a predominant involvement of ADAM8 in the observed high cleavage rates. Both the use of an antibody recognizing the extracellular domain of ADAM8 as well as the detectable proteolytical activity indicate a topological orientation of ADAM8 towards the extracellular compartment. It is tempting to speculate that ADAM8 may exert its tumor-promoting functions not only by being taken up by recipient cells but also by the proteolytic activity on the surface of exosomes. Interestingly, the proteolytic activity of several proteases on the surface of exosomes has been described in previous studies (Sanderson *et al.*, 2019). Among these, a protease termed membrane-type1 MMP (MT1-MMP, MMP14) embedded in the bilayer structure of exosomes has been reported to degrade type I collagen and proenzyme MMP-2 (Hakulinen *et al.*, 2008). In addition, enhanced TNF-α and amphiregulin shedding activity of ADAM17 on the surface of exosomes were shown by Groth *et al.* (Groth *et al.*, 2016). This data suggests a possible regulatory and ECM shaping role for ADAM8 on exosomes since it can also cleave several ECM molecules and regulate protease activities (Conrad *et al.*, 2019; Scharfenberg *et al.*, 2020).

Considering the heterogeneity of PDAC tumors, detecting, or profiling several different biomolecules in exosomes is thought to have greater diagnostic value than focusing on just one biomarker. Based on the finding that miRNAs can be packed into EVs, we were interested in exosomal miRNAs that are correlated with the presence of ADAM8 (Soung *et al.*, 2017). By means of a cancer-associated miRNA screening, we identified two miRNAs affected by the disease status of PDAC patients compared to healthy probands. One of them has already been described in connection with ADAM8. For instance, Das *et al.* reported downregulation of miR-720 in ADAM8-deficient breast cancer cells and their derived exosomes (Das *et al.*, 2016). In contrast, our study found a significant decrease of mirR-720 levels in exosomes derived from the blood of CP and PDAC

patients compared to exosomes from healthy controls and patients with precursor lesions. The validation of these results in exosomes derived from Panc89 ADAM8 knockout cells revealed, contrary to Das *et al.*, an upregulation of exosomal miR-720 in Panc89 ADAM8 knockout cells suggesting a rather tumor-promoting role for the ADAM8-regulated release of miR-720 in PDAC. A study reinforced this assumption by demonstrating that upregulation of miR-720 acts as a tumor suppressor, thereby preventing pancreatic tumor cell proliferation and invasion ability (Zhang *et al.*, 2017). In addition, it was shown that high miR-720 expression in pancreatic cancer cells downregulated epithelial-mesenchymal transition (EMT)-associated genes (Lemberger *et al.*, 2019). By further analyzing the isolated sEVs' content, we observed a significant upregulation of miR-451 in samples of precursor lesions or PDAC patients and a simultaneous reduction of miR-451 expression in EVs from ADAM8 knockout Panc89 cells. A study that has been retracted claimed a tumor-promoting role for miR-451 by targeting calcium-binding protein 39 (CAB39), thus increasing cell proliferation and invasion of pancreatic cancer cells (Retracted article (Guo *et al.*, 2017; International, 2021). Although this article was retracted, the use of TargetScan (v8.0; targetscan.org; accessed on 01 March 2022) revealed a target site in the 3’ untranslated region (UTR) of CAB39. Considering these results and the tumor-promoting effects and regulatory functions that have been described for ADAM8 in PDAC, it seems plausible to speculate that ADAM8 may regulate tumor progression by upregulation of miR-451. Despite this, the regulatory role of ADAM8 for miR-451 must be investigated further.

To conclude, our study provides insights into the content of exosomes derived from PDAC patients compared to healthy individuals. We successfully detected ADAM8 in exosomes and identified ADAM8-dependent exosomal miR-720 and miR-451 levels as a potential biomarker profile. The different regulatory patterns of miRNAs might help to differentiate between CP, precursor lesions, and PDAC disease and to improve the early detection of pancreatic cancer, particularly the curative treatment of the disease. Furthermore, the presence of exosomal ADAM8 and its proteolytic activity on exosomes' surface could extend the additional important functions of ADAM8 in the TME of PDAC regarding tumor progression and metastasis. Again, ADAM8 has emerged as a potential therapeutic target in pancreatic cancer.

3.3 ADAM8-Dependent Extracellular Signaling in the Tumor Microenvironment Involves Regulated Release of Lipocalin 2 and MMP-9

The TME in PDAC has emerged as a complex network of cancer cells as well as tumor-associated cells, ECM proteins, and signaling molecules (Hessmann *et al.*, 2020). During tumorigenesis, cells within the TME communicate either by cell-to-cell contact or exchange of soluble factors and EVs (Dominiak *et al.*, 2020; Yang *et al.*, 2020). In the article published by Verel-Yilmaz *et al.*, we demonstrated the proteolytic activity and the potential regulatory function of ADAM8-positive exosomes that have been isolated from PDAC patients' blood (Verel-Yilmaz *et al.*, 2021). Since there is evidence that ADAM8 is expressed in tumor-associated macrophages in the tumor tissue of PDAC patients, we were interested in the role of the multifunctional protein ADAM8 in communication between macrophages and tumor cells in PDAC (Jaworek *et al.*, 2021).

Firstly, the characterization of the Panc89 ADAM8 knockout cell line used in our studies revealed a reduced cell migration and invasion. These findings are in accordance with data of a previous study in that Schlomann *et al.* reported a decrease in migration and invasion upon ADAM8 knockdown in another pancreatic cancer cell line (Schlomann *et al.*, 2015). However, ADAM8 not only affects cancer cell migration and invasion in PDAC but also in breast, brain, and lung cancer, as well as in hepatocellular carcinoma suggesting that ADAM8 is involved in general tumor-promoting and cancer dissemination processes (Wildeboer *et al.*, 2006; Hernández *et al.*, 2010; Romagnoli *et al.*, 2014; Awan *et al.*, 2021b). The underlying mechanisms also include the complex coordination and interaction of different MMPs and ADAMs. Previous studies demonstrated an ADAM8-dependent regulation of MMP-2, MMP-9, MMP-14, and ADAM17 activities, leading to the investigation of an activity profile in both Panc89 cell lines (Schlomann *et al.*, 2015; Conrad *et al.*, 2018; Scharfenberg *et al.*, 2020). As a result, the inferred proteolytic activities of MMP-2 and ADAM17 were hardly measurable, whereas ADAM8 and MMP-9 cleavage rates were comparably high and downregulated in ADAM8 knockout cells. Hence, the data indicated that functional active ADAM8 might regulate high MMP-9 activity levels in Panc89 cells. Due to its ability to degrade ECM molecules such as collagen, fibronectin, and laminin, MMP-9 has been described to facilitate extravasation and dissemination of tumor cells, thus accelerating metastasis formations in several cancer diseases (Xu *et al.*, 2010a; Hagemann *et al.*, 2012; Yabluchanskiy *et al.*, 2013; Farina and Mackay, 2014; Mehner *et al.*, 2014; Huang, 2018). A recent study addressing proteolytic functions in breast cancer implied an ADAM8-dependent regulation of the transcription and proteolytic activity of MMP-9 via

activation of extracellular signal-regulated kinases 1/2 (ERK1/2) and cyclic adenosine monophosphate responsive element-binding protein (CREB) signaling. Consequently, the transmigration of tumor cells through the endothelial cell layer was induced, and metastasis to the brain occurred (Conrad *et al.*, 2018). Additionally, in brain cancer, the latest results indicate that MMP-9 expression induced by ADAM8 via MAPK signaling is mediated by a downregulation of miR-181a-5p that has evolved as a tumor suppressor in glioma cells, suggesting a plausible mechanism for ADAM8-dependent regulation of MMP-9 activity in PDAC (Shi *et al.*, 2008); Schäfer *et al.*, Manuscript in press). Based on these findings, the noted ADAM8-dependent proteolytic activity of MMP-9 could explain the increased invasive behavior of Panc89 control cells compared to ADAM8 knockout cells. Nevertheless, unlike what was shown by Conrad *et al.*, we could not ascertain a transcriptional regulation of MMP-9 by ADAM8 expression in Panc89 cells since MMP-9 mRNA and protein levels were almost not detectable. Consequently, we were interested in the regulatory mechanisms underlying MMP-9 activity and therefore performed a protease/inhibitory array to investigate potential proteins regulated by ADAM8 to promote MMP-9 activity.

Among these proteins, our data revealed a decreased LCN2 expression in cells lacking ADAM8, which became much more interesting for us since LCN2 has been described to regulate MMP-9 activity by forming a complex, thus protecting it from degradation (Tschesche *et al.*, 2001; Yan *et al.*, 2001). The role and function of LCN2 expression in pancreatic diseases are contrarily discussed in the literature (Gumpper *et al.*, 2020). Nevertheless, it has been demonstrated that the depletion of LCN2 in pancreatic cancer cell lines diminished invasive behavior, as shown by a lower proteolytic activity of MMP-9 in gelatin zymography and the reduced ability to degrade ECM molecules in an invasion assay. Furthermore, pancreatic cancer cells lacking LCN2 expression were more sensitive to gemcitabine treatment than cells exhibiting LCN2 (Leung *et al.*, 2012). In addition, *in vivo* data of a constitutive *Lcn2* knockout in KPC mice revealed increased overall survival, reduced ECM secretion, less PanIN development, diminished tumor growth, and impaired macrophage recruitment (Gomez-Chou *et al.*, 2017). Considering the observed effects of ADAM8 on pancreatic cancer cells and PDAC development, we suggested that ADAM8 could regulate MMP-9 activity indirectly by controlling LCN2 levels. Since no ADAM8-mediated cleavage or activation of pro-MMP-9 is known so far, we hypothesize that ADAM8-dependent regulation of LCN2 results in higher levels of enzymatically active MMP-9. As a result, ADAM8 could thereby increase tumor cells' invasive behavior and enhance tumor progression and metastasis. A possible mechanism for regulating LCN2 expression could be the activation of nuclear factor kappa-light-chain-enhancer of activated B cells (NF-κB). In chondrosarcoma cells,

ADAM8 has been described to regulate migration and invasion of tumor cells by the activation of NF-κB (Liu *et al.*, 2019). In hepatoma cells, the binding of ADAM8 to β1-integrin is responsible for the activation of FAK/MAPK/Src kinase and ras homolog guanosine triphosphate hydrolyzing enzyme (Rho GTPase) that in turn can activate NF-κB (Lee *et al.*, 2007; Awan *et al.*, 2021a). Since the promotor of LCN2 contains a binding site for NF-κB, this type of regulation would be possible and requires further research (Zhao *et al.*, 2014). In addition, upon IL-10 stimulation, signal transducer and activator of transcription 3 (STAT3) phosphorylation led to an increased LCN2 expression in macrophages, as described by another study (Jung *et al.*, 2012). In GBM cells as well as in macrophages, ADAM8 has been found to regulate angiogenesis by inducing OPN expression via janus kinase (JAK)/STAT3 activation, suggesting a possible regulatory link between ADAM8-dependent activation of STAT3 and induced LCN2 expression.

Furthermore, ADAM8 has been reported to regulate miRNAs involved in pancreatic, breast, and brain cancer progression (Das *et al.*, 2016; Verel-Yilmaz *et al.*, 2021). Thus, miRNA-mediated regulation of LCN2 by ADAM8 should not be ruled out. Several studies reported miRNAs that are found to target LCN2 expression. For instance, in the context of ischemic stroke, exosomal miR-138-5p has been shown to inhibit LCN2 expression, whereas the investigation of miR-761 revealed the inhibition of EMT by blocking LCN2 transcription during chronic rhinosinusitis (Deng *et al.*, 2019; Cheng *et al.*, 2020). The latter could be a potential miRNA downregulated by ADAM8 and thus promote EMT-associated processes. Moreover, the results of a miRNA expression analysis of GBM ADAM8 knockout cells of one of our master's students have turned out to be informative and revealed a negative correlation of ADAM8 with miR-130a (master's thesis by Lara Meier; unpublished data). The overexpression of miR-130a in a murine granulocytic precursor cell line led to decreased LCN2 mRNA expression, suggesting a regulatory mechanism in which LCN2 expression is induced by ADAM8-mediated downregulation of miR-130a (Larsen *et al.*, 2014).

When Panc89 control and ADAM8 knockout cells were co-cultivated with THP-1-derived macrophages, LCN2 expression was significantly enhanced in both cell lines but substantially higher in Panc89 control cells. Although MMP-9 mRNA and protein levels in Panc89 cells were elevated independent of ADAM8 and macrophage polarization, gelatin zymography displayed the ADAM8-dependent upregulation of MMP-9 activity. The presence of macrophage increased the observed effect of ADAM8 on LCN2 and MMP-9 activity; hence we expect a more invasive phenotype of Panc89 control than ADAM8 knockout cells. A study supporting this assumption published by Puolakkainen *et al.* could also indicate an increased induction of MMP-9 expression using a similar experimental setup. Unlike our study, ADAM8 was additionally upregulated in tumor cells

upon co-culture with macrophages. However, the invasion rate of co-cultivated tumor cells correlated with increased ADAM8 and MMP-9 expression levels (Puolakkainen *et al.*, 2014). In addition, Tekin *et al.* reported that the secretion of MMP-9 by macrophages which leads to the activation of EMT by MMP-9-mediated cleavage of protease-activated receptor (PAR1). Other than described here, we assume that independent of its origin, tumor cell-derived MMP-9 might also lead to the activation of PAR1 and, consequently, induce the transcription of EMT-associated genes (Tekin *et al.*, 2020). Based on these studies, our data suggest that the invasiveness of Panc89 control cells compared to ADAM8 knockout cells should increase upon co-culture. Experiments addressing these assumptions should provide further insights.

Another possible underlying mechanism of ADAM8-dependent upregulation of LCN2 expression could be the complex network of TNF-α signaling. In 2010, Bartsch *et al.* provided evidence that ADAM8 expression is upregulated after the stimulation with TNF-α, which in turn led to shedding processes of TNF-R1 by ADAM8 (Bartsch *et al.*, 2010). Since pro-inflammatory macrophages (M1) secrete inflammatory cytokines such as TNF-α and the inducibility of LCN2 expression by TNF-α has been reported by an earlier study, one could assume that macrophage-derived TNF-α is responsible for the described upregulation (Zhao *et al.*, 2014). It is tempting to speculate that TNF-α, released by macrophages, somehow induces the ADAM8-mediated cleavage of soluble TNF-R1, thus increasing LCN2 secretion in tumor cells. Our data supports this assumption, as pro-inflammatory macrophages have a relatively more substantial inducing effect on LCN2 expression in Panc89 control cells compared to anti-inflammatory macrophages (M2).

Our study revealed that ADAM8 was packaged as an active enzyme in EVs derived from Panc89 and MB-231 control cells, suggesting that the secretion of ADAM8 in EVs might mediate the ADAM8-based communication within the TME. Upon closer examination, we showed that the extracellular release of LCN2 and MMP-9 in EVs was dependent on the presence of ADAM8. EVs without ADAM8 as a cargo had lower levels of LCN2, whereas exosomal MMP-9 was hardly detectable. Since we could not find any evidence that ADAM8 is sorted into EVs by binding ESCRT-I protein TSG101 via PTAP-motif, other mechanisms independent of TSG101 need to be investigated (Nabhan *et al.*, 2012). For instance, the presence of lipid rafts was shown to facilitate the formation of exosomes, thereby encapsulating proteins that are embedded in these structures (Tan *et al.*, 2013). ADAM17 was associated with lipid rafts and was also detected in EVs, presenting an alternative mechanism for directing ADAM8 into EVs (Tellier *et al.*, 2006; Groth *et al.*, 2016). Furthermore, the association with ceramides or tetraspanins, which have been described to be involved in exosomal sorting processes, could also allow

ADAM8 to be packaged into exosomes (Wei *et al.*, 2021). Previous studies could demonstrate an association for ADAM10 with tetraspanins, thus supporting the proposed mechanism (Arduise *et al.*, 2008; Harrison *et al.*, 2021).

In conclusion, it became clear from the results presented here that ADAM8 in the TME significantly affects tumor development and progression. Its multidomain structure enables the execution of essential functions for tumor-associated processes such as enzymatic processing of receptors and proteins or signaling by interaction with regulatory factors (Conrad *et al.*, 2019). Our results proved that ADAM8 was not only detected in tumor cells but also in tumor-associated cells such as neutrophils, NK cells, and macrophages. In addition, the determination of ADAM8-positive neutrophil density in venules of pancreatic tumors has been shown to be useful as a prognostic marker in PDAC (Jaworek *et al.*, 2021). It has turned out that ADAM8 is important for the recruitment of immune cells as well as for the motility and transendothelial migration of these cells, contributing to a tumor-supportive microenvironment (Dreymueller *et al.*, 2017; Jaworek *et al.*, 2021; Conrad *et al.*, 2022). Besides its ability to recruit immune cells to the tumor site, ADAM8 can also activate regulatory proteins such as β1-integrin, STAT3, or MAPK/CREB leading to the upregulation of tumor-promoting proteins such as LCN2, OPN, and MMP-9 and increased migration, invasion, and angiogenesis. In addition, the presence of immune cells such as macrophages can enhance the ADAM8-dependent upregulation of these proteins (Schlomann *et al.*, 2015; Conrad *et al.*, 2018; Li *et al.*, 2021; Cook *et al.*, 2022). Furthermore, as a cargo of extracellular vesicles, we could conclusively show that ADAM8 exerts its functions in the TME by either regulating the molecular content or acting as an active protease on the surface of these vesicles. For instance, ADAM8 has been described to regulate the expression and sorting of miRNAs such as miR-451, miR-720, and miR-181a into extracellular vesicles, but also proteins such as LCN2 and MMP-9. (Verel-Yilmaz *et al.*, 2021; Cook *et al.*, 2022; Schäfer *et al.*, Manuscript in press). The uptake of these vesicles by recipient cells could lead to either expression changes of genes involved in tumor progression or activation of signaling pathways. Moreover, the outward-facing metalloprotease domain of ADAM8 could potentially degrade ECM molecules during dissemination processes or receptor-ectodomain shedding on recipient cells, creating a tumor-promoting microenvironment. In addition, ADAM8 present in exosomes derived from serum of PDAC patients is a suitable method for diagnostic purposes since exosomal ADAM8 abundance correlated with disease progression that needs to be improved by identification of markers that are regulated by ADAM8 in order to provide a higher specificity of diagnoses (Verel-Yilmaz *et al.*, 2021).

Further elucidation of the ADAM8-dependent regulation of miRNAs as well as tumor-promoting proteins is crucial. Furthermore, a more detailed understanding of regulatory mechanisms underlying ADAM8-dependent cargo loading of extracellular vesicles may provide more insight into ADAM8-driven communication of tumor and immune cells in the TME and support the development of diagnostic and therapeutic approaches in PDAC.

4 Summary

The expression of the membrane-bound protein ADAM8 is associated with various diseases such as respiratory diseases, liver injury, neuroinflammation, and cancer. Despite its low expression level in distinct cell types, ADAM8 can be upregulated to significant levels upon specific stimuli. Unlike inflammatory processes, ADAM8 is constitutively overexpressed in cancer diseases as it has been described for brain, breast, lung, and pancreatic cancer, and correlates almost exclusively with poor survival. Most importantly, PDAC demonstrated that ADAM8 plays an essential role in tumor cell migration, invasion, and metastasis *in vitro* and in *vivo*. The treatment of PDAC is impeded by its high metastatic ability and the lack of specific symptoms leading to late detection of the tumor disease and a high mortality rate. Therefore, there is a high urgency to identify biomarkers for early detection as well as specific therapeutic targets. The first aim of this thesis was to detect ADAM8 in tumor tissue sections of the Marburg PDAC patient cohort. DAB staining of all patients revealed a positive detection of ADAM8 in all sections, suggesting an essential role for ADAM8 in PDAC tumor and disease progression. Nevertheless, ADAM8 expression did not correlate with patient overall survival. ADAM8 expression was also detected in tumor-associated macrophages, NK cells, and neutrophils, indicating that ADAM8 is involved in the recruitment of immune cells to the tumor microenvironment and thus might promote tumor progression. However, the quantification and subsequent analysis of the neutrophil density in post-capillary venules within the tumor areas disclosed the significant negative correlation of neutrophils positive for ADAM8 with overall survival, emphasizing the potential of ADAM8 for diagnosis and prognosis of PDAC.

In the second part of this study, ADAM8 was identified as an active protease in exosomes derived from sera of PDAC patients by applying a bead-coupled FACS analysis. Elevated ADAM8 levels in exosomes correlated with disease progression. In addition, two miRNAs, miR-451 and miR-720, that are reported to exert tumor-promoting functions, were dysregulated in exosomes derived from PDAC patients compared to healthy individuals. The validation of these two miRNAs in exosomes from pancreatic cancer cell lines Panc89 control and Panc89 ADAM8 knockout cells revealed the ADAM8-dependent upregulation of miR-720 and downregulation of miR-451. Based on these results, the detection of ADAM8, miR-451, and miR-720 in exosomes may facilitate diagnosis, as this regulatory profile allows the differentiation between different stages of PDAC disease.

The final part of this work investigates the regulatory function of ADAM8 in the tumor microenvironment. As a protease involved in tumor cell invasion and metastasis, MMP-

9 was previously described to be regulated by ADAM8 via MAPK/CREB signaling. Based on this finding, MMP-9 expression was validated in Panc89 control and ADAM8 knockout cells. However, ADAM8 was shown to regulate MMP-9 activity but not MMP-9 expression. Further analysis of other regulatory proteins revealed the ADAM8-dependent downregulation of LCN2, a protein that promotes PDAC progression and is involved in the regulation of MMP-9 activity. These data suggest that ADAM8 regulates LCN2 expression levels to control MMP-9 activity, promoting invasion and metastasis in PDAC. In addition, the described regulatory effect of ADAM8 on LCN2 and MMP-9 was enhanced by the co-culture of Panc89 cell with THP-1 derived macrophages demonstrating the essential role of ADAM8 in the PDAC tumor microenvironment and thus underlining the potential as a therapeutic target. The functional analysis of exosomes derived from Panc89 control and ADAM8 knockout cells demonstrated an ADAM8-dependent release of LCN2 and revealed that ADAM8 is sorted as a proteolytically active enzyme in exosomes.

The presence of the ADAM8 in extracellular vesicles and the ability to exert specific regulatory functions in the tumor microenvironment by either cleavage of essential proteins or regulating particular genes involved in tumor progression offers the possibility to develop advanced treatment strategies and to improve the early detection of PDAC disease.

5 Zusammenfassung

Die Expression des membrangebundenen Proteins ADAM8 wird mit verschiedenen Krankheiten wie Atemwegserkrankungen, Leberschäden, Entzündung des Nervengewebes und Krebserkrankungen in Verbindung gebracht. Trotz seiner geringen Expression in bestimmten Zelltypen kann ADAM8 durch spezifische Stimuli auf ein beträchtliches Maß hochreguliert werden. Im Gegensatz zu entzündlichen Prozessen ist ADAM8 bei Krebserkrankungen konstitutiv überexprimiert, wie es für Gehirn-, Brust-, Lungen- und Bauchspeicheldrüsenkrebs beschrieben wurde und korreliert fast ausschließlich mit einem schlechten Überleben. Vor allem konnte beim PDAC nachgewiesen werden, dass ADAM8 für die Migration, Invasion und Metastasierung von Tumorzellen *in vitro* und *in vivo* eine wichtige Rolle spielt. Die Behandlung des duktalen Adenokarzinoms des Pankreas wird durch seine hohe Metastasierungsfähigkeit und das Fehlen spezifischer Symptome erschwert, was zu einer späten Erkennung der Tumorerkrankung und einer hohen Sterblichkeit führt. Daher ist es dringend notwendig, sowohl Biomarker für die frühe Erkennung als auch spezifische therapeutische Ziele zu finden.

Das erste Ziel dieser Arbeit war der Nachweis von ADAM8 in den Tumorgewebeschnitten der Marburger PDAC-Patientenkohorte. Die DAB-Färbung aller Patienten ergab einen positiven Nachweis von ADAM8 in allen Schnitten, was auf eine wesentliche Rolle von ADAM8 bei der Progression des Tumors und Entwicklung der Erkrankung hindeutet. Dennoch korrelierte die ADAM8-Expression nicht mit dem Überleben der Patienten. Die Expression von ADAM8 wurde auch in tumorassoziierten Makrophagen, NK-Zellen und Neutrophilen nachgewiesen, was darauf hindeutet, dass ADAM8 an der Rekrutierung von Immunzellen in die Tumormikroumgebung beteiligt ist, und somit die Tumorprogression fördern könnte. Die Quantifizierung und anschließende Analyse der Neutrophilen-Dichte in den postkapillären Venolen innerhalb des Tumors ergab jedoch eine signifikante negative Korrelation der ADAM8-positiven Neutrophilen mit dem Gesamtüberleben, was das Potenzial von ADAM8 für die Diagnose und Prognose von PDAC unterstreicht.

Im zweiten Teil dieser Studie wurde ADAM8 mit Hilfe einer „Bead“-gekoppelten FACS-Analyse als aktive Protease in Exosomen aus Seren von PDAC-Patienten nachgewiesen. Ein erhöhter ADAM8-Spiegel in Exosomen korrelierte mit dem Fortschreiten der Erkrankung. Darüber hinaus wurde festgestellt, dass die zwei miRNAs miR-451 und miR-720, von denen berichtet wird, dass sie tumorfördernde Funktionen ausüben, in Exosomen von PDAC-Patienten im Vergleich zu gesunden Personen dysreguliert sind. Die Validierung dieser beiden miRNAs in Exosomen, die von den

Pankreaskrebs-Zelllinien Panc89 Kontrolle und Panc89 ADAM8 Knockout sekretiert wurden, zeigte die ADAM8-abhängige Hochregulierung von miR-720 und die Herunterregulierung von miR-451. Auf der Grundlage dieser Ergebnisse könnte der Nachweis von ADAM8, miR-451 und miR-720 in Exosomen die Diagnosestellung erleichtern, da durch dieses Regulationsprofil die Unterscheidung zwischen verschiedenen Stadien der PDAC-Erkrankung ermöglicht.

Im letzten Teil dieser Arbeit wurde die regulatorische Funktion von ADAM8 in der Mikroumgebung von Tumoren untersucht. Als eine Protease, die an der Invasion und Metastasierung von Tumorzellen beteiligt ist, wird MMP-9 nachweislich von ADAM8 über MAPK/CREB-Signale reguliert. Auf dieser Grundlage wurde die Expression von MMP-9 in Panc89 Kontroll- und ADAM8-Knockout-Zellen validiert. Es zeigte sich jedoch, dass ADAM8 zwar die Aktivität, aber nicht die Expression von MMP-9 reguliert. Eine weitere Analyse anderer regulatorischer Proteine zeigte die ADAM8-abhängige Herabregulierung von LCN2, einem Protein, das die PDAC-Progression fördert und die MMP-9 Aktivität bestimmen kann. Darüber hinaus wurde die beschriebene regulierende Wirkung von ADAM8 auf LCN2 und MMP-9 durch die Co-Kultur von Panc89-Zellen mit THP-1-Makrophagen verstärkt, was die wesentliche Rolle von ADAM8 in der Tumormikroumgebung von PDAC zeigt und damit das Potential als therapeutisches Ziel unterstreicht. Die funktionelle Analyse von Exosomen, die aus Panc89 Kontroll- und ADAM8-Knockout Zellen isoliert wurden, zeigte die ADAM8-abhängige Freisetzung von LCN2 und dass ADAM8 als aktives Enzym in Exosomen sekretiert wird.

Das Vorhandensein von ADAM8 in extrazellulären Vesikeln und die Fähigkeit, spezifische regulatorische Funktionen in der Mikroumgebung des Tumors auszuüben, wie zum Beispiel die proteolytische Spaltung von essenziellen Proteinen oder die Regulierung bestimmter tumorfördernder Gene, bietet die Möglichkeit, fortschrittliche Behandlungsstrategien zu entwickelnd und die Früherkennung von PDAC zu verbessern.

6 References

Ainola, M., Li, T.-F., Mandelin, J., Hukkanen, M., Choi, S.J., Salo, J. and Konttinen, Y.T. (2009), “Involvement of a disintegrin and a metalloproteinase 8 (ADAM8) in osteoclastogenesis and pathological bone destruction”, *Annals of the rheumatic diseases*, Vol. 68 No. 3, pp. 427–434.

Akers, J.C., Gonda, D., Kim, R., Carter, B.S. and Chen, C.C. (2013), “Biogenesis of extracellular vesicles (EV): exosomes, microvesicles, retrovirus-like vesicles, and apoptotic bodies”, *Journal of neuro-oncology*, Vol. 113 No. 1, pp. 1–11.

Almoguera, C., Shibata, D., Forrester, K., Martin, J., Arnheim, N. and Perucho, M. (1988), “Most human carcinomas of the exocrine pancreas contain mutant c-K-ras genes”, *Cell*, Vol. 53 No. 4, pp. 549–554.

Arduise, C., Abache, T., Li, L., Billard, M., Chabanon, A., Ludwig, A., Mauduit, P., Boucheix, C., Rubinstein, E. and Le Naour, F. (2008), “Tetraspanins regulate ADAM10-mediated cleavage of TNF-alpha and epidermal growth factor”, *Journal of immunology (Baltimore, Md. 1950)*, Vol. 181 No. 10, pp. 7002–7013.

Awan, T., Babendreyer, A., Mahmood Alvi, A., Düsterhöft, S., Lambertz, D., Bartsch, J.W., Liedtke, C. and Ludwig, A. (2021a), “Expression levels of the metalloproteinase ADAM8 critically regulate proliferation, migration and malignant signalling events in hepatoma cells”, *Journal of cellular and molecular medicine*, Vol. 25 No. 4, pp. 1982–1999.

Awan, T., Babendreyer, A., Wozniak, J., Alvi, A.M., Sterzer, V., Cook, L., Bartsch, J.W., Liedtke, C., Yildiz, D. and Ludwig, A. (2021b), “Expression of the Metalloproteinase ADAM8 Is Upregulated in Liver Inflammation Models and Enhances Cytokine Release In Vitro”, *Mediators of inflammation*, Vol. 2021, p. 6665028.

Ballehaninna, U.K. and Chamberlain, R.S. (2012), “The clinical utility of serum CA 19-9 in the diagnosis, prognosis and management of pancreatic adenocarcinoma: An evidence based appraisal”, *Journal of gastrointestinal oncology*, Vol. 3 No. 2, pp. 105–119.

Bardeesy, N., Cheng, K.-H., Berger, J.H., Chu, G.C., Pahler, J., Olson, P., Hezel, A.F., Horner, J., Lauwers, G.Y., Hanahan, D. and Depinho, R.A. (2006), “Smad4 is dispensable for normal pancreas development yet critical in progression and tumor biology of pancreas cancer”, *Genes & development*, Vol. 20 No. 22, pp. 3130–3146.

Bartsch, J.W., Wildeboer, D., Koller, G., Naus, S., Rittger, A., Moss, M.L., Minai, Y. and Jockusch, H. (2010), “Tumor necrosis factor-alpha (TNF-alpha) regulates shedding of TNF-alpha receptor 1 by the metalloprotease-disintegrin ADAM8: evidence for a

protease-regulated feedback loop in neuroprotection", *The Journal of Neuroscience*, Vol. 30 No. 36, pp. 12210–12218.

Biswas, S.K. and Mantovani, A. (2010), "Macrophage plasticity and interaction with lymphocyte subsets: cancer as a paradigm", *Nature immunology*, Vol. 11 No. 10, pp. 889–896.

Bode, W., Grams, F., Reinemer, P., Gomis-Rüth, F.X., Baumann, U., McKay, D.B. and Stöcker, W. (1996), "The metzincin-superfamily of zinc-peptidases", *Advances in experimental medicine and biology*, Vol. 389, pp. 1–11.

Brierley, J., Gospodarowicz, M.K. and Wittekind, C. (Eds.) (2017), *TNM classification of malignant tumours,* Eighth edition, John Wiley & Sons Inc, Chichester, West Sussex, UK, Hoboken, NJ.

Caldas, C., Hahn, S.A., da Costa, L.T., Redston, M.S., Schutte, M., Seymour, A.B., Weinstein, C.L., Hruban, R.H., Yeo, C.J. and Kern, S.E. (1994), "Frequent somatic mutations and homozygous deletions of the p16 (MTS1) gene in pancreatic adenocarcinoma", *Nature genetics*, Vol. 8 No. 1, pp. 27–32.

Chang, C.-H. and Pauklin, S. (2021), "Extracellular vesicles in pancreatic cancer progression and therapies", *Cell death & disease*, Vol. 12 No. 11, p. 973.

Chen, J., Deng, L., Dreymüller, D., Jiang, X., Long, J., Duan, Y., Wang, Y., Luo, M., Lin, F., Mao, L., Müller, B., Koller, G. and Bartsch, J.W. (2016), "A novel peptide ADAM8 inhibitor attenuates bronchial hyperresponsiveness and Th2 cytokine mediated inflammation of murine asthmatic models", *Scientific reports*, Vol. 6, p. 30451.

Chen, J., Jiang, X., Duan, Y., Long, J., Bartsch, J.W. and Deng, L. (2013), "ADAM8 in asthma. Friend or foe to airway inflammation?", *American journal of respiratory cell and molecular biology*, Vol. 49 No. 6, pp. 875–884.

Cheng, J., Chen, J., Zhao, Y., Yang, J., Xue, K. and Wang, Z. (2020), "MicroRNA-761 suppresses remodeling of nasal mucosa and epithelial-mesenchymal transition in mice with chronic rhinosinusitis through LCN2", *Stem cell research & therapy*, Vol. 11 No. 1, p. 151.

Choi, S.J., Han, J.H. and Roodman, G.D. (2001), "ADAM8: a novel osteoclast stimulating factor", *Journal of bone and mineral research the official journal of the American Society for Bone and Mineral Research*, Vol. 16 No. 5, pp. 814–822.

Chung, H.W., Kim, J.J., Choi, J.I., Lee, H.R. and Lim, J.B. (2019), "A Disintegrin and Metalloproteinase 8 as a Potential Blood Biomarker for Early Diagnosis of Gastric Cancer", *Yonsei medical journal*, Vol. 60 No. 8, pp. 713–719.

Conrad, C., Benzel, J., Dorzweiler, K., Cook, L., Schlomann, U., Zarbock, A., Slater, E.P., Nimsky, C. and Bartsch, J.W. (2019), "ADAM8 in invasive cancers: links to

tumor progression, metastasis, and chemoresistance", *Clinical science (London, England 1979)*, Vol. 133 No. 1, pp. 83–99.

Conrad, C., Götte, M., Schlomann, U., Roessler, M., Pagenstecher, A., Anderson, P., Preston, J., Pruessmeyer, J., Ludwig, A., Li, R., Kamm, R.D., Ritz, R., Carl, B., Nimsky, C. and Bartsch, J.W. (2018), "ADAM8 expression in breast cancer derived brain metastases: Functional implications on MMP-9 expression and transendothelial migration in breast cancer cells", *International journal of cancer*, Vol. 142 No. 4, pp. 779–791.

Conrad, C., Yildiz, D., Cleary, S.J., Margraf, A., Cook, L., Schlomann, U., Panaretou, B., Bowser, J.L., Karmouty-Quintana, H., Li, J., Berg, N.K., Martin, S.C., Aljohmani, A., Moussavi-Harami, S.F., Wang, K.M., Tian, J.J., Magnen, M., Valet, C., Qiu, L., Singer, J.P., Eltzschig, H.K., Bertrams, W., Herold, S., Suttorp, N., Schmeck, B., Ball, Z.T., Zarbock, A., Looney, M.R. and Bartsch, J.W. (2022), "ADAM8 signaling drives neutrophil migration and ARDS severity", *JCI insight*, Vol. 7 No. 3.

Conroy, T., Desseigne, F., Ychou, M., Bouché, O., Guimbaud, R., Bécouarn, Y., Adenis, A., Raoul, J.-L., Gourgou-Bourgade, S., La Fouchardière, C. de, Bennouna, J., Bachet, J.-B., Khemissa-Akouz, F., Péré-Vergé, D., Delbaldo, C., Assenat, E., Chauffert, B., Michel, P., Montoto-Grillot, C. and Ducreux, M. (2011), "FOLFIRINOX versus gemcitabine for metastatic pancreatic cancer", *The New England journal of medicine*, Vol. 364 No. 19, pp. 1817–1825.

Conroy, T., Hammel, P., Hebbar, M., Ben Abdelghani, M., Wei, A.C., Raoul, J.-L., Choné, L., Francois, E., Artru, P., Biagi, J.J., Lecomte, T., Assenat, E., Faroux, R., Ychou, M., Volet, J., Sauvanet, A., Breysacher, G., Di Fiore, F., Cripps, C., Kavan, P., Texereau, P., Bouhier-Leporrier, K., Khemissa-Akouz, F., Legoux, J.-L., Juzyna, B., Gourgou, S., O'Callaghan, C.J., Jouffroy-Zeller, C., Rat, P., Malka, D., Castan, F. and Bachet, J.-B. (2018), "FOLFIRINOX or Gemcitabine as Adjuvant Therapy for Pancreatic Cancer", *The New England journal of medicine*, Vol. 379 No. 25, pp. 2395–2406.

Cook, L., Sengelmann, M., Winkler, B., Nagl, C., Koch, S., Schlomann, U., Slater, E.P., Miller, M.A., Strandmann, E.P. von, Dörsam, B., Preußer, C. and Bartsch, J.W. (2022), "ADAM8-Dependent Extracellular Signaling in the Tumor Microenvironment Involves Regulated Release of Lipocalin 2 and MMP-9", *International Journal of Molecular Sciences*, Vol. 23 No. 4, p. 1976.

Das, A., Mohan, V., Krishnaswamy, V.R., Solomonov, I. and Sagi, I. (2019), "Exosomes as a storehouse of tissue remodeling proteases and mediators of cancer progression", *Cancer metastasis reviews*, Vol. 38 No. 3, pp. 455–468.

Das, S.G., Romagnoli, M., Mineva, N.D., Barillé-Nion, S., Jézéquel, P., Campone, M. and Sonenshein, G.E. (2016), “miR-720 is a downstream target of an ADAM8-induced ERK signaling cascade that promotes the migratory and invasive phenotype of triple-negative breast cancer cells”, *Breast cancer research BCR*, Vol. 18 No. 1, p. 40.

Deng, Y., Chen, D., Gao, F., Lv, H., Zhang, G., Sun, X., Liu, L., Mo, D., Ma, N., Song, L., Huo, X., Yan, T., Zhang, J. and Miao, Z. (2019), “Exosomes derived from microRNA-138-5p-overexpressing bone marrow-derived mesenchymal stem cells confer neuroprotection to astrocytes following ischemic stroke via inhibition of LCN2”, *Journal of Biological Engineering*, Vol. 13 No. 1, p. 71.

Dominiak, A., Chełstowska, B., Olejarz, W. and Nowicka, G. (2020), “Communication in the Cancer Microenvironment as a Target for Therapeutic Interventions”, *Cancers*, Vol. 12 No. 5.

Dong, F., Eibach, M., Bartsch, J.W., Dolga, A.M., Schlomann, U., Conrad, C., Schieber, S., Schilling, O., Biniossek, M.L., Culmsee, C., Strik, H., Koller, G., Carl, B. and Nimsky, C. (2015), “The metalloprotease-disintegrin ADAM8 contributes to temozolomide chemoresistance and enhanced invasiveness of human glioblastoma cells”, *Neuro-oncology*, Vol. 17 No. 11, pp. 1474–1485.

Dreymueller, D., Pruessmeyer, J., Schumacher, J., Fellendorf, S., Hess, F.M., Seifert, A., Babendreyer, A., Bartsch, J.W. and Ludwig, A. (2017), “The metalloproteinase ADAM8 promotes leukocyte recruitment in vitro and in acute lung inflammation”, *American journal of physiology. Lung cellular and molecular physiology*, Vol. 313 No. 3, L602-L614.

Farina, A.R. and Mackay, A.R. (2014), “Gelatinase B/MMP-9 in Tumour Pathogenesis and Progression”, *Cancers*, Vol. 6 No. 1, pp. 240–296.

Feig, C., Gopinathan, A., Neesse, A., Chan, D.S., Cook, N. and Tuveson, D.A. (2012), “The pancreas cancer microenvironment”, *Clinical cancer research an official journal of the American Association for Cancer Research*, Vol. 18 No. 16, pp. 4266–4276.

Fourie, A.M., Coles, F., Moreno, V. and Karlsson, L. (2003), “Catalytic activity of ADAM8, ADAM15, and MDC-L (ADAM28) on synthetic peptide substrates and in ectodomain cleavage of CD23”, *The Journal of biological chemistry*, Vol. 278 No. 33, pp. 30469–30477.

Fuhrmann, G., Serio, A., Mazo, M., Nair, R. and Stevens, M.M. (2015), “Active loading into extracellular vesicles significantly improves the cellular uptake and photodynamic effect of porphyrins”, *Journal of controlled release official journal of the Controlled Release Society*, Vol. 205, pp. 35–44.

Gjorgjevski, M., Hannen, R., Carl, B., Li, Y., Landmann, E., Buchholz, M., Bartsch, J.W. and Nimsky, C. (2019), “Molecular profiling of the tumor microenvironment in glioblastoma patients: correlation of microglia/macrophage polarization state with metalloprotease expression profiles and survival”, *Bioscience reports*, Vol. 39 No. 6.

Goggins, M., Schutte, M., Lu, J., Moskaluk, C.A., Weinstein, C.L., Petersen, G.M., Yeo, C.J., Jackson, C.E., Lynch, H.T., Hruban, R.H. and Kern, S.E. (1996), “Germline BRCA2 gene mutations in patients with apparently sporadic pancreatic carcinomas”, *Cancer research*, Vol. 56 No. 23, pp. 5360–5364.

Gomez-Chou, S.B., Swidnicka-Siergiejko, A.K., Badi, N., Chavez-Tomar, M., Lesinski, G.B., Bekaii-Saab, T., Farren, M.R., Mace, T.A., Schmidt, C., Liu, Y., Deng, D., Hwang, R.F., Zhou, L., Moore, T., Chatterjee, D., Wang, H., Leng, X., Arlinghaus, R.B., Logsdon, C.D. and Cruz-Monserrate, Z. (2017), “Lipocalin-2 Promotes Pancreatic Ductal Adenocarcinoma by Regulating Inflammation in the Tumor Microenvironment”, *Cancer research*, Vol. 77 No. 10, pp. 2647–2660.

Gómez-Gaviro, M., Domínguez-Luis, M., Canchado, J., Calafat, J., Janssen, H., Lara-Pezzi, E., Fourie, A., Tugores, A., Valenzuela-Fernández, A., Mollinedo, F., Sánchez-Madrid, F. and Díaz-González, F. (2007), “Expression and regulation of the metalloproteinase ADAM-8 during human neutrophil pathophysiological activation and its catalytic activity on L-selectin shedding”, *Journal of immunology (Baltimore, Md. 1950)*, Vol. 178 No. 12, pp. 8053–8063.

Gordon, S. and Taylor, P.R. (2005), “Monocyte and macrophage heterogeneity”, *Nature reviews. Immunology*, Vol. 5 No. 12, pp. 953–964.

Griesmann, H., Drexel, C., Milosevic, N., Sipos, B., Rosendahl, J., Gress, T.M. and Michl, P. (2017), “Pharmacological macrophage inhibition decreases metastasis formation in a genetic model of pancreatic cancer”, *Gut*, Vol. 66 No. 7, pp. 1278–1285.

Groth, E., Pruessmeyer, J., Babendreyer, A., Schumacher, J., Pasqualon, T., Dreymueller, D., Higashiyama, S., Lorenzen, I., Grötzinger, J., Cataldo, D. and Ludwig, A. (2016), “Stimulated release and functional activity of surface expressed metalloproteinase ADAM17 in exosomes”, *Biochimica et biophysica acta*, Vol. 1863 No. 11, pp. 2795–2808.

Guaiquil, V.H., Swendeman, S., Zhou, W., Guaiquil, P., Weskamp, G., Bartsch, J.W. and Blobel, C.P. (2010), “ADAM8 is a negative regulator of retinal neovascularization and of the growth of heterotopically injected tumor cells in mice”, *Journal of molecular medicine (Berlin, Germany)*, Vol. 88 No. 5, pp. 497–505.

Gumpper, K., Dangel, A.W., Pita-Grisanti, V., Krishna, S.G., Lara, L.F., Mace, T., Papachristou, G.I., Conwell, D.L., Hart, P.A. and Cruz-Monserrate, Z. (2020), “Lipocalin-2 expression and function in pancreatic diseases”, *Pancreatology official*

journal of the International Association of Pancreatology (IAP) … [et al.], Vol. 20 No. 3, pp. 419–424.

Guo, R., Gu, J., Zhang, Z., Wang, Y. and Gu, C. (2017), “MiR-451 Promotes Cell Proliferation and Metastasis in Pancreatic Cancer through Targeting CAB39”, *BioMed research international*, Vol. 2017, p. 2381482.

Hagemann, C., Anacker, J., Ernestus, R.-I. and Vince, G.H. (2012), “A complete compilation of matrix metalloproteinase expression in human malignant gliomas”, *World journal of clinical oncology*, Vol. 3 No. 5, pp. 67–79.

Hakulinen, J., Sankkila, L., Sugiyama, N., Lehti, K. and Keski-Oja, J. (2008), “Secretion of active membrane type 1 matrix metalloproteinase (MMP-14) into extracellular space in microvesicular exosomes”, *Journal of cellular biochemistry*, Vol. 105 No. 5, pp. 1211–1218.

Hall, T., Leone, J.W., Wiese, J.F., Griggs, D.W., Pegg, L.E., Pauley, A.M., Tomasselli, A.G. and Zack, M.D. (2009), “Autoactivation of human ADAM8: a novel pre-processing step is required for catalytic activity”, *Bioscience reports*, Vol. 29 No. 4, pp. 217–228.

Harrison, N., Koo, C.Z. and Tomlinson, M.G. (2021), “Regulation of ADAM10 by the TspanC8 Family of Tetraspanins and Their Therapeutic Potential”, *International journal of molecular sciences*, Vol. 22 No. 13.

Hawari, F.I., Rouhani, F.N., Cui, X., Yu, Z.-X., Buckley, C., Kaler, M. and Levine, S.J. (2004), “Release of full-length 55-kDa TNF receptor 1 in exosome-like vesicles: a mechanism for generation of soluble cytokine receptors”, *Proceedings of the National Academy of Sciences of the United States of America*, Vol. 101 No. 5, pp. 1297–1302.

Hayes, T.K., Neel, N.F., Hu, C., Gautam, P., Chenard, M., Long, B., Aziz, M., Kassner, M., Bryant, K.L., Pierobon, M., Marayati, R., Kher, S., George, S.D., Xu, M., Wang-Gillam, A., Samatar, A.A., Maitra, A., Wennerberg, K., Petricoin, E.F., Yin, H.H., Nelkin, B., Cox, A.D., Yeh, J.J. and Der, C.J. (2016), “Long-Term ERK Inhibition in KRAS-Mutant Pancreatic Cancer Is Associated with MYC Degradation and Senescence-like Growth Suppression”, *Cancer cell*, Vol. 29 No. 1, pp. 75–89.

He, S., Ding, L., Cao, Y., Li, G., Deng, J., Tu, Y. and Wang, B. (2012), “Overexpression of a disintegrin and metalloprotease 8 in human gliomas is implicated in tumor progression and prognosis”, *Medical oncology (Northwood, London, England)*, Vol. 29 No. 3, pp. 2032–2037.

Hernández, I., Moreno, J.L., Zandueta, C., Montuenga, L. and Lecanda, F. (2010), “Novel alternatively spliced ADAM8 isoforms contribute to the aggressive bone metastatic phenotype of lung cancer”, *Oncogene*, Vol. 29 No. 26, pp. 3758–3769.

Hessmann, E., Buchholz, S.M., Demir, I.E., Singh, S.K., Gress, T.M., Ellenrieder, V. and Neesse, A. (2020), “Microenvironmental Determinants of Pancreatic Cancer”, *Physiological reviews*, Vol. 100 No. 4, pp. 1707–1751.

Hezel, A.F., Kimmelman, A.C., Stanger, B.Z., Bardeesy, N. and Depinho, R.A. (2006), “Genetics and biology of pancreatic ductal adenocarcinoma”, *Genes & development*, Vol. 20 No. 10, pp. 1218–1249.

Hodgkinson, C.P. and Ye, S. (2003), “Microarray analysis of peroxisome proliferator-activated receptor-γ induced changes in gene expression in macrophages”, *Biochemical and Biophysical Research Communications*, Vol. 308 No. 3, pp. 505–510.

Hoff, D.D. von, Ervin, T., Arena, F.P., Chiorean, E.G., Infante, J., Moore, M., Seay, T., Tjulandin, S.A., Ma, W.W., Saleh, M.N., Harris, M., Reni, M., Dowden, S., Laheru, D., Bahary, N., Ramanathan, R.K., Tabernero, J., Hidalgo, M., Goldstein, D., van Cutsem, E., Wei, X., Iglesias, J. and Renschler, M.F. (2013), “Increased survival in pancreatic cancer with nab-paclitaxel plus gemcitabine”, *The New England journal of medicine*, Vol. 369 No. 18, pp. 1691–1703.

Howard, L., Maciewicz, R.A. and Blobel, C.P. (2000), “Cloning and characterization of ADAM28: evidence for autocatalytic pro-domain removal and for cell surface localization of mature ADAM28”, *Biochemical Journal*, 348 Pt 1 No. Pt 1, pp. 21–27.

Hruban, R.H., van Mansfeld, A.D., Offerhaus, G.J., van Weering, D.H., Allison, D.C., Goodman, S.N., Kensler, T.W., Bose, K.K., Cameron, J.L. and Bos, J.L. (1993), “K-ras oncogene activation in adenocarcinoma of the human pancreas. A study of 82 carcinomas using a combination of mutant-enriched polymerase chain reaction analysis and allele-specific oligonucleotide hybridization”, *The American Journal of Pathology*, Vol. 143 No. 2, pp. 545–554.

Hruban, R.H., Wilentz, R.E. and Kern, S.E. (2000), “Genetic Progression in the Pancreatic Ducts”, *The American Journal of Pathology*, Vol. 156 No. 6, pp. 1821–1825.

Huang, H. (2018), “Matrix Metalloproteinase-9 (MMP-9) as a Cancer Biomarker and MMP-9 Biosensors: Recent Advances”, *Sensors (Basel, Switzerland)*, Vol. 18 No. 10.

Huber, M., Brehm, C.U., Gress, T.M., Buchholz, M., Alashkar Alhamwe, B., Strandmann, E.P. von, Slater, E.P., Bartsch, J.W., Bauer, C. and Lauth, M. (2020), “The Immune Microenvironment in Pancreatic Cancer”, *International journal of molecular sciences*, Vol. 21 No. 19.

Ino, Y., Yamazaki-Itoh, R., Shimada, K., Iwasaki, M., Kosuge, T., Kanai, Y. and Hiraoka, N. (2013), “Immune cell infiltration as an indicator of the immune microenvironment of pancreatic cancer”, *British journal of cancer*, Vol. 108 No. 4, pp. 914–923.

International, B.R. (2021), “Retracted: MiR-451 Promotes Cell Proliferation and Metastasis in Pancreatic Cancer through Targeting CAB39”, *BioMed research international*, Vol. 2021, p. 3702061.

Ishikawa, N., Daigo, Y., Yasui, W., Inai, K., Nishimura, H., Tsuchiya, E., Kohno, N. and Nakamura, Y. (2004), “ADAM8 as a novel serological and histochemical marker for lung cancer”, *Clinical cancer research an official journal of the American Association for Cancer Research*, Vol. 10 No. 24, pp. 8363–8370.

Iwai, N., Okuda, T., Sakagami, J., Harada, T., Ohara, T., Taniguchi, M., Sakai, H., Oka, K., Hara, T., Tsuji, T., Komaki, T., Kagawa, K., Yasuda, H., Naito, Y. and Itoh, Y. (2020), “Neutrophil to lymphocyte ratio predicts prognosis in unresectable pancreatic cancer”, *Scientific reports*, Vol. 10 No. 1, p. 18758.

Jaworek, C., Verel-Yilmaz, Y., Driesch, S., Ostgathe, S., Cook, L., Wagner, S., Bartsch, D.K., Slater, E.P. and Bartsch, J.W. (2021), “Cohort Analysis of ADAM8 Expression in the PDAC Tumor Stroma”, *Journal of personalized medicine*, Vol. 11 No. 2.

Jung, M., Weigert, A., Tausendschön, M., Mora, J., Ören, B., Sola, A., Hotter, G., Muta, T. and Brüne, B. (2012), “Interleukin-10-induced neutrophil gelatinase-associated lipocalin production in macrophages with consequences for tumor growth”, *Molecular and cellular biology*, Vol. 32 No. 19, pp. 3938–3948.

Kelly, K., Hutchinson, G., Nebenius-Oosthuizen, D., Smith, A.J.H., Bartsch, J.W., Horiuchi, K., Rittger, A., Manova, K., Docherty, A.J.P. and Blobel, C.P. (2005), “Metalloprotease-disintegrin ADAM8: expression analysis and targeted deletion in mice”, *Developmental dynamics an official publication of the American Association of Anatomists*, Vol. 232 No. 1, pp. 221–231.

Kim, S., Park, B.K., Seo, J.H., Choi, J., Choi, J.W., Lee, C.K., Chung, J.B., Park, Y. and Kim, D.W. (2020), “Carbohydrate antigen 19-9 elevation without evidence of malignant or pancreatobiliary diseases”, *Scientific reports*, Vol. 10 No. 1, p. 8820.

King, N.E., Zimmermann, N., Pope, S.M., Fulkerson, P.C., Nikolaidis, N.M., Mishra, A., Witte, D.P. and Rothenberg, M.E. (2004), “Expression and regulation of a disintegrin and metalloproteinase (ADAM) 8 in experimental asthma”, *American journal of respiratory cell and molecular biology*, Vol. 31 No. 3, pp. 257–265.

Kleino, I., Järviluoma, A., Hepojoki, J., Huovila, A.P. and Saksela, K. (2015), “Preferred SH3 domain partners of ADAM metalloproteases include shared and ADAM-specific SH3 interactions”, *PloS one*, Vol. 10 No. 3, e0121301.

Knolle, M.D., Nakajima, T., Hergrueter, A., Gupta, K., Polverino, F., Craig, V.J., Fyfe, S.E., Zahid, M., Permaul, P., Cernadas, M., Montano, G., Tesfaigzi, Y., Sholl, L., Kobzik, L., Israel, E. and Owen, C.A. (2013), “Adam8 limits the development of allergic airway inflammation in mice”, *Journal of immunology (Baltimore, Md. 1950)*, Vol. 190 No. 12, pp. 6434–6449.

Knudsen, E.S., Vail, P., Balaji, U., Ngo, H., Botros, I.W., Makarov, V., Riaz, N., Balachandran, V., Leach, S., Thompson, D.M., Chan, T.A. and Witkiewicz, A.K. (2017), “Stratification of Pancreatic Ductal Adenocarcinoma: Combinatorial Genetic, Stromal, and Immunologic Markers”, *Clinical cancer research an official journal of the American Association for Cancer Research*, Vol. 23 No. 15, pp. 4429–4440.

Kurahara, H., Shinchi, H., Mataki, Y., Maemura, K., Noma, H., Kubo, F., Sakoda, M., Ueno, S., Natsugoe, S. and Takao, S. (2011), “Significance of M2-polarized tumor-associated macrophage in pancreatic cancer”, *The Journal of surgical research*, Vol. 167 No. 2, e211-9.

Larsen, M.T., Häger, M., Glenthøj, A., Asmar, F., Clemmensen, S.N., Mora-Jensen, H., Borregaard, N. and Cowland, J.B. (2014), “miRNA-130a regulates C/EBP-ε expression during granulopoiesis”, *Blood*, Vol. 123 No. 7, pp. 1079–1089.

Lee, H.D., Koo, B.-H., Kim, Y.H., Jeon, O.-H. and Kim, D.-S. (2012), “Exosome release of ADAM15 and the functional implications of human macrophage-derived ADAM15 exosomes”, *FASEB journal official publication of the Federation of American Societies for Experimental Biology*, Vol. 26 No. 7, pp. 3084–3095.

Lee, H.S., Moon, C., Lee, H.W., Park, E.-M., Cho, M.-S. and Kang, J.L. (2007), “Src tyrosine kinases mediate activations of NF-kappaB and integrin signal during lipopolysaccharide-induced acute lung injury”, *Journal of immunology (Baltimore, Md. 1950)*, Vol. 179 No. 10, pp. 7001–7011.

Lemberger, M., Loewenstein, S., Lubezky, N., Nizri, E., Pasmanik-Chor, M., Barazovsky, E., Klausner, J.M. and Lahat, G. (2019), “MicroRNA profiling of pancreatic ductal adenocarcinoma (PDAC) reveals signature expression related to lymph node metastasis”, *Oncotarget*, Vol. 10 No. 27, pp. 2644–2656.

Leung, L., Radulovich, N., Zhu, C.-Q., Organ, S., Bandarchi, B., Pintilie, M., To, C., Panchal, D. and Tsao, M.S. (2012), “Lipocalin2 promotes invasion, tumorigenicity and gemcitabine resistance in pancreatic ductal adenocarcinoma”, *PloS one*, Vol. 7 No. 10, e46677.

Li, Y., Guo, S., Zhao, K., Conrad, C., Driescher, C., Rothbart, V., Schlomann, U., Guerreiro, H., Bopp, M.H., König, A., Carl, B., Pagenstecher, A., Nimsky, C. and Bartsch, J.W. (2021), “ADAM8 affects glioblastoma progression by regulating

osteopontin-mediated angiogenesis", *Biological chemistry*, Vol. 402 No. 2, pp. 195–206.

Li, Z., Liao, Q., Wu, Y., Liao, M., Hao, Y., Zhang, S., Song, S., Li, B. and Zhang, Y. (2012), "Upregulation of a disintegrin and metalloprotease 8 influences tumor metastasis and prognosis in patients with osteosarcoma", *Pathology oncology research POR*, Vol. 18 No. 3, pp. 657–661.

Liu, Y., Li, Z.-H., Zhang, L. and Lu, S.-B. (2019), "ADAM8 promotes chondrosarcoma cell migration and invasion by activating the NF-κB/MMP-13 signaling axis", *Anti-cancer drugs*, Vol. 30 No. 7, e0790.

Mahoney, E.T., Benton, R.L., Maddie, M.A., Whittemore, S.R. and Hagg, T. (2009), "ADAM8 is selectively up-regulated in endothelial cells and is associated with angiogenesis after spinal cord injury in adult mice", *The Journal of comparative neurology*, Vol. 512 No. 2, pp. 243–255.

Maia, J., Caja, S., Strano Moraes, M.C., Couto, N. and Costa-Silva, B. (2018), "Exosome-Based Cell-Cell Communication in the Tumor Microenvironment", *Frontiers in cell and developmental biology*, Vol. 6, p. 18.

Mathews, J.A., Gibb, D.R., Chen, B.-H., Scherle, P. and Conrad, D.H. (2010), "CD23 Sheddase A disintegrin and metalloproteinase 10 (ADAM10) is also required for CD23 sorting into B cell-derived exosomes", *The Journal of biological chemistry*, Vol. 285 No. 48, pp. 37531–37541.

Matsuo, Y., Ochi, N., Sawai, H., Yasuda, A., Takahashi, H., Funahashi, H., Takeyama, H., Tong, Z. and Guha, S. (2009), "CXCL8/IL-8 and CXCL12/SDF-1alpha co-operatively promote invasiveness and angiogenesis in pancreatic cancer", *International Journal of Cancer*, Vol. 124 No. 4, pp. 853–861.

Mehner, C., Hockla, A., Miller, E., Ran, S., Radisky, D.C. and Radisky, E.S. (2014), "Tumor cell-produced matrix metalloproteinase 9 (MMP-9) drives malignant progression and metastasis of basal-like triple negative breast cancer", *Oncotarget*, Vol. 5 No. 9, pp. 2736–2749.

Miller, M.A., Barkal, L., Jeng, K., Herrlich, A., Moss, M., Griffith, L.G. and Lauffenburger, D.A. (2011), "Proteolytic Activity Matrix Analysis (PrAMA) for simultaneous determination of multiple protease activities", *Integrative biology quantitative biosciences from nano to macro*, Vol. 3 No. 4, pp. 422–438.

Miquel, M., Zhang, S. and Pilarsky, C. (2021), "Pre-clinical Models of Metastasis in Pancreatic Cancer", *Frontiers in cell and developmental biology*, Vol. 9, p. 748631.

Mir, B. and Goettsch, C. (2020), "Extracellular Vesicles as Delivery Vehicles of Specific Cellular Cargo", *Cells*, Vol. 9 No. 7.

Mosser, D.M. and Edwards, J.P. (2008), “Exploring the full spectrum of macrophage activation”, *Nature reviews. Immunology*, Vol. 8 No. 12, pp. 958–969.

Nabhan, J.F., Hu, R., Oh, R.S., Cohen, S.N. and Lu, Q. (2012), “Formation and release of arrestin domain-containing protein 1-mediated microvesicles (ARMMs) at plasma membrane by recruitment of TSG101 protein”, *Proceedings of the National Academy of Sciences of the United States of America*, Vol. 109 No. 11, pp. 4146–4151.

Naso, J.R., Topham, J.T., Karasinska, J.M., Lee, M.K.C., Kalloger, S.E., Wong, H.-L., Nelson, J., Moore, R.A., Mungall, A.J., Jones, S.J.M., Laskin, J., Marra, M.A., Renouf, D.J. and Schaeffer, D.F. (2021), “Tumor infiltrating neutrophils and gland formation predict overall survival and molecular subgroups in pancreatic ductal adenocarcinoma”, *Cancer medicine*, Vol. 10 No. 3, pp. 1155–1165.

Naus, S., Blanchet, M.-R., Gossens, K., Zaph, C., Bartsch, J.W., McNagny, K.M. and Ziltener, H.J. (2010), “The metalloprotease-disintegrin ADAM8 is essential for the development of experimental asthma”, *American journal of respiratory and critical care medicine*, Vol. 181 No. 12, pp. 1318–1328.

Naus, S., Reipschläger, S., Wildeboer, D., Lichtenthaler, S.F., Mitterreiter, S., Guan, Z., Moss, M.L. and Bartsch, J.W. (2006), “Identification of candidate substrates for ectodomain shedding by the metalloprotease-disintegrin ADAM8”, *Biological chemistry*, Vol. 387 No. 3, pp. 337–346.

Neesse, A., Algül, H., Tuveson, D.A. and Gress, T.M. (2015), “Stromal biology and therapy in pancreatic cancer: a changing paradigm”, *Gut*, Vol. 64 No. 9, pp. 1476–1484.

Nishimura, D., Sakai, H., Sato, T., Sato, F., Nishimura, S., Toyama-Sorimachi, N., Bartsch, J.W. and Sehara-Fujisawa, A. (2015), “Roles of ADAM8 in elimination of injured muscle fibers prior to skeletal muscle regeneration”, *Mechanisms of development*, Vol. 135, pp. 58–67.

Nywening, T.M., Belt, B.A., Cullinan, D.R., Panni, R.Z., Han, B.J., Sanford, D.E., Jacobs, R.C., Ye, J., Patel, A.A., Gillanders, W.E., Fields, R.C., DeNardo, D.G., Hawkins, W.G., Goedegebuure, P. and Linehan, D.C. (2018), “Targeting both tumour-associated CXCR2+ neutrophils and CCR2+ macrophages disrupts myeloid recruitment and improves chemotherapeutic responses in pancreatic ductal adenocarcinoma”, *Gut*, Vol. 67 No. 6, pp. 1112–1123.

Orth, M., Metzger, P., Gerum, S., Mayerle, J., Schneider, G., Belka, C., Schnurr, M. and Lauber, K. (2019), “Pancreatic ductal adenocarcinoma: biological hallmarks, current status, and future perspectives of combined modality treatment approaches”, *Radiation oncology (London, England)*, Vol. 14 No. 1, p. 141.

Osaki, M. and Okada, F. (2019), “Exosomes and Their Role in Cancer Progression”, *Yonago acta medica*, Vol. 62 No. 2, pp. 182–190.

Park (2009), “ICAM-3 enhances the migratory and invasive potential of human non-small cell lung cancer cells by inducing MMP-2 and MMP-9 via Akt and CREB”, *International Journal of Oncology*, Vol. 36 No. 01.

Peng, Y. and Croce, C.M. (2016), “The role of MicroRNAs in human cancer”, *Signal transduction and targeted therapy*, Vol. 1, p. 15004.

Piciucchi, M., Stigliano, S., Archibugi, L., Zerboni, G., Signoretti, M., Barucca, V., Valente, R., Fave, G.D. and Capurso, G. (2017), “The Neutrophil/Lymphocyte Ratio at Diagnosis Is Significantly Associated with Survival in Metastatic Pancreatic Cancer Patients”, *International journal of molecular sciences*, Vol. 18 No. 4.

Polverino, F., Rojas-Quintero, J., Wang, X., Petersen, H., Zhang, L., Gai, X., Higham, A., Zhang, D., Gupta, K., Rout, A., Yambayev, I., Pinto-Plata, V., Sholl, L.M., Cunoosamy, D., Celli, B.R., Goldring, J., Singh, D., Tesfaigzi, Y., Wedzicha, J., Olsson, H. and Owen, C.A. (2018), “A Disintegrin and Metalloproteinase Domain-8: A Novel Protective Proteinase in Chronic Obstructive Pulmonary Disease”, *American journal of respiratory and critical care medicine*, Vol. 198 No. 10, pp. 1254–1267.

Principe, D.R., Diaz, A.M., Torres, C., Mangan, R.J., DeCant, B., McKinney, R., Tsao, M.-S., Lowy, A., Munshi, H.G., Jung, B. and Grippo, P.J. (2017), “TGFβ engages MEK/ERK to differentially regulate benign and malignant pancreas cell function”, *Oncogene*, Vol. 36 No. 30, pp. 4336–4348.

Puolakkainen, P., Koski, A., Vainionpää, S., Shen, Z., Repo, H., Kemppainen, E., Mustonen, H. and Seppänen, H. (2014), “Anti-inflammatory macrophages activate invasion in pancreatic adenocarcinoma by increasing the MMP9 and ADAM8 expression”, *Medical oncology (Northwood, London, England)*, Vol. 31 No. 3, p. 884.

Redston, M.S., Caldas, C., Seymour, A.B., Hruban, R.H., da Costa, L., Yeo, C.J. and Kern, S.E. (1994), “p53 mutations in pancreatic carcinoma and evidence of common involvement of homocopolymer tracts in DNA microdeletions”, *Cancer research*, Vol. 54 No. 11, pp. 3025–3033.

Robbins, P.D. and Morelli, A.E. (2014), “Regulation of immune responses by extracellular vesicles”, *Nature reviews. Immunology*, Vol. 14 No. 3, pp. 195–208.

Romagnoli, M., Mineva, N.D., Polmear, M., Conrad, C., Srinivasan, S., Loussouarn, D., Barillé-Nion, S., Georgakoudi, I., Dagg, Á., McDermott, E.W., Duffy, M.J., McGowan, P.M., Schlomann, U., Parsons, M., Bartsch, J.W. and Sonenshein, G.E. (2014), “ADAM8 expression in invasive breast cancer promotes tumor dissemination and metastasis”, *EMBO molecular medicine*, Vol. 6 No. 2, pp. 278–294.

Sanderson, R.D., Bandari, S.K. and Vlodavsky, I. (2019), “Proteases and glycosidases on the surface of exosomes: Newly discovered mechanisms for extracellular remodeling”, *Matrix biology journal of the International Society for Matrix Biology*, 75-76, pp. 160–169.

Santoni, M., Bracarda, S., Nabissi, M., Massari, F., Conti, A., Bria, E., Tortora, G., Santoni, G. and Cascinu, S. (2014), “CXC and CC chemokines as angiogenic modulators in nonhaematological tumors”, *BioMed research international*, Vol. 2014, p. 768758.

Scharfenberg, F., Helbig, A., Sammel, M., Benzel, J., Schlomann, U., Peters, F., Wichert, R., Bettendorff, M., Schmidt-Arras, D., Rose-John, S., Moali, C., Lichtenthaler, S.F., Pietrzik, C.U., Bartsch, J.W., Tholey, A. and Becker-Pauly, C. (2020), “Degradome of soluble ADAM10 and ADAM17 metalloproteases”, *Cellular and molecular life sciences CMLS*, Vol. 77 No. 2, pp. 331–350.

Schlomann, U., Koller, G., Conrad, C., Ferdous, T., Golfi, P., Garcia, A.M., Höfling, S., Parsons, M., Costa, P., Soper, R., Bossard, M., Hagemann, T., Roshani, R., Sewald, N., Ketchem, R.R., Moss, M.L., Rasmussen, F.H., Miller, M.A., Lauffenburger, D.A., Tuveson, D.A., Nimsky, C. and Bartsch, J.W. (2015), “ADAM8 as a drug target in pancreatic cancer”, *Nature communications*, Vol. 6, p. 6175.

Schlomann, U., Rathke-Hartlieb, S., Yamamoto, S., Jockusch, H. and Bartsch, J.W. (2000), “Tumor Necrosis Factor α Induces a Metalloprotease-Disintegrin, ADAM8 (CD 156): Implications for Neuron–Glia Interactions during Neurodegeneration”, *The Journal of Neuroscience*, Vol. 20 No. 21, pp. 7964–7971.

Schlomann, U., Wildeboer, D., Webster, A., Antropova, O., Zeuschner, D., Knight, C.G., Docherty, A.J.P., Lambert, M., Skelton, L., Jockusch, H. and Bartsch, J.W. (2002), “The metalloprotease disintegrin ADAM8. Processing by autocatalysis is required for proteolytic activity and cell adhesion”, *The Journal of biological chemistry*, Vol. 277 No. 50, pp. 48210–48219.

Shi, L., Cheng, Z., Zhang, J., Li, R., Zhao, P., Fu, Z. and You, Y. (2008), “hsa-mir-181a and hsa-mir-181b function as tumor suppressors in human glioma cells”, *Brain research*, Vol. 1236, pp. 185–193.

Shimoda, M. and Khokha, R. (2017), “Metalloproteinases in extracellular vesicles”, *Biochimica et biophysica acta. Molecular cell research*, Vol. 1864 No. 11 Pt A, pp. 1989–2000.

Siegel, R.L., Miller, K.D., Fuchs, H.E. and Jemal, A. (2021), “Cancer Statistics, 2021”, *CA: a cancer journal for clinicians*, Vol. 71 No. 1, pp. 7–33.

Soung, Y.H., Ford, S., Zhang, V. and Chung, J. (2017), “Exosomes in Cancer Diagnostics”, *Cancers*, Vol. 9 No. 1.

Stoeck, A., Keller, S., Riedle, S., Sanderson, M.P., Runz, S., Le Naour, F., Gutwein, P., Ludwig, A., Rubinstein, E. and Altevogt, P. (2006), “A role for exosomes in the constitutive and stimulus-induced ectodomain cleavage of L1 and CD44”, *Biochemical Journal*, Vol. 393 No. Pt 3, pp. 609–618.

Stotz, M., Gerger, A., Eisner, F., Szkandera, J., Loibner, H., Ress, A.L., Kornprat, P., AlZoughbi, W., Zoughbi, W.A., Seggewies, F.S., Lackner, C., Stojakovic, T., Samonigg, H., Hoefler, G. and Pichler, M. (2013), “Increased neutrophil-lymphocyte ratio is a poor prognostic factor in patients with primary operable and inoperable pancreatic cancer”, *British journal of cancer*, Vol. 109 No. 2, pp. 416–421.

Sumrin, A., Moazzam, S., Khan, A.A., Ramzan, I., Batool, Z., Kaleem, S., Ali, M., Bashir, H. and Bilal, M. (2018), “Exosomes as Biomarker of Cancer”, *Brazilian Archives of Biology and Technology*, Vol. 61 No. 0.

Tan, S.S., Yin, Y., Lee, T., Lai, R.C., Yeo, R.W.Y., Zhang, B., Choo, A. and Lim, S.K. (2013), “Therapeutic MSC exosomes are derived from lipid raft microdomains in the plasma membrane”, *Journal of extracellular vesicles*, Vol. 2.

Tekin, C., Aberson, H.L., Waasdorp, C., Hooijer, G.K.J., Boer, O.J. de, Dijk, F., Bijlsma, M.F. and Spek, C.A. (2020), “Macrophage-secreted MMP9 induces mesenchymal transition in pancreatic cancer cells via PAR1 activation”, *Cellular oncology (Dordrecht)*, Vol. 43 No. 6, pp. 1161–1174.

Tellier, E., Canault, M., Rebsomen, L., Bonardo, B., Juhan-Vague, I., Nalbone, G. and Peiretti, F. (2006), “The shedding activity of ADAM17 is sequestered in lipid rafts”, *Experimental cell research*, Vol. 312 No. 20, pp. 3969–3980.

Théry, C., Witwer, K.W., Aikawa, E., Alcaraz, M.J., Anderson, J.D., Andriantsitohaina, R., Antoniou, A., Arab, T., Archer, F., Atkin-Smith, G.K., Ayre, D.C., Bach, J.-M., Bachurski, D., Baharvand, H., Balaj, L., Baldacchino, S., Bauer, N.N., Baxter, A.A., Bebawy, M., Beckham, C., Bedina Zavec, A., Benmoussa, A., Berardi, A.C., Bergese, P., Bielska, E., Blenkiron, C., Bobis-Wozowicz, S., Boilard, E., Boireau, W., Bongiovanni, A., Borràs, F.E., Bosch, S., Boulanger, C.M., Breakefield, X., Breglio, A.M., Brennan, M.Á., Brigstock, D.R., Brisson, A., Broekman, M.L., Bromberg, J.F., Bryl-Górecka, P., Buch, S., Buck, A.H., Burger, D., Busatto, S., Buschmann, D., Bussolati, B., Buzás, E.I., Byrd, J.B., Camussi, G., Carter, D.R., Caruso, S., Chamley, L.W., Chang, Y.-T., Chen, C., Chen, S., Cheng, L., Chin, A.R., Clayton, A., Clerici, S.P., Cocks, A., Cocucci, E., Coffey, R.J., Cordeiro-da-Silva, A., Couch, Y., Coumans, F.A., Coyle, B., Crescitelli, R., Criado, M.F., D'Souza-Schorey, C., Das, S., Datta Chaudhuri, A., Candia, P. de, Santana, E.F. de, Wever, O. de, Del Portillo, H.A., Demaret, T., Deville, S., Devitt, A., Dhondt, B., Di Vizio, D., Dieterich, L.C., Dolo, V., Dominguez Rubio, A.P., Dominici, M., Dourado, M.R., Driedonks, T.A., Duarte,

F.V., Duncan, H.M., Eichenberger, R.M., Ekström, K., El Andaloussi, S., Elie-Caille, C., Erdbrügger, U., Falcón-Pérez, J.M., Fatima, F., Fish, J.E., Flores-Bellver, M., Försönits, A., Frelet-Barrand, A., Fricke, F., Fuhrmann, G., Gabrielsson, S., Gámez-Valero, A., Gardiner, C., Gärtner, K., Gaudin, R., Gho, Y.S., Giebel, B., Gilbert, C., Gimona, M., Giusti, I., Goberdhan, D.C., Görgens, A., Gorski, S.M., Greening, D.W., Gross, J.C., Gualerzi, A., Gupta, G.N., Gustafson, D., Handberg, A., Haraszti, R.A., Harrison, P., Hegyesi, H., an Hendrix, Hill, A.F., Hochberg, F.H., Hoffmann, K.F., Holder, B., Holthofer, H., Hosseinkhani, B., Hu, G., Huang, Y., Huber, V., Hunt, S., Ibrahim, A.G.-E., Ikezu, T., Inal, J.M., Isin, M., Ivanova, A., Jackson, H.K., Jacobsen, S., Jay, S.M., Jayachandran, M., Jenster, G., Jiang, L., Johnson, S.M., Jones, J.C., Jong, A., Jovanovic-Talisman, T., Jung, S., Kalluri, R., Kano, S.-I., Kaur, S., Kawamura, Y., Keller, E.T., Khamari, D., Khomyakova, E., Khvorova, A., Kierulf, P., Kim, K.P., Kislinger, T., Klingeborn, M., Klinke, D.J., Kornek, M., Kosanović, M.M., Kovács, Á.F., Krämer-Albers, E.-M., Krasemann, S., Krause, M., Kurochkin, I.V., Kusuma, G.D., Kuypers, S., Laitinen, S., Langevin, S.M., Languino, L.R., Lannigan, J., Lässer, C., Laurent, L.C., Lavieu, G., Lázaro-Ibáñez, E., Le Lay, S., Lee, M.-S., Lee, Y.X.F., Lemos, D.S., Lenassi, M., Leszczynska, A., Li, I.T., Liao, K., Libregts, S.F., Ligeti, E., Lim, R., Lim, S.K., Linē, A., Linnemannstöns, K., Llorente, A., Lombard, C.A., Lorenowicz, M.J., Lörincz, Á.M., Lötvall, J., Lovett, J., Lowry, M.C., Loyer, X., Lu, Q., Lukomska, B., Lunavat, T.R., Maas, S.L., Malhi, H., Marcilla, A., Mariani, J., Mariscal, J., Martens-Uzunova, E.S., Martin-Jaular, L., Martinez, M.C., Martins, V.R., Mathieu, M., Mathivanan, S., Maugeri, M., McGinnis, L.K., McVey, M.J., Meckes, D.G., Meehan, K.L., Mertens, I., Minciacchi, V.R., Möller, A., Møller Jørgensen, M., Morales-Kastresana, A., Morhayim, J., Mullier, F., Muraca, M., Musante, L., Mussack, V., Muth, D.C., Myburgh, K.H., Najrana, T., Nawaz, M., Nazarenko, I., Nejsum, P., Neri, C., Neri, T., Nieuwland, R., Nimrichter, L., Nolan, J.P., Nolte-'t Hoen, E.N., Noren Hooten, N., O'Driscoll, L., O'Grady, T., O'Loghlen, A., Ochiya, T., Olivier, M., Ortiz, A., Ortiz, L.A., Osteikoetxea, X., Østergaard, O., Ostrowski, M., Park, J., Pegtel, D.M., Peinado, H., Perut, F., Pfaffl, M.W., Phinney, D.G., Pieters, B.C., Pink, R.C., Pisetsky, D.S., Pogge von Strandmann, E., Polakovicova, I., Poon, I.K., Powell, B.H., Prada, I., Pulliam, L., Quesenberry, P., Radeghieri, A., Raffai, R.L., Raimondo, S., Rak, J., Ramirez, M.I., Raposo, G., Rayyan, M.S., Regev-Rudzki, N., Ricklefs, F.L., Robbins, P.D., Roberts, D.D., Rodrigues, S.C., Rohde, E., Rome, S., Rouschop, K.M., Rughetti, A., Russell, A.E., Saá, P., Sahoo, S., Salas-Huenuleo, E., Sánchez, C., Saugstad, J.A., Saul, M.J., Schiffelers, R.M., Schneider, R., Schøyen, T.H., Scott, A., Shahaj, E., Sharma, S., Shatnyeva, O., Shekari, F., Shelke, G.V., Shetty, A.K., Shiba, K., Siljander, P.R.-M.,

Silva, A.M., Skowronek, A., Snyder, O.L., Soares, R.P., Sódar, B.W., Soekmadji, C., Sotillo, J., Stahl, P.D., Stoorvogel, W., Stott, S.L., Strasser, E.F., Swift, S., Tahara, H., Tewari, M., Timms, K., Tiwari, S., Tixeira, R., Tkach, M., Toh, W.S., Tomasini, R., Torrecilhas, A.C., Tosar, J.P., Toxavidis, V., Urbanelli, L., Vader, P., van Balkom, B.W., van der Grein, S.G., van Deun, J., van Herwijnen, M.J., van Keuren-Jensen, K., van Niel, G., van Royen, M.E., van Wijnen, A.J., Vasconcelos, M.H., Vechetti, I.J., Veit, T.D., Vella, L.J., Velot, É., Verweij, F.J., Vestad, B., Viñas, J.L., Visnovitz, T., Vukman, K.V., Wahlgren, J., Watson, D.C., Wauben, M.H., Weaver, A., Webber, J.P., Weber, V., Wehman, A.M., Weiss, D.J., Welsh, J.A., Wendt, S., Wheelock, A.M., Wiener, Z., Witte, L., Wolfram, J., Xagorari, A., Xander, P., Xu, J., Yan, X., Yáñez-Mó, M., Yin, H., Yuana, Y., Zappulli, V., Zarubova, J., Žėkas, V., Zhang, J.-Y., Zhao, Z., Zheng, L., Zheutlin, A.R., Zickler, A.M., Zimmermann, P., Zivkovic, A.M., Zocco, D. and Zuba-Surma, E.K. (2018), “Minimal information for studies of extracellular vesicles 2018 (MISEV2018): a position statement of the International Society for Extracellular Vesicles and update of the MISEV2014 guidelines”, *Journal of extracellular vesicles*, Vol. 7 No. 1, p. 1535750.

Tschesche, H., Zölzer, V., Triebel, S. and Bartsch, S. (2001), “The human neutrophil lipocalin supports the allosteric activation of matrix metalloproteinases”, *European journal of biochemistry*, Vol. 268 No. 7, pp. 1918–1928.

Valkovskaya, N., Kayed, H., Felix, K., Hartmann, D., Giese, N.A., Osinsky, S.P., Friess, H. and Kleeff, J. (2007), “ADAM8 expression is associated with increased invasiveness and reduced patient survival in pancreatic cancer”, *Journal of cellular and molecular medicine*, Vol. 11 No. 5, pp. 1162–1174.

Valkovskaya, N.V. (2008), “Hypoxia-dependent expression of ADAM8 in human pancreatic cancer cell lines”, *Experimental oncology*, Vol. 30 No. 2, pp. 129–132.

Verel-Yilmaz, Y., Fernández, J.P., Schäfer, A., Nevermann, S., Cook, L., Gercke, N., Helmprobst, F., Jaworek, C., Pogge von Strandmann, E., Pagenstecher, A., Bartsch, D.K., Bartsch, J.W. and Slater, E.P. (2021), “Extracellular Vesicle-Based Detection of Pancreatic Cancer”, *Frontiers in cell and developmental biology*, Vol. 9, p. 697939.

Vincent, A., Herman, J., Schulick, R., Hruban, R.H. and Goggins, M. (2011), “Pancreatic cancer”, *The Lancet*, Vol. 378 No. 9791, pp. 607–620.

Wei, H., Chen, Q., Lin, L., Sha, C., Li, T., Liu, Y., Yin, X., Xu, Y., Chen, L., Gao, W., Li, Y. and Zhu, X. (2021), “Regulation of exosome production and cargo sorting”, *International journal of biological sciences*, Vol. 17 No. 1, pp. 163–177.

Wikberg, M.L., Ling, A., Li, X., Öberg, Å., Edin, S. and Palmqvist, R. (2017), “Neutrophil infiltration is a favorable prognostic factor in early stages of colon cancer”, *Human pathology*, Vol. 68, pp. 193–202.

Wildeboer, D., Naus, S., Amy Sang, Q.-X., Bartsch, J.W. and Pagenstecher, A. (2006), “Metalloproteinase disintegrins ADAM8 and ADAM19 are highly regulated in human primary brain tumors and their expression levels and activities are associated with invasiveness”, *Journal of neuropathology and experimental neurology*, Vol. 65 No. 5, pp. 516–527.

Xu, D., McKee, C.M., Cao, Y., Ding, Y., Kessler, B.M. and Muschel, R.J. (2010a), “Matrix metalloproteinase-9 regulates tumor cell invasion through cleavage of protease nexin-1”, *Cancer research*, Vol. 70 No. 17, pp. 6988–6998.

Xu, Z., Vonlaufen, A., Phillips, P.A., Fiala-Beer, E., Zhang, X., Yang, L., Biankin, A.V., Goldstein, D., Pirola, R.C., Wilson, J.S. and Apte, M.V. (2010b), “Role of pancreatic stellate cells in pancreatic cancer metastasis”, *The American Journal of Pathology*, Vol. 177 No. 5, pp. 2585–2596.

Yabluchanskiy, A., Ma, Y., Iyer, R.P., Hall, M.E. and Lindsey, M.L. (2013), “Matrix metalloproteinase-9: Many shades of function in cardiovascular disease”, *Physiology (Bethesda, Md.)*, Vol. 28 No. 6, pp. 391–403.

Yachida, S. and Iacobuzio-Donahue, C.A. (2009), “The pathology and genetics of metastatic pancreatic cancer”, *Archives of pathology & laboratory medicine*, Vol. 133 No. 3, pp. 413–422.

Yammine, L., Zablocki, A., Baron, W., Terzi, F. and Gallazzini, M. (2019), “Lipocalin-2 Regulates Epidermal Growth Factor Receptor Intracellular Trafficking”, *Cell reports*, Vol. 29 No. 7, 2067-2077.e6.

Yan, L., Borregaard, N., Kjeldsen, L. and Moses, M.A. (2001), “The high molecular weight urinary matrix metalloproteinase (MMP) activity is a complex of gelatinase B/MMP-9 and neutrophil gelatinase-associated lipocalin (NGAL). Modulation of MMP-9 activity by NGAL”, *The Journal of biological chemistry*, Vol. 276 No. 40, pp. 37258–37265.

Yang, S., Liu, Q. and Liao, Q. (2020), “Tumor-Associated Macrophages in Pancreatic Ductal Adenocarcinoma: Origin, Polarization, Function, and Reprogramming”, *Frontiers in cell and developmental biology*, Vol. 8, p. 607209.

Yang, Z., Bai, Y., Huo, L., Chen, H., Huang, J., Li, J., Fan, X., Yang, Z., Wang, L. and Wang, J. (2014), “Expression of A disintegrin and metalloprotease 8 is associated with cell growth and poor survival in colorectal cancer”, *BMC cancer*, Vol. 14, p. 568.

Yee, N.S., Lengerich, E.J., Schmitz, K.H., Maranki, J.L., Gusani, N.J., Tchelebi, L., Mackley, H.B., Krok, K.L., Baker, M.J., Boer, C. de and Yee, J.D. (2018), “Frontiers in Gastrointestinal Oncology: Advances in Multi-Disciplinary Patient Care”, *Biomedicines*, Vol. 6 No. 2.

Yee, N.S., Zhang, S., He, H.-Z. and Zheng, S.-Y. (2020), “Extracellular Vesicles as Potential Biomarkers for Early Detection and Diagnosis of Pancreatic Cancer”, *Biomedicines*, Vol. 8 No. 12.

Yoshida, S., Setoguchi, M., Higuchi, Y., Akizuki, S. and Yamamoto, S. (1990), “Molecular cloning of cDNA encoding MS2 antigen, a novel cell surface antigen strongly expressed in murine monocytic lineage”, *International immunology*, Vol. 2 No. 6, pp. 585–591.

Yoshiyama, K., Higuchi, Y., Kataoka, M., Matsuura, K. and Yamamoto, S. (1997), “CD156 (human ADAM8): expression, primary amino acid sequence, and gene location”, *Genomics*, Vol. 41 No. 1, pp. 56–62.

Zack, M.D., Malfait, A.-M., Skepner, A.P., Yates, M.P., Griggs, D.W., Hall, T., Hills, R.L., Alston, J.T., Nemirovskiy, O.V., Radabaugh, M.R., Leone, J.W., Arner, E.C. and Tortorella, M.D. (2009), “ADAM-8 isolated from human osteoarthritic chondrocytes cleaves fibronectin at Ala(271)”, *Arthritis and rheumatism*, Vol. 60 No. 9, pp. 2704–2713.

Zhang, W., Wan, M., Ma, L., Liu, X. and He, J. (2013), “Protective effects of ADAM8 against cisplatin-mediated apoptosis in non-small-cell lung cancer”, *Cell biology international*, Vol. 37 No. 1, pp. 47–53.

Zhang, X., Shi, S., Zhang, B., Ni, Q., Yu, X. and Xu, J. (2018), “Circulating biomarkers for early diagnosis of pancreatic cancer: facts and hopes”, *American Journal of Cancer Research*, Vol. 8 No. 3, pp. 332–353.

Zhang, Y., Su, Y., Zhao, Y., Lv, G. and Luo, Y. (2017), “MicroRNA-720 inhibits pancreatic cancer cell proliferation and invasion by directly targeting cyclin D1”, *Molecular medicine reports*, Vol. 16 No. 6, pp. 9256–9262.

Zhao, P., Elks, C.M. and Stephens, J.M. (2014), “The induction of lipocalin-2 protein expression in vivo and in vitro”, *The Journal of biological chemistry*, Vol. 289 No. 9, pp. 5960–5969.

Zhu, Y., Herndon, J.M., Sojka, D.K., Kim, K.-W., Knolhoff, B.L., Zuo, C., Cullinan, D.R., Luo, J., Bearden, A.R., Lavine, K.J., Yokoyama, W.M., Hawkins, W.G., Fields, R.C., Randolph, G.J. and DeNardo, D.G. (2017), “Tissue-Resident Macrophages in Pancreatic Ductal Adenocarcinoma Originate from Embryonic Hematopoiesis and Promote Tumor Progression”, *Immunity*, Vol. 47 No. 2, 323-338.e6.

7 Publications

Journal of *Personalized Medicine*

MDPI

Article

Cohort Analysis of ADAM8 Expression in the PDAC Tumor Stroma

Christian Jaworek [1,†], Yesim Verel-Yilmaz [2,†], Sarah Driesch [2], Sarah Ostgathe [1], Lena Cook [1], Steffen Wagner [3], Detlef K. Bartsch [2], Emily P. Slater [2,†] and Jörg W. Bartsch [1,*,†]

[1] Department of Neurosurgery, Philipps University Marburg, Baldingerstrasse, 35033 Marburg, Germany; christian@jaworek.org (C.J.); sarah.ostgathe@googlemail.com (S.O.); cookl@staff.uni-marburg.de (L.C.)
[2] Department of Visceral Surgery, Philipps University Marburg, Baldingerstrasse, 35033 Marburg, Germany; yesimverel@hotmail.de (Y.V.-Y.); sarahdriesch@hotmail.de (S.D.); bartsch@med.uni-marburg.de (D.K.B.); slater@med.uni-marburg.de (E.P.S.)
[3] Head and Neck Surgery, Department of Otorhinolaryngology, Justus Liebig University Giessen, Aulweg 128 (ForMED), 35392 Giessen, Germany; Steffen.Wagner@hno.med.uni-giessen.de
* Correspondence: jbartsch@med.uni-marburg.de; Tel.: +49-6421-58-61173
† Equal contribution.

Abstract: Pancreatic ductal adenocarcinoma (PDAC) is a cancer type with one of the highest mortalities. The metalloprotease-disintegrin ADAM8 is highly expressed in pancreatic cancer cells and is correlated with an unfavorable patient prognosis. However, no information is available on ADAM8 expression in cells of the tumor microenvironment. We used immunohistochemistry (IHC) to describe the stromal cell types expressing ADAM8 in PDAC patients using a cohort of 72 PDAC patients. We found ADAM8 expressed significantly in macrophages (6%), natural killer cells (40%), and neutrophils (63%), which showed the highest percentage of ADAM8 expressing stromal cells. We quantified the amount of ADAM8$^+$ neutrophils in post-capillary venules in PDAC sections by IHC. Notably, the amount of ADAM8$^+$ neutrophils could be correlated with post-operative patient survival times. In contrast, neither the total neutrophil count in peripheral blood nor the neutrophil-to-lymphocyte ratio showed a comparable correlation. We conclude from our data that ADAM8 is, in addition to high expression levels in tumor cells, present in tumor-associated stromal macrophages, NK cells, and neutrophils and, in addition to functional implications, the ADAM8-expressing neutrophil density in post-capillary venules is a diagnostic parameter for PDAC patients when the numbers of ADAM8$^+$ neutrophils are quantified.

Keywords: pancreatic cancer; tumor microenvironment; tumor stroma; neutrophils; ADAM8 protease

Citation: Jaworek, C.; Verel-Yilmaz, Y.; Driesch, S.; Ostgathe, S.; Cook, L.; Wagner, S.; Bartsch, D.K.; Slater, E.P.; Bartsch, J.W. Cohort Analysis of ADAM8 Expression in the PDAC Tumor Stroma. *J. Pers. Med.* **2021**, *11*, 113. https://doi.org/10.3390/jpm11020113

Academic Editor: Lisa Salvatore
Received: 26 January 2021
Accepted: 7 February 2021
Published: 10 February 2021

1. Introduction

Pancreatic ductal adenocarcinoma (PDAC) is a highly heterogeneous tumor entity with a grim prognosis with a 5-year survival rate of less than 8% [1]. Desmoplastic reaction is very common in PDAC and accounts for a massive activation of stroma and stromal cells in the tumor microenvironment. The PDAC tumor microenvironment (TME) with its inflammatory nature activates many immune cell types in response to tumor cell derived signals (reviewed in [2]). As creators of and responders to signals in the tumor microenvironment, ADAM proteases (A disintegrin and metalloprotease) have been found to be associated with numerous functions ranging from immune cell migration and invasion [3], degradation of extracellular matrix molecules (Collagens I, IV) [4] to proteolytic inactivation of immune checkpoint inhibitors such as PD-L1 [5,6]. With their multidomain structures, ADAM proteases are capable of multiple physiological functions associated with cell adhesion, cell fusion, cell signaling, and proteolysis. Proteolysis of membrane-anchored precursor proteins by ADAMs is a key event for the generation of signaling cascades within the TME. In PDAC, a significant contribution of ADAM

proteases to tumor progression was reported for ADAM8 [4], ADAM9 [7,8], ADAM10 [9], ADAM12 [10], and ADAM17 [11]. Notably, higher expression levels of these ADAM proteases were reported to be associated with a poor patient prognosis in PDAC. Similar to other solid cancers, shedding of EGF-ligands and EGFR by ADAM10 and 17 are clearly relevant for tumor signaling in pancreatic cancer [11,12]. Furthermore, there are a number of ADAM proteases lacking phenotypes in knockout mice but with a possible role in different tumor entities and specifically in PDAC, which applies for ADAM8 and ADAM9 [8]. In particular, high expression levels of ADAM8 and 9 are associated with a worsened patient prognosis [13]. In previous studies, ADAM8 in particular was described in tumor cells and functional analyses revealed a tumor-promoting effect of ADAM8 in pancreatic cancer cells [4], so that inhibition of ADAM8 in pancreatic cancer (KPC) mice using a cyclic ADAM8 inhibiting peptide (BK-1361) leads to prolonged survival and improved metrics of pathological parameters (metastasis formation, invasion of tumor cells, acinar structures). However, since ADAM8 was reported to be highly expressed in tumor-associated immune cells as shown in glioblastoma [14], the goal of the present study was to analyze the presence of ADAM8 in tumor stroma of PDAC in a cohort of 72 in-house patients.

2. Materials and Methods

2.1. Patients and Tissue Samples

A total of 72 patients with PDAC who underwent a pancreas resection in the Department of Visceral Surgery at the University Hospital Marburg were enrolled in our study (see Table 1). All tumors were histologically staged by an experienced pathologist according to UICC-TNM (Union for International Cancer Control; tumor, node, metastasis) classification 2017 [15]. All samples were obtained from the tumor bank of the Department of Pathology. Ethical approval was obtained by the local ethics committee at Marburg University, Faculty of Medicine (File Nr. 5/03). All patients provided written informed consent prior to participating in this study.

Table 1. Clinical data on pancreatic ductal adenocarcinoma (PDAC) patient cohort used in this study (n = 72); abbreviations used: *: NLR: neutrophil-to-lymphocyte ratio; UICC: Union for International Cancer Control.

Gender	Males (%)	37 (51%)
	Females (%)	35 (49%)
Median Age at Surgery, Years (Range)		68 (47 to 85)
UICC Stage, Number of Patients (%)	I	11 (15.3%)
	II	10 (13.9%)
	III	46 (63.9%)
	IV	5 (6.9%)
Median Survival, Months (Range)		22 (1 to 92)
Location	head	65 (90%)
	body or tail	7 (10%)
Median NLR * (Range)		3.14 (1.53 to 31.67)

2.2. Immunohistochemistry (IHC)

For ADAM8 immunostaining, formalin-fixed and paraffin-embedded archived tumor samples and corresponding normal tissues were stained as follows. Paraffin sections (4 µm thickness) from PDAC patients were stained for ADAM8 using a polyclonal anti-ADAM8 antibody and a standard VectaStain Protocol. For double-staining of PDAC sections, sections were stained for ADAM8 and the respective markers for T cell markers CD3, CD4, and CD8, stellate cell marker SMA, macrophage marker CD68, natural killer cell marker CD56, and neutrophil marker myeloperoxidase (MPO). Antibodies, concentrations,

and sources of primary antibodies are listed below (Table 2). Briefly, slides were heated to 60 °C for 1 h, deparaffinized using xylene, and hydrated by a graded series of ethanol washes. Antigen retrieval was accomplished by steam-heating in Target Retrieval Solution, pH9 (Agilent Dako, Waldbronn, Germany) for 30 min. For immunohistochemistry, endogenous peroxidase activity was quenched by 5 min incubation in 3% H_2O_2. Sections were then incubated with primary antibodies for 45 min at RT followed by biotinylated secondary antibodies for 20 min also at RT. Bound antibodies were detected using the avidin-biotin complex (ABC) peroxidase method (ABC Elite Kit; Vector Labs, Burlingame, CA, USA). Final staining was developed with the Dako DAB peroxidase substrate kit. For double staining, HRP Magenta Substrate Chromogen System was employed. Counterstaining was performed using hematoxylin. All steps following the antigen retrieval were performed using the DakoCytomation Autostainer Plus.

Table 2. Concentrations and sources of primary antibodies.

Antibody	Species	Working Dilution	Source
ADAM8	rabbit	1:200	R&D Systems (AF1031)
CD3	mouse	1:50	Dako (M7254)
CD56	mouse	1:10	Monosan (MON 9006)
CD68	mouse	1:200	Novus Biologicals (NB100-683)
CD163	mouse	1:50	ThermoFisher (MA5-11458)
CD4	mouse	1:100	Dako (M7310)
CD8	mouse	1:200	R&D Systems (MAB3801)
α Smooth muscle actin	mouse	1:2000	R&D Systems (MAB1420)
MPO	mouse	1:50	R&D systems (MAB3174)

2.3. Selection of Patient Samples for Double-Staining

A total of 10 patients were selected for double-staining that reflect our total cohort by having 7 stage III (among them 2 R0) and 3 stage II samples and from these 5 patients with survival times of less than 18 months and 5 patients with survival time longer than 18 months (one patient alive with disease).

2.4. Quantitation

The quantitation of ADAM8-positive and marker-positive cells in paraffin-embedded and stained sections was performed using the virtual software programs Fiji Image J [16].

2.5. Cell Counting and Scoring of Neutrophils in PDAC Patients

Samples from 51 patients were included in neutrophil analyses and none of these patients received a neoadjuvant therapy. Planimetry measurements of three venous blood vessels on each ADAM8-stained section were performed. Later, the number of $ADAM8^+$ neutrophils in the lumen of the blood vessels was scored and a ratio was calculated (cells per area). The sum of the three data sets of each patient are listed in the last column of Table A1. The blood vessels analyzed fulfilled the following criteria. The vessels were located in the center of tumor with a minimal luminal area of 2000 μm^2. The distance between the vessels was such that three different areas of the tumor could be analyzed randomly. Blood vessels displaying fixation-related artifacts were excluded. Only cells that could be identified clearly as neutrophils with a positive staining for ADAM8 were counted.

2.6. Statistical Analysis

Two-way ANOVA was used for stroma cell quantifications and survival analyses. For neutrophil/survival analyses, a Pearson correlation coefficient was determined in conjunction with t statistics and p-value. Analyses were performed using Prism 6 for

Mac OSX from GraphPad, San Diego, CA, USA. A value of $p < 0.05$ was considered to be significant.

3. Results

3.1. ADAM8 Expression in PDAC

The PDAC patient cohort (tumor, stromal cells, co-localization) consists of patients who were clinically diagnosed with PDAC in the department of visceral surgery and included in the study (see Materials and Methods section for information on exclusion criteria). From all tumor patients, paraffin-embedded sections were stained and scored for ADAM8 expression (Figure 1).

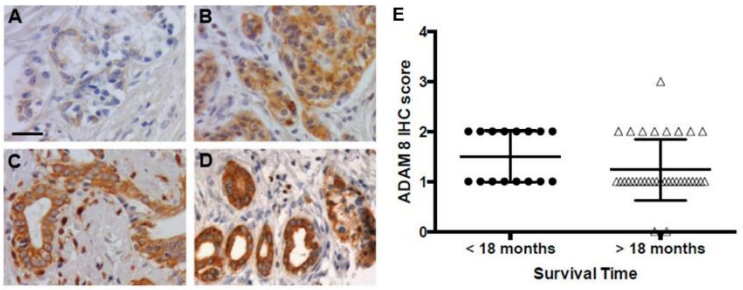

Figure 1. Correlation of ADAM8 staining scores with survival in patients of the PDAC cohort ($n = 50$). Four exemplary images illustrating varying levels of ADAM8 staining in patient samples. The scale bar is 25 µm. Staining intensities were determined for each section based on analysis of 5 viewing fields per section and were between 0 and 3 with no (0; (**A**)), low (1; (**B**)), moderate (2; (**C**)) and strong (3; (**D**)) ADAM8 staining. (**E**): Patients in the cohort were split into 2 groups with group 1, survival less than 18 months (•; $n = 16$) and group 2 (Δ; $n = 34$), patient survival longer than 18 months. Note that only two PDAC sections were almost negative for ADAM8. Difference is not significant.

Staining intensities in tumor cells were assessed by IHC score (0–3) according to earlier studies [17] in our in house cohort. Groups were separated into two according to median survival times either shorter or longer than 18 months. No significant differences were observed between the two groups with regard to ADAM8 IHC scores.

3.2. Co-Localization of ADAM8 and Stromal Cell Markers in PDAC Tissue

In all PDAC sections stained for ADAM8, a notable expression was also observed in stromal cells (Figure 2A). To identify the stromal cell types expressing ADAM8 in PDAC, double staining of tissue with respective cell markers for T cells (CD3, CD4, CD8), natural killer (NK) cells (CD56), macrophages (CD68), neutrophils (MPO), and smooth muscle actin for stellate cells (SMA) was performed on a representative cohort of ten patients reflecting our total cohort (see Materials and Methods section for details).

We identified ADAM8-positive cells not only in the duct-like structures of the tumor area (Figure 2A), but also in the tumor microenvironment (Figure 2A–H). Stromal cells show moderate to high levels of ADAM8 staining. Significant co-staining of ADAM8 with markers for CD68 (macrophages, Figure 2B), for CD56 (NK cells, Figure 2F), and for MPO (neutrophils, Figure 2H) can be seen in Figure 2. Cells stained positively for both MPO and ADAM8 were identified to be neutrophils as evidenced by their granulocytic morphology.

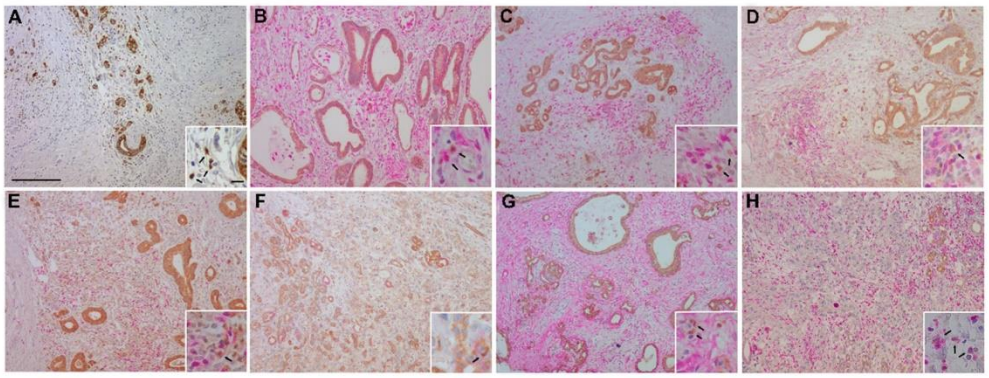

Figure 2. ADAM8 staining (**A**) in PDAC sections and co-localization of ADAM8 (brown) with markers (pink) for CD68 (macrophages, (**B**)), CD3 ($CD3^+$ T cells, (**C**)), CD4 ($CD4^+$ T cells, (**D**)), CD8 ($CD8^+$ T cells, (**E**)), CD56 (NK cells, (**F**)), SMA (stellate cells, (**G**)), and MPO (neutrophils, (**H**)). In (**A**), a control stain for ADAM8 alone is shown. Bar in A, 800 μm; bar in insert (**A**), 100 μm.

3.3. Quantitative Analysis of Co-Localization

ImageJ analysis on double-stained sections from a representative group of 10 patients was performed to quantify the number of specific stromal cells that were ADAM8 positive (Figure 3). Whereas T cells identified with distinct markers (CD3, CD4, and CD8) and pancreatic stellate cells (SMA) show a low percentage of co-localization, significant ADAM8-positive cell populations were observed for macrophages (CD68, 0–17%), NK cells (CD56, 18–75%), and neutrophils (MPO, 30–90%).

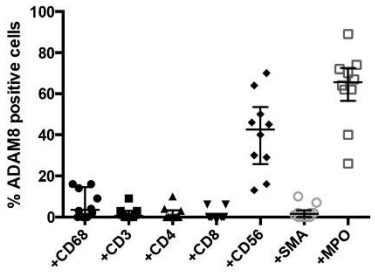

Figure 3. Scatter dot plot of the percentage of double-positive ADAM8/marker cells as analyzed in 10 representative PDAC sections stained for CD68 (●), CD3 (■), CD4 (▲), CD8 (▼), CD56 (♦), SMA (○) and MPO (□). Note that the frequency of $ADAM8^+$ stromal cells is highest for macrophages (CD68), NK cells (CD56), and neutrophils (MPO). For each section analyzed, data are derived from quantification of 5 viewing fields in the tumor proximal stroma areas. Median values with interquartile ranges are indicated. Note that the highest frequency of co-localization of ADAM8 with stromal markers is observed for MPO (neutrophils).

3.4. ADAM8 Expression in Neutrophils

We confirmed ADAM8 expression in neutrophils and their association with blood vessels in PDAC sections (Figure 3). Neutrophils enter the tissue from post-capillary venules in a process called leukodiapedesis. Thus, the likelihood of detecting neutrophils in these blood vessels is higher than in any other type of capillaries. Since post-capillary venules are large vessels, we sought to determine their frequency in PDAC sections.

To obtain comparable results, neutrophils were quantified in at least 3 independent post-capillary venules with an area of >2000 μm^2 in the core tumor tissue (Figure 4 and Table A1 in Appendix A).

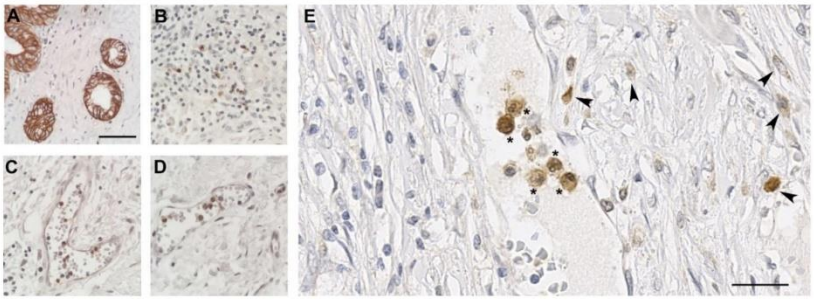

Figure 4. ADAM8 positive neutrophils located in tumor stromal post-capillary venules. (**A**), ADAM8 staining in duct-like structures; (**B**), ADAM8 staining in PDAC tumor stroma adjacent to duct-like structures reveals mainly ADAM8$^+$ neutrophils; (**C**) and (**D**) overview venules in tumor areas with ADAM8$^+$ neutrophils. (**E**), detailed view of venules with ADAM8$^+$ neutrophils in vessels (asterisks) and adjacent infiltrated neutrophils (arrowheads) in a representative PDAC section. Scale bar in (**A**), valid for (**A**–**D**), 120 μm; Scale bar in (**E**), 55 μm.

Neutrophil numbers were correlated with patient survival data in the entire PDAC patient cohort (Figure 5A,B) where respective structures (venules) were analyzable. Moreover, we determined the neutrophil-to-leukocyte ratio (NLR) in PDAC patients where data were available and correlated these and the total blood neutrophil counts (Figure 5C,D) with survival data, respectively.

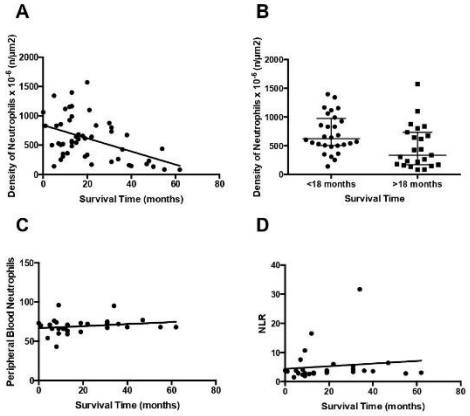

Figure 5. (**A**) Correlation analyses of ADAM8$^+$ neutrophil counts in post-capillary venules. Each data point is the average of 3 independent post-capillary venules of an area > 2000 μm^2 in the core tumor tissue (n = 50). Pearson correlation revealed r = −0.463 with p = 0.0006. (**B**) Neutrophil density diagram from our PDAC patient cohort split into survival time less than and greater than 18 months, p = 0.0128. (**C**) Neutrophil counts in peripheral blood of PDAC patients from the same cohort, p = 0.2797. (**D**) Neutrophil-to-lymphocyte ratio in the PDAC patient cohort, p = 0.5143. Note that only the ADAM8$^+$ neutrophil counts in post-capillary venules are significantly correlated with PDAC patient survival.

4. Discussion

Due to high expression levels in PDAC tumor cells, ADAM8 was previously identified as a potential therapeutic target in PDAC [4,13]. Here we confirmed earlier results in our cohort that ADAM8 is expressed in almost all PDAC samples, but no significant correlation between ADAM8 expression in tumors and survival could be drawn. Interestingly, no previous study has mentioned expression of ADAM8 in stromal cells of PDAC. Given a distinct physiological expression profile of ADAM8 in immune cells such as macrophages and leukocytes, an ADAM8 expression in stromal cells of PDAC is likely and suggests an important role of ADAM8 in the tumor microenvironment of PDAC. However, the relatively low abundance of ADAM8-positive macrophages is unexpected as under physiological conditions, e.g., in the bone marrow, macrophages are constitutively expressing ADAM8 [14,18]. In macrophages, there is experimental evidence that ADAM8 can trigger their migratory behavior into the tissue under inflammatory conditions. This has been demonstrated in muscle regeneration when ADAM8-deficient macrophages are unable to remove muscle cell debris after muscle degeneration due to lack of motility [19]. A more general effect of ADAM8 on several immune related cells was observed in allergic asthma in mice where deficiency in ADAM8 caused a significantly reduced recruitment of macrophages, neutrophils, and eosinophils to the airway inflammation site to dampen the allergic response and the asthma severity [20]. By analyzing ADAM8 expression in neutrophils, we were able to show that an increased number of ADAM8-positive neutrophils particularly in venules of the tumor areas can be of prognostic value for PDAC patients. Mechanistically, this observation could point towards a detrimental effect of ADAM8-positive neutrophils in PDAC by regulating neutrophil transmigration from the vasculature to the tumor site. A neutrophil-to-lymphocyte ratio (NLR) has been reported to be a predictive parameter in clinical studies with PDAC patients. Higher ratios have been associated with poor outcome in some studies [21–23]. However, the value of this ratio in terms of prognosis is controversial [24]. In addition, whereas low tumor infiltration of neutrophils has been associated with poor prognosis [25], others report neutrophil infiltration to be observed in pancreatic tumors with the poorest prognosis [26]. It is interesting to note that the number of ADAM8-positive neutrophils in venules of PDAC patients shows a better correlation than either peripheral blood neutrophil count or the NLR. Although controversial, the general findings suggest that, in pretherapy PDAC patients, the NLR is not indicative for overall survival [24], which is in accordance with our findings.

5. Conclusions

In PDAC, ADAM8 is significantly expressed in stromal cells, in particular in macrophages, NK cells, and neutrophils. Given the diagnostic value of neutrophil counts as reported previously [21–23], we propose that determination of neutrophil density in venules of tumor areas is a reliable indicator of disease progression and patient survival and could be used to stratify PDAC patients.

Author Contributions: Conceptualization, D.K.B., E.P.S. and J.W.B.; methodology, E.P.S. and J.W.B.; investigation, C.J., S.O., S.D. and Y.V.-Y.; resources, D.K.B. and E.P.S.; data curation, C.J., Y.V.-Y., S.O., S.W., L.C., E.P.S. and J.W.B.; writing—original draft preparation, C.J., J.W.B. and E.P.S.; writing—review and editing, C.J., D.K.B. and J.W.B.; supervision, D.K.B., E.P.S. and J.W.B.; project administration, E.P.S. and J.W.B.; funding acquisition, E.P.S. and J.W.B. All authors have read and agreed to the published version of the manuscript.

Funding: This research was funded by the DFG Clinical Research Unit (CRU) 325 (Clinical relevance of Tumor-microenvironment interactions in pancreatic cancer) grant number BA1606/4-1 and SL17/5-1. C.J. and S.D. received funding from the CRU 325 by a doctoral stipend; article processing charge was generously funded by Philipps University Marburg.

Institutional Review Board Statement: This study was conducted in accordance with the guidelines of the Declaration of Helsinki and approved by the local ethics committee, Medical Faculty of the Philipps University Marburg, file number 05/03.

Informed Consent Statement: Informed consent was obtained from all subjects involved in the study.

Data Availability Statement: Patient data can be made available upon request.

Acknowledgments: Authors would like to thank A. Ramaswamy for expert pathological advice, V. Wischmann for expert IHC staining, and N. Gercke for excellent technical assistance.

Conflicts of Interest: The authors declare no conflict of interest.

Appendix A

Table A1. Summarizes clinical data and neutrophil counts in venules of PDAC patients in the cohort investigated. Abbreviations used: UICC: Union for International Cancer Control.; NLR: neutrophil-to-lymphocyte ratio.

Number	Gender	Age at Surgery (Years)	UICC Stage	Survival (Months)	Location	NLR	Density of Neutrophils (n/µm^2)
1	f	71	II	92	head	4.60	
2	m	85	IV	20	head	n.a.	334×10^6
3	f	75	III	11	head	2.64	360×10^6
4	m	65	III	31	head	4.29	216×10^6
5	m	74	III	30	head	n.a.	878×10^6
6	m	61	III	55	head	2.83	84×10^6
7	m	56	III	62	head	3.09	81×10^6
8	f	55	III	19	head	3.84	305×10^6
9	m	73	III	6	body	2.87	831×10^6
10	m	49	II	8	head	2.39	856×10^6
11	m	67	III	5	head	n.a.	139×10^6
12	f	51	III	40	head	3.58	146×10^6
13	m	68	III	50	head	n.a.	134×10^6
14	w	77	II	34	head	31.67	260×10^6
15	f	85	II	0	head	3.84	1061×10^6
16	m	52	IV	16	body	n.a.	603×10^6
17	f	68	III	20	tail	n.a.	1573×10^6
18	f	82	III	22	head	6.00	643×10^6
19	f	53	III	35	head	n.a.	
20	f	69	IV	15	body	n.a.	540×10^6
21	f	74	III	4	head	1.53	501×10^6
22	m	68	III	4	head	n.a.	
23	f	78	III	39	head	n.a.	159×10^6
24	m	56	III	30	head	n.a.	
25	f	65	III	38	head	n.a.	672×10^6
26	f	50	III	13	head	2.81	484×10^6
27	f	62	I	42	head	n.a.	
28	m	78	III	31	head	3.35	800×10^6
29	f	75	I	32	head	n.a.	
30	m	68	I	1	head	3.50	831×10^6
31	m	72	III	36	head	n.a.	
32	m	66	II	33	head	n.a.	
33	m	78	I	28	head	n.a.	
34	f	75	I	35	head	6.83	
35	f	79	III	22	head	n.a.	168×10^6
36	m	60	III	9	head	2.87	519×10^6
37	f	60	I	33	head	2.75	
38	f	58	III	27	head	2.79	
39	f	57	III	19	head	3.10	616×10^6
40	m	67	III	28	head	n.a.	
41	m	64	III	24	head	n.a.	836×10^6
42	f	68	I	29	head	n.a.	
43	m	60	I	n.a.	head	n.a.	
44	m	60	III	28	head	2.87	
45	f	51	III	16	head	n.a.	682×10^6

Table A1. *Cont.*

Number	Gender	Age at Surgery (Years)	UICC Stage	Survival (Months)	Location	NLR	Density of Neutrophils (n/µm²)
46	f	78	III	28	head	2.00	
47	f	79	I	26	head	n.a.	
48	m	47	III	10	head	n.a.	1117×10^6
49	m	65	II	12	body	16.50	1154×10^6
50	f	79	III	13	head	2.86	569×10^6
51	m	72	III	13	head	2.86	1398×10^6
52	m	58	III	48	head	n.a.	230×10^6
53	f	71	II	75	head	2.67	
54	m	78	III	12	head	n.a.	926×10^6
55	m	64	III	54	head	n.a.	438×10^6
56	m	70	I	36	body	3.79	425×10^6
57	f	61	III	31	head	5.36	733×10^6
58	m	71	III	13	head	n.a.	1164×10^6
59	m	68	III	21	head	n.a.	1099×10^6
60	m	75	II	47	head	6.42	179×10^6
61	f	77	III	57	head	3.14	
62	f	75	III	9	head	1.94	349×10^6
63	m	80	II	8	head	4.11	252×10^6
64	m	52	III	13	head	n.a.	991×10^6
65	f	78	III	7	head	7.60	529×10^6
66	m	80	II	9	head	10.67	308×10^6
67	m	67	III	15	head	n.a.	643×10^6
68	f	64	IV	13	body	3.09	553×10^6
69	f	68	IV	18	head	n.a.	658×10^6
70	f	73	III	5	head	3.74	1342×10^6
71	f	72	III	8	head	n.a.	506×10^6
72	m	77	I	16	head	n.a.	

References

1. Siegel, R.L.; Miller, K.D.; Jemal, A. Cancer statistics, 2020. *CA Cancer J. Clin.* **2020**, *70*, 7–30. [CrossRef]
2. Huber, M.; Brehm, C.U.; Gress, T.M.; Buchholz, M.; Alhamwe, B.A.; von Strandmann, E.P.; Slater, E.P.; Bartsch, J.W.; Bauer, C.; Lauth, M. The immune microenvironment in pancreatic cancer. *Int. J. Mol. Sci.* **2020**, *21*, 7307. [CrossRef]
3. Conrad, C.; Benzel, J.; Dorzweiler, K.; Cook, L.; Schlomann, U.; Zarbock, A.; Slater, E.P.; Nimsky, C.; Bartsch, J.W. ADAM8 in invasive cancers: Links to tumor progression, metastasis, and chemoresistance. *Clin. Sci. (London)* **2019**, *133*, 83–99. [CrossRef]
4. Schlomann, U.; Koller, G.; Conrad, C.; Ferdous, T.; Golfi, P.; Garcia, A.M.; Höfling, S.; Parsons, M.; Costa, P.; Soper, R.; et al. ADAM8 as a drug target in pancreatic cancer. *Nat. Commun.* **2015**, *6*, 6175. [CrossRef] [PubMed]
5. Romero, Y.; Wise, R.; Zolkiewska, A. Proteolytic processing of PD-L1 by ADAM proteases in breast cancer cells. *Cancer Immunol. Immunother.* **2020**, *69*, 43–55. [CrossRef]
6. Orme, J.J.; Jazieh, K.A.; Xie, T.; Harrington, S.; Liu, X.; Ball, M.; Madden, B.; Charlesworth, M.C.; Azam, T.U.; Lucien, F.; et al. ADAM10 and ADAM17 cleave PD-L1 to mediate PD-(L)1 inhibitor resistance. *Oncoimmunology* **2020**, *9*, 1744980. [CrossRef]
7. Grützmann, R.; Lüttges, J.; Sipos, B.; Ammerpohl, O.; Dobrowolski, F.; Alldinger, I.; Kersting, S.; Ockert, D.; Koch, R.; Kalthoff, H.; et al. ADAM9 expression in pancreatic cancer is associated with tumour type and is a prognostic factor in ductal adenocarcinoma. *Br. J. Cancer* **2004**, *90*, 1053–1058. [CrossRef] [PubMed]
8. Oria, V.O.; Lopatta, P.; Schmitz, T.; Preca, B.T.; Nyström, A.; Conrad, C.; Bartsch, J.W.; Kulemann, B.; Hoeppner, J.; Maurer, J.; et al. ADAM9 contributes to vascular invasion in pancreatic ductal adenocarcinoma. *Mol. Oncol.* **2019**, *13*, 456–479. [CrossRef]
9. Gaida, M.M.; Haag, N.; Günther, F.; Tschaharganeh, D.F.; Schirmacher, P.; Friess, H.; Giese, N.A.; Schmidt, J.; Wente, M.N. Expression of A disintegrin and metalloprotease 10 in pancreatic carcinoma. *Int. J. Mol. Med.* **2010**, *26*, 281–288. [CrossRef] [PubMed]
10. Veenstra, V.L.; Damhofer, H.; Waasdorp, C.; van Rijssen, L.B.; van de Vijver, M.J.; Dijk, F.; Wilmink, H.W.; Besselink, M.G.; Busch, O.R.; Chang, D.K.; et al. ADAM12 is a circulating marker for stromal activation in pancreatic cancer and predicts response to chemotherapy. *Oncogenesis* **2018**, *7*, 87. [CrossRef] [PubMed]
11. Ardito, C.M.; Grüner, B.M.; Takeuchi, K.K.; Lubeseder-Martellato, C.; Teichmann, N.; Mazur, P.K.; Delgiorno, K.E.; Carpenter, E.S.; Halbrook, C.J.; Hall, J.C.; et al. EGF receptor is required for KRAS-induced pancreatic tumorigenesis. *Cancer Cell* **2012**, *22*, 304–317. [CrossRef]

12. Blobel, C.P. ADAMs: Key components in EGFR signalling and development. *Nat. Rev. Mol. Cell Biol.* **2005**, *6*, 32–43. [CrossRef] [PubMed]
13. Valkovskaya, N.; Kayed, H.; Felix, K.; Hartmann, D.; Giese, N.A.; Osinsky, S.P.; Friess, H.; Kleeff, J. ADAM8 expression is associated with increased invasiveness and reduced patient survival in pancreatic cancer. *J. Cell. Mol. Med.* **2007**, *11*, 1162–1174. [CrossRef] [PubMed]
14. Gjorgjevski, M.; Hannen, R.; Carl, B.; Li, Y.; Landmann, E.; Buchholz, M.; Bartsch, J.W.; Nimsky, C. Molecular profiling of the tumor microenvironment in glioblastoma patients: Correlation of microglia/macrophage polarization state with metalloprotease expression profiles and survival. *Biosci. Rep.* **2019**, *39*. [CrossRef]
15. Gospodarowicz, M.K.; Brierley, J.D. *TNM Classification of Malignant Tumors*; Wiley-Blackwell: Oxford, UK, 2017.
16. Schindelin, J.; Arganda-Carreras, I.; Frise, E.; Kaynig, V.; Longair, M.; Pietzsch, T.; Preibisch, S.; Rueden, C.; Saalfeld, S.; Schmid, B.; et al. Fiji: An open-source platform for biological-image analysis. *Nat. Methods* **2012**, *9*, 676–682. [CrossRef] [PubMed]
17. Conrad, C.; Götte, M.; Schlomann, U.; Roessler, M.; Pagenstecher, A.; Anderson, P.; Preston, J.; Pruessmeyer, J.; Ludwig, A.; Li, R.; et al. ADAM8 expression in breast cancer derived brain metastases: Functional implications on MMP-9 expression and transendothelial migration in breast cancer cells. *Int. J. Cancer* **2018**, *142*, 779–791. [CrossRef] [PubMed]
18. Li, Y.; Guo, S.; Zhao, K.; Conrad, C.; Driescher, C.; Rothbart, V.; Schlomann, U.; Guerreiro, H.; Bopp, M.H.; König, A.; et al. ADAM8 affects glioblastoma progression by regulating osteopontin-mediated angiogenesis. *Biol. Chem.* **2020**. [CrossRef]
19. Nishimura, D.; Sakai, H.; Sato, T.; Sato, F.; Nishimura, S.; Toyama-Sorimachi, N.; Bartsch, J.W.; Sehara-Fujisawa, A. Roles of ADAM8 in elimination of injured muscle fibers prior to skeletal muscle regeneration. *Mech. Dev.* **2015**, *135*, 58–67. [CrossRef]
20. Naus, S.; Blanchet, M.R.; Gossens, K.; Zaph, C.; Bartsch, J.W.; McNagny, K.; Ziltener, H.J. The metalloprotease-disintegrin ADAM8 is essential for the development of experimental asthma. *Am. J. Respir. Crit. Care Med.* **2010**, *181*, 1318–1328. [CrossRef]
21. Arima, K.; Okabe, H.; Hashimoto, D.; Chikamoto, A.; Tsuji, A.; Yamamura, K.; Kitano, Y.; Inoue, R.; Kaida, T.; Higashi, T.; et al. The diagnostic role of the neutrophil-to-lymphocyte ratio in predicting pancreatic ductal adenocarcinoma in patients with pancreatic diseases. *Int. J. Clin. Oncol.* **2016**, *21*, 940–945. [CrossRef] [PubMed]
22. Ben, Q.; An, W.; Wang, L.; Wang, W.; Yu, L.; Yuan, Y. Validation of the pretreatment neutrophil-lymphocyte ratio as a predictor of overall survival in a cohort of patients with pancreatic ductal adenocarcinoma. *Pancreas* **2015**, *44*, 471–477. [CrossRef]
23. Tao, L.; Zhang, L.; Peng, Y.; Tao, M.; Li, G.; Xiu, D.; Yuan, C.; Ma, C.; Jiang, B. Preoperative neutrophil-to-lymphocyte ratio and tumor-related factors to predict lymph node metastasis in patients with pancreatic ductal adenocarcinoma (PDAC). *Oncotarget* **2016**, *7*, 74314–74324. [CrossRef] [PubMed]
24. Chawla, A.; Huang, T.L.; Ibrahim, A.M.; Hardacre, J.M.; Siegel, C.; Ammori, J.B. Pretherapy neutrophil to lymphocyte ration and platelet to lymphocyte ratio do not predict survival in resectable pancreatic cancer. *HPB (Oxford)* **2018**, *20*, 398–404. [CrossRef]
25. Naso, J.R.; Topham, J.T.; Karasinska, J.M.; Lee, M.K.C.; Kalloger, S.E.; Wong, H.L.; Nelson, J.; Moore, R.A.; Mungall, A.J.; Jones, S.J.M.; et al. Tumor infiltrating neutrophils and gland formation predict overall survival and molecular subgroups in pancreatic ductal adenocarcinoma. *Cancer Med.* **2020**. [CrossRef] [PubMed]
26. Steele, C.W.; Karim, S.A.; Leach, J.D.G.; Bailey, P.; Upstill-Goddard, R.; Rishi, L.; Foth, M.; Bryson, S.; McDaid, K.; Wilson, Z.; et al. CXCR2 inhibition profoundly suppresses metastases and augments immunotherapy in pancreatic ductal adenocarcinoma. *Cancer Cell* **2016**, *29*, 832–845. [CrossRef] [PubMed]

frontiers in Cell and Developmental Biology

BRIEF RESEARCH REPORT
published: 23 July 2021
doi: 10.3389/fcell.2021.697939

Extracellular Vesicle-Based Detection of Pancreatic Cancer

Yesim Verel-Yilmaz[1†], Juan Pablo Fernández[1†], Agnes Schäfer[2], Sheila Nevermann[1], Lena Cook[2], Norman Gercke[1], Frederik Helmprobst[3,4], Christian Jaworek[2], Elke Pogge von Strandmann[5], Axel Pagenstecher[3], Detlef K. Bartsch[1], Jörg W. Bartsch[2†] and Emily P. Slater[1†]*

[1] Department of Visceral, Thoracic and Vascular Surgery, Philipps University Marburg, Marburg, Germany, [2] Department of Neurosurgery, Philipps University Marburg, Marburg, Germany, [3] Department of Neuropathology, Philipps University Marburg, Marburg, Germany, [4] Core Facility-Mouse Pathology and Electron Microscopy (MPEM), Philipps University Marburg, Marburg, Germany, [5] Institute for Tumorimmunology, Philipps University Marburg, Marburg, Germany

OPEN ACCESS

Edited by:
Jeffrey David Galley,
The Ohio State University,
United States

Reviewed by:
Cheng Wang,
Nanjing University, China
Xinlei Li,
Nationwide Children's Hospital,
United States

***Correspondence:**
Emily P. Slater
slater@med.uni-marburg.de

[†]These authors have contributed equally to this work

Specialty section:
This article was submitted to Molecular and Cellular Pathology, a section of the journal Frontiers in Cell and Developmental Biology

Received: 20 April 2021
Accepted: 29 June 2021
Published: 23 July 2021

Citation:
Verel-Yilmaz Y, Fernández JP, Schäfer A, Nevermann S, Cook L, Gercke N, Helmprobst F, Jaworek C, Pogge von Strandmann E, Pagenstecher A, Bartsch DK, Bartsch JW and Slater EP (2021) Extracellular Vesicle-Based Detection of Pancreatic Cancer. Front. Cell Dev. Biol. 9:697939. doi: 10.3389/fcell.2021.697939

Due to a grim prognosis, there is an urgent need to detect pancreatic ductal adenocarcinoma (PDAC) prior to metastasis. However, reliable diagnostic imaging methods or biomarkers for PDAC or its precursor lesions are still scarce. ADAM8, a metalloprotease-disintegrin, is highly expressed in PDAC tissue and negatively correlates with patient survival. The aim of our study was to determine the ability of ADAM8-positive extracellular vesicles (EVs) and cargo microRNAs (miRNAs) to discriminate precursor lesions or PDAC from healthy controls. In order to investigate enrichment of ADAM8 on EVs, these were isolated from serum of patients with PDAC (n = 52), precursor lesions (n = 7) and healthy individuals (n = 20). Nanoparticle Tracking Analysis and electron microscopy indicated successful preparation of EVs that were analyzed for ADAM8 by FACS. Additionally, EV cargo analyses of miRNAs from the same serum samples revealed the presence of miR-720 and miR-451 by qPCR and was validated in 20 additional PDAC samples. Statistical analyses included Wilcoxon rank test and ROC curves. FACS analysis detected significant enrichment of ADAM8 in EVs from patients with PDAC or precursor lesions compared to healthy individuals (p = 0.0005). ADAM8-dependent co-variates, miR-451 and miR-720 were also diagnostic, as patients with PDAC had significantly higher serum levels of miR-451 and lower serum levels of miR-720 than healthy controls and reached high sensitivity and specificity (AUC = 0.93 and 1.00, respectively) to discriminate PDAC from healthy control. Thus, detection of ADAM8-positive EVs and related cargo miR-720 and miR-451 may constitute a specific biomarker set for screening individuals at risk for PDAC.

Keywords: pancreatic cancer, extracellular vesicles, ADAM8, serum biomarkers, miRNA

INTRODUCTION

Pancreatic cancer is the fourth leading cause of cancer-related deaths in the world with an incidence of 45 in 100,000 and a 5-year survival rate of around 9% (Siegel et al., 2020). Among pancreatic cancer, pancreatic ductal adenocarcinoma (PDAC) is the most common type with more than 90% of all cases. A number of factors are responsible for the poor prognosis of PDAC that combines the difficulties in detecting the tumor in early stages, an aggressive biological behavior to account

for metastasis and the resistance to existing adjuvant therapies. To detect PDAC in early stages, only a few biomarkers are used routinely that are able to detect its presence and the lesions prior to its derivation (Bartsch et al., 2018). Exosomes are a defined type of extracellular vesicle (EV) ranging in size from 30 to 100 nm and secreted by all cell types including cancer cells. In the context of cancer, exosomes produced in tumor cells contain an abundance of cell-specific molecules that may facilitate the discrimination between cancer afflicted patients and healthy individuals (Sumrin et al., 2018).

Exosome cargo consists of proteins, nucleic acids and lipids (Colombo et al., 2014). Their composition is not only a reflection of the cell they originated from, but also appears to be a regulated process that remains not completely understood (Minciacchi et al., 2015). Content sorting and exosome release seem to not only depend on the type of donor cell, but also on its physiological or pathological state, different stimuli and the pathway of exosome biogenesis (Minciacchi et al., 2015). There are, however, marker proteins that have been found to be specific to EVs because they are related to their pathway of biogenesis. These proteins are, for example, members of the tetraspanin family (CD9, CD81) that are characteristic to exosomes, or flotillins (flotillin-1–2), which are frequently observed in exosomes and microvesicles alike (Kowal et al., 2016). Because exosome content is specific to their donor cell and exosomes can be isolated from bodily fluids such as blood, saliva, ascites or urine, they make promising candidates for early tumor diagnostics.

One rationale to use EVs as early diagnostic markers is their potential to transport tumor-associated micro RNAs (miRNAs) encapsulated in serum exosomes. MiRNAs are small non-coding RNAs of about 18–22 nt long that can be transferred to adjacent cells in the tumor microenvironment to modulate gene expression (Zonari et al., 2013; Su et al., 2016).

As protein cargo, membrane proteins involved in extracellular communication and remodeling are excellent candidates for exosome loading. Among these proteins metalloprotease-disintegrins (ADAM) are potential cargo proteins (reviewed in Shimoda and Khokha, 2017). Due to the interaction with the exosomal marker protein CD9, ADAM10 was one of the first members of the ADAM protease family found to be associated with exosomes (Keller et al., 2009). In previous studies, ADAM8 was defined as an ADAM protease associated with tumor progression and metastasis formation in PDAC (Valkovskaya et al., 2007; Schlomann et al., 2015). In addition, ADAM8 is expressed in tumor associated immune cells such as macrophages, NK cells and neutrophils (Jaworek et al., 2021). These data suggest that ADAM8 itself could be a diffusible molecule that is, similarly to the ADAM protease ADAM10, released in exosomes. Recently, much attention has been addressed to EVs, which may serve as a strategy of monitoring and managing disease status (Cufaro et al., 2019). Since ADAM8 expression is high in PDAC, it is likely that EVs isolated from its precursor lesions, Pancreatic intraepithelial Neoplasia (PanINs) types 2 and 3, could be packed with ADAM8 and ADAM8-associated molecular markers such as miRNAs as shown for breast cancer with correlated expression levels of ADAM8 and miRNA-720 (Das et al., 2016). MiRNAs are integral components of almost every cancer-related biological process, including cellular differentiation, proliferation, migration, apoptosis, EMT and angiogenesis. Here we hypothesized that high ADAM8 expression levels in pancreatic cancer is reflected by release of EVs expressing ADAM8 on their surface and that ADAM8 expression might cause miRNAs associated with ADAM8 expression to be cargo for ADAM8-positive EVs, so that these EVs can be used to detect pancreatic cancer in patient serum at early stages.

MATERIALS AND METHODS

Patient Cohort

Patients with familial pancreatic cancer (FPC) or PDAC treated at the Department of Visceral Surgery at University Hospital Marburg were enrolled in our study. All patients provided written informed consent prior to participating in this study. Ethical approval was granted from the local ethics committee at Marburg University, Faculty of Medicine (File No. 5/03). All tumors were histologically staged by an experienced pathologist according to the UICC-TNM (Union for International Cancer Control; tumor, node, metastasis) classification 2017 (Gospodarowicz and Brierley, 2017).

Extracellular Vesicle Preparation

250 µl of serum were diluted with 4.5 ml Hank's Salt Saline Buffer in a 15 ml falcon tube in order to lower sample viscosity and centrifuged at 800 × g for 5 min in order to eliminate any remaining cells. The supernatant was transferred to a new 15 ml falcon tube and centrifuged at 2,000 × g for 10 min to remove dead cells or cell debris (Théry et al., 2006; Melo et al., 2015). The supernatant was then transferred to a 5 ml syringe and filtered through a 0.2 µm pore filter and transferred to a 6.0 ml polypropylene bell-top quick-seal centrifuge tube and filled with Hank's Balanced Salt Solution (HBSS). The tubes were centrifuged at 100,000 × g and 4°C for 70 min. The pellet was resuspended in HBSS and transferred to a polypropylene 1.5 ml microcentrifuge tube and was centrifuged with an Optima MAX-XP Ultracentrifuge in a TLA-55 fixed angle rotor at 100,000 × g and 4°C for 100 min. The supernatant was discarded, and the pellet resuspended with 50 µl HBSS. Samples were stored at −80°C. In order to determine the particle size and concentration of isolated EVs, NTA was performed with the ZetaView® BASIC PMX-120 and the corresponding software ZetaView®.

Western Blot Analysis

To further phenotype isolated EVs, enriched proteins were detected in Western blots. Twenty µg protein determined by standard BCA were boiled in Laemmli buffer without β-Mercaptoethanol (60 mM Tris-HCl, pH = 6.8; 2% SDS; 10% Glycerol; 0.01% Bromphenol-Blue) for 5 min. Protein separation was performed by SDS-PAGE followed by a transfer onto PVDF membranes. Successful transfer was confirmed by Ponceau S staining. To block unspecific binding, membranes were immersed in 4% BSA in TBST (50 mM

Tris, pH = 7.5; 150 mM NaCl; 0.1% Tween-20) for 1 h, followed by incubation with primary antibody against CD9 (CBL162; Chemicon International, Temecula, CA, United States, 1:1,000 in 4% BSA in TBST) at 4°C overnight. After washing three times, blots were incubated with the respective secondary antibody for 1 h. After an additional washing step, signals were detected with SuperSignal™ West Pico PLUS Chemiluminescent Substrate (Thermo Fisher Scientific, Rockford, IL, United States). Additional antibodies were used to characterize the EVs isolated. These included CD81 (sc-166029; Santa Cruz Biotechnology), Flotillin-1 (PA5-18053; Thermo Fisher Scientific), hADAM8 (MAB10311; R&D Systems) and Calnexin (2679; Cell Signaling Technology).

FACS Analyses

FACS analyses were performed as previously described (Bartsch et al., 2018). Briefly, 1.5×10^9 EVs were coupled to 10 µl of 4 µm aldehyde/sulfate latex beads, 4% w/v in 100 µl PBS and incubated for 15 min at room temperature. Then 900 µl of PBS were added to reach a final volume of 1,000 µl and EVs and beads were incubated for another 30 min at room temperature. Beads were then blocked by adding 50 µl 10% BSA. Samples were centrifuged at 9,900 rpm for 1 min. Supernatant was discarded leaving a volume of 100 µl in the tubes. Samples were further blocked by incubation with 5 µl Human True Stain FcX Blocking Solution for 10 min at room temperature. Samples were then centrifuged again at 9,000 rpm for 1 min and the supernatant was discarded. Pellets were resuspended in 20 µl 2% BSA. Now, one half of the samples was incubated with 3 µl anti-ADAM8 (MAB10311, R&D Systems) at 4°C overnight. The next day, all samples were washed in 1 ml 2% BSA and centrifuged at 9,900 rpm for 1 min. All samples were treated with 20 µl of a blocking solution consisting of Human True Stain FcX Blocking Solution (BioLegend, San Diego, CA, United States) and 2% BSA and incubated with 3 µl alexa-488-tagged secondary antibody (Abcam, Cambridge, United Kingdom) at 4°C for 1 h. In a final step, samples were washed twice in 1 ml 2% BSA. The final bead pellet was resuspended in 1 ml PBS and transferred to 5 ml Flow Cytometry Tubes. Samples were stored at 4°C in the dark until measurement. The percentage of ADAM8-positive beads out of 100,000 total events was then calculated in a FACS analysis.

Electron Microscopy

EVs were stained for electron microscopy as previously described (Théry et al., 2006). Briefly, purified extracellular vesicles were fixed with an equal amount of 4% PFA. An amount of 5–7 µl was placed on a Formvar/carbon coated 200 mesh copper (Ted Pella Inc., Redding, CA) electron microscopy grid and incubated for 20 min. After the membrane adsorbed the vesicles the grids were washed with sterile filtered PBS and fixed for 5 min with 1% glutaraldehyde. The grids were washed 8 times for 2 min with sterile filtered water and then incubated with 1% uranyl acetate for 5 min. After an additional incubation with 2% methyl cellulose supplemented with 4% uranyl acetate (ratio 9:1) on ice, the excess fluid was removed with filter paper and the grids were air dried for up to 10 min. The exosomes were imaged with a Zeiss EM 900 at 80 kV.

Protease Activity Assay

Serum EVs isolated from either PDAC patients or healthy individuals were tested for ADAM8 activity by determining cleavage of a FRET-based polypeptide substrate with a high Kcat/Km for ADAM8 (PEPDab13, BioZyme, Inc., North Carolina, United States) as previously described (Schlomann et al., 2019). Briefly, 10 µM of PEPDab13 in 50 µl assay buffer (1 mM $ZnCl_2$, 20 mM Tris-HCl pH 8.0, 10 mM $CaCl_2$, 150 mM NaCl, 0.0006% Brij-35) was incubated with 3.75×10^8 EVs in a total volume of 100 µl. Resulting fluorescence was monitored every 2 min for 6 h at 37°C with a multiwell plate reader (FLUOstar OPTIMA, BMG Labtech, Offenburg, Germany) using λ_{ex} of 485 nm and an λ_{em} of 530 nm.

Serum Exosome miRNA Analysis

Total RNA carried by exosomes or other EVs in 250 µl of serum was extracted using the ExoRNeasy Serum/Plasma Midi Kit from Qiagen (Hilden, Germany) with the addition of a spike of 25 fmol of synthetic cel-miR-54 DNA as recommended by the manufacturer. The RNA was converted to cDNA using the miRNA Reverse Transcription Kit, miScript II RT Kit, also from Qiagen. The cDNA synthesis reaction was diluted and incubated with QuantiTect® SYBR Green PCR Master Mix, miScript Universal Primer and specific miScript Primer Assays. The real-time PCR reactions were run in a StepOnePlus Real time PCR System from Applied Biosystems (Darmstadt, Germany). The Δ threshold cycle (Ct) values were then calculated by subtracting the *cel*-miR-54 Ct value from the specific miRNA Ct value. For the analyses of cell lines SNORD95 was chosen as the endogenous control as previously described (Sperveslage et al., 2014). Ct values of each target miRNA transcript were normalized against the Ct value of SNORD95. Relative change in exosomal miRNA expression comparing wild type and knock-out cells was calculated using the ΔΔCt method.

Statistical Analyses

A Wilcoxon signed-rank test and a *t*-test were performed to assess whether the patient values were significantly different from control samples. A p-value of < 0.05 was considered to be statistically significant. The receiver operating characteristic curve analyses were performed using GraphPad Prism version 6 (GraphPad Software, La Jolla, CA, United States).

RESULTS

Clinicopathological Characteristics of the Recruited Patients, Including IAR With High-Risk Precursor Lesions

The characteristics of the 72 PDAC patients that were included in the study are presented in **Table 1**.

Preparation of Extracellular Vesicles From Patient Serum Samples

Extracellular vesicles including exosomes with an average diameter < 120 nm were isolated from patient serum using

TABLE 1 | Clinicopathological characteristics of the recruited patients.

		Cohort (n = 72)
Gender		
	Males (%)	37 (51%)
	Females (%)	35 (49%)
Median age at surgery, years (range)		68 (47–85)
UICC stage		
	I	11 (15.3%)
	II	10 (13.9%)
	III	46 (63.9%)
	IV	5 (6.9%)
Median survival, months (range)		22 (1–92)
Location	Pancreas	
	Head	65 (90.3%)
	body or tail	7 (9.7%)

In addition, 7 individuals at risk (IAR) who had undergone surgery for removal of precursor lesions were also recruited. These included 2 males and 5 females with a median age of 54 years. Histologically verified precursor lesions included 1 main duct intraductal papillary mucinous neoplasm (IPMN) with high grade dysplasia, 2 PanIN 3 and 4 PanIN 2. The healthy controls (n = 20) had a median age of 40 years and included 10 males and 10 females.

a range of purification steps including ultracentrifugation and filtration. The exosomes present in these preparations were identified by a number of analytical methods including ZetaView® analyses and electron microscopy to confirm existence of a double membrane and the proper size corresponding to exosomes (**Figures 1A–C**). The particle size and vesicle concentration did not vary among the preparations from the different sources (**Figures 1D,E**). In addition, CD9 was found in all preparations. However, whereas the control samples had relatively constant amounts of CD9 (**Figure 1F**), the tumor samples varied in abundance (**Figure 1G**). Additional markers were also tested to characterize the EVs. The preparations were also positive for CD81, Flotillin-1 and ADAM8, but were negative for calnexin (**Supplementary Figure 1**).

Diagnostic FACS Analysis of ADAM8 in Exosomes

In order to detect ADAM8 on the surface of exosomes, a bead-coupled FACS analysis was performed (**Figure 2**). Positive ADAM8 signals were observed both in control individuals and in PDAC patients. However, their proportion was significantly different, so that an enrichment of ADAM8 in serum exosomes from patients with PDAC or its precursor lesions compared to healthy individuals was observed ($p < 0.0001$ or $p = 0.0139$, respectively).

Cargo Analysis of Serum Derived EVs From Control and PDAC Patients

Since ADAM8 is located on EVs as shown by bead-coupled FACS analysis, we investigated whether ADAM8 confers enzymatic activity to EVs enriched in ADAM8. Activity of ADAM8 can

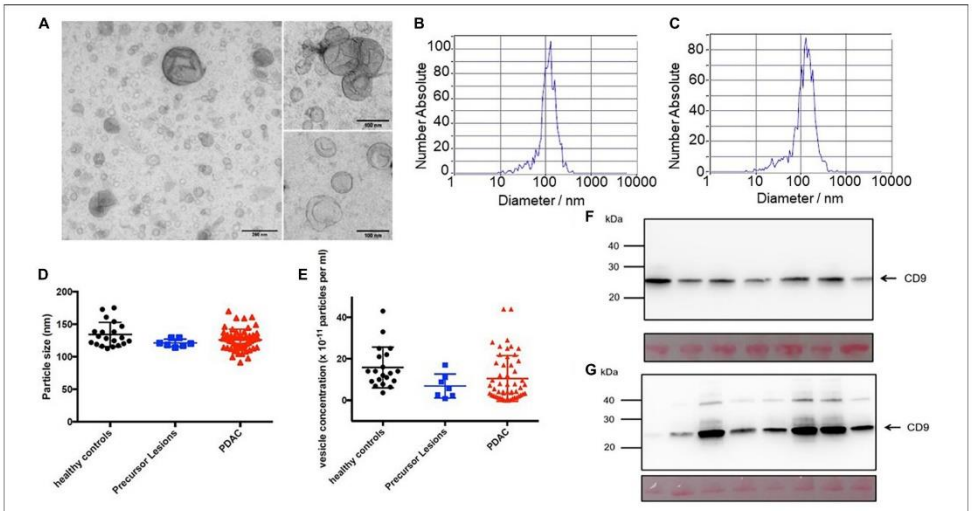

FIGURE 1 | Extracellular vesicles prepared from serum. Electron micrograph of EVs isolated from PDAC patient's serum **(A)**. Border is clearly delimited. ZetaView measurements of serum EVs isolated from healthy control **(B)** and PDAC patient **(C)**. Mean particle size **(D)** and mean vesicle concentration **(E)** of serum EVs from 7 patients with pancreatic precursor lesions (blue) and 52 patients with PDAC (red) compared to 20 healthy individuals (black). Immunoblots of serum EVs isolated from healthy individuals (n = 7, **F**) and PDAC patients (n = 8, **G**). Twenty µg protein determined by standard BCA were separated in an SDS-PAGE, blotted to PVDF membranes, stained with Ponceau S to confirm equal loading (lanes below), and probed with antibody against exosomal protein CD9.

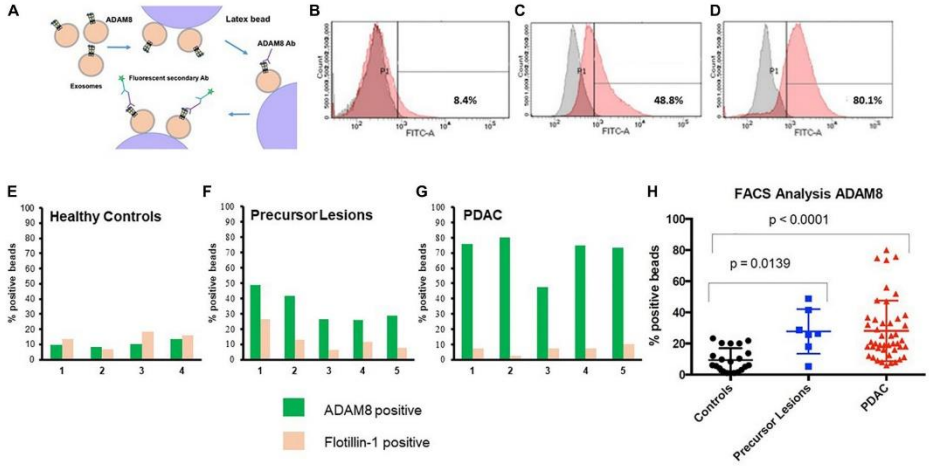

FIGURE 2 | Cartoon of protocol for flow cytometry (FACS) **(A)**. FACS analyses of serum EVs isolated from healthy individuals **(B)**, patients with precursor lesions **(C)** or PDAC **(D)**, attached to beads and detected with ADAM8 antibody. Results with secondary antibody alone appear in gray and those with both ADAM8 antibody and secondary antibody appear in red. Exemplary comparison of results for FACS analyses of serum exosomes from healthy controls (n = 4, **E**), precursor lesions (n = 5, **F**) or PDAC (n = 5, **G**) with ADAM8 (green) or Flotillin-1 (ochre) antibodies. Graphic representation of results from FACS analysis of EVs isolated from healthy individuals, patients with precursor lesions or PDAC from the total cohort, attached to beads and detected with ADAM8 antibody **(H)**.

be detected by using a FRET-based peptide representing the cleavage site of CD23 (Schlomann et al., 2019). Cleavage analysis of EVs isolated from either a control individual or a PDAC patient revealed a strongly enhanced proteolytic activity in EVs from the PDAC patient (**Figures 3A,B**). Although the FRET-based peptide is not specific for ADAM8 activity, it is very likely that the increased activity originates from ADAM8 as a protease with enhanced expression in EVs from PDAC patients as the FACS analysis suggests. In addition to the protein cargo analysis, a systematic screening for miRNAs was performed on EVs derived from control individuals and PDAC patients (**Figure 3C**). Interestingly, a set of 7 oncomiRNAs were found to be differentially regulated with the strongest upregulation for miRNA-451 and the strongest down-regulation for miRNA-720 (**Figure 3C**). To confirm differential regulation of these miRNAs in the PDAC patient cohort, exosomal miRNAs were isolated from the same serum samples and analyzed for miR-720 and miR-451 by semi-quantitative real time RT-PCR. Serum samples had been spiked with synthetic *C. elegans* miR-54 before miRNA isolation to be used as a normalization control. Statistical analyses were performed using the Wilcoxon rank test and ROC curve analysis. The miR-720 and miR-451 were also diagnostic, as patients with PDAC had significantly higher serum exosome levels of miR-451 and lower serum exosome levels of miR-720 than healthy controls and reached high sensitivity and specificity with an AUC = 0.9329 and 1.000, respectively, to discriminate PDAC (**Figures 3D–G**). In addition, serum exosomes were also isolated from patients with chronic pancreatitis (CP; n = 10) and precursor lesions (n = 7). Whereas serum exosomes from patients with precursor lesions had increased levels of miR-451, approaching the levels found in PDACs, CP patient serum exosomes did not. In contrast, the serum exosomes isolated from CP patients had lower levels of miR-720, similar to the PDAC serum exosomes, while the exosomes derived from serum of patients with precursor lesions had levels comparable to the healthy controls. Analysis of these miRNAs in Panc89 wild type and ADAM8 knock-out cells demonstrated that the levels of exosomal miR-451 decrease and the levels of exosomal miR-720 increase upon knock-out of ADAM8, suggesting a regulatory component of ADAM8 on these miRNAs (**Figure 3H**).

DISCUSSION

EV based serum diagnostics provides an additional and powerful diagnostic component in the field of liquid biopsies (Yee et al., 2020). With regard to EV diagnostic in PDAC, the concentration and size of EVs in patient serum has been correlated with tumor differentiation and overall survival in PDAC patients (Badovinac et al., 2021), but no specific cargo analysis of "diagnostic" EVs in serum has been reported up to now. In this respect, our results provide some novelties: First of all, we identified ADAM8, a protease with a therapeutic potential in PDAC, to be located in EVs that meet all criteria for exosomes. By establishing a bead-supported FACS analysis method to analyze surface located ADAM8 in EVs, we demonstrated that ADAM8-positive EVs

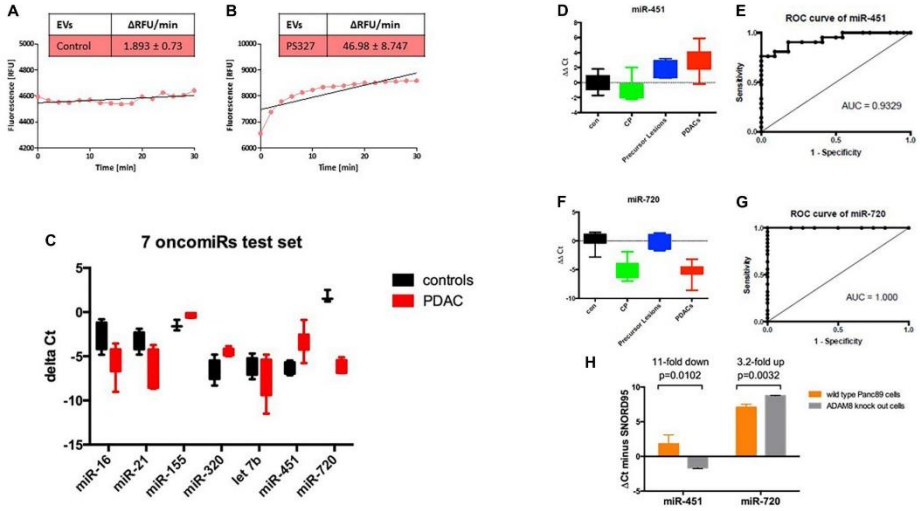

FIGURE 3 | Activity assay of ADAM8 in serum EVs isolated from healthy control **(A)** or PDAC patient **(B)**. Results of the test set using 7 oncomiRs with black boxes, controls, and red boxes, PDAC patients **(C)**. Boxplots of the (miR-451–*Cel*-54) **(D)** and (miR-720—*Cel*-54) **(F)** ΔΔCt values (patient minus healthy control) in the four groups (con, healthy control; CP, chronic pancreatitis; precursor lesions; and PDACs, pancreatic ductal adenocarcinoma). ROC curves for the comparison of exo-miR-451 **(E)** and exo-miR-720 **(G)** expression levels between patients with PDAC and healthy controls. ΔCt values for miRNAs isolated from EVs secreted by wild type Panc89 (orange) and ADAM8 knock-out cells (gray) **(H)**.

were significantly enriched in PDAC patients and were gradually increased with increasing tumor staging, at least when comparing precursor lesions with fully developed adenocarcinoma. From the biochemical point of view, we hypothesized that ADAM8 integrated in EV membranes should be enzymatically active. By peptide cleavage assays, we were able to confirm that ADAM8-enriched EVs show remarkable activities compared to those EVs from control individuals. These data support the notion that a FACS based analysis of EVs from PDAC patients can be performed to detect membrane proteins that are topologically oriented to the extracellular compartment.

In addition to the pure presence of ADAM8, we investigated potential exosomal miRNAs as EV cargo that could be regulated by ADAM8. A panel of "oncomiRNAs" including let-7b was screened from exosomal miRNAs extracted from healthy control individuals and PDAC patients, respectively. We found that ADAM8-positive EVs are specifically equipped with miRNAs that show a functional relevance in PDAC as exemplified by the results with miR-451 and miR-720 in serum EVs from these patients. From all miRNAs examined, exosomal (exo)-miRNA-720 and exo-miRNA-451 were the most significantly dysregulated. Exosomal miRNA-720 was significantly down-regulated in serum samples from chronic pancreatitis and PDAC patients and therefore suggested perfect accuracy in the diagnosis of CP and PDAC either in its hereditary or sporadic form (AUC = 1), exosomal miRNA-451 showed the highest up-regulation in precursor lesions and in PDAC, but not in samples from CP patients and was able to discriminate between precursor lesion or PDAC-afflicted patients and healthy individuals with relatively high accuracy and an AUC of 0.9329.

To further analyze the correlation of ADAM8 expression with miRNA expression levels, we used the PDAC cell line Panc89 with a genetic knockout of the *ADAM8* gene (Cook et al., manuscript in preparation). Using these cell lines, we further demonstrate that the regulation of miRNA-451 and miRNA-720 is dependent on ADAM8 expression levels, respectively. ADAM8 expression is inversely correlated with miRNA-720 levels, as an ADAM8-knockout in Panc89 cells leads to an increase in miRNA-720 levels (average 3.2-fold higher in Panc89_A8KO cells vs. Panc89_A8Ctrl cells), in accordance with the finding that we found decreased levels of miRNA-720 and increased ADAM8 levels in PDAC patients compared to control individuals. In contrast, miRNA-451 is positively correlated with ADAM8 expression levels, as this miRNA is decreased in Panc89_A8KO cells vs. Panc89_A8Ctrl cells. Similarly, we found increased miRNA-451 levels in PDAC patients with a higher ADAM8 expression. For both these miRNAs, functional roles in PDAC were reported that are in accordance with their described abundance in PDAC patient sera. In particular, it was shown that miRNA-720 inhibits pancreatic cancer cell proliferation and invasion by directly targeting cyclin D1 (Zhang et al., 2017)

so that down-regulation of miRNA-720 as observed in PDAC patients compared to healthy individuals has a potential tumor-promoting effect. ADAM8-dependent regulation of miRNA-720 was reported earlier in the breast cancer cell line MDA-MB-231 (Das et al., 2016) however in the opposite direction, an observation that we could reproduce with a CRISPR/Cas9 generated knockout of *ADAM8* in this cell line. In contrast, miRNA-451 can promote cell proliferation and metastasis in PDAC by down-regulating CAB39 (Calcium binding protein 39), a tumor suppressor upstream of STK11 (serine-threonine kinase 11) (Guo et al., 2017). Thus, as observed here, upregulation of miRNA-451 downregulated a tumor suppressor pathway. With miRNA-451 detecting precursor lesions and PDAC, but not chronic pancreatitis (CP) and miRNA 720 detecting CP but not precursor lesions in conjunction with ADAM8-positive EVs, we can achieve a high degree of specificity and sensitivity in serum EV analysis to predict pancreatic precursor lesion and PDAC while discriminating between chronic pancreatitis patients and healthy individuals.

CONCLUSION

Enrichment of ADAM8 in serum exosomes as well as the measurement of exosomal miRNAs, miR-720 and miR-451, may contribute to a biomarker profile for the screening of individuals for PDAC. More generally, our data provide evidence for an EV based communication in the PDAC tumor microenvironment that can be triggered in the pro-oncogenic direction by the presence of ADAM8. This biological signature in turn can be exploited for diagnostic purposes to detect PDAC lesions and fully developed PDAC, as demonstrated here.

DATA AVAILABILITY STATEMENT

The raw data supporting the conclusions of this article will be made available by the authors, without undue reservation.

ETHICS STATEMENT

The studies involving human participants were reviewed and approved by the Ethics Committee of the Marburg University, Faculty of Medicine (File No. 5/03). The patients/participants provided their written informed consent to participate in this study.

AUTHOR CONTRIBUTIONS

ES, DB, and JB conceived the study. YV-Y, JF, AS, SN, LC, NG, FH, CJ, EP, and AP performed the experiments and provided resources. ES and JB wrote the manuscript. All authors approved the submitted version.

FUNDING

Work was supported by the Deutsche Forschungsgemeinschaft (DFG) with a Clinical Research Unit grant (CRU 325) and grants to JB (BA-1606/4-1), to ES (SL-17/5-1), to DB (BA-1467/6-1), and to EP (PO-1408/14-1 and GRK 2573/1).

ACKNOWLEDGMENTS

We wish to thank all patients for participation in the study, Günter Klöppel for histological verification of precursor lesions and all members of the Department of Pathology, Marburg University, in particular Annette Ramaswamy, Corinna Keber and Carsten Denkert.

SUPPLEMENTARY MATERIAL

The Supplementary Material for this article can be found online at: https://www.frontiersin.org/articles/10.3389/fcell.2021.697939/full#supplementary-material

REFERENCES

Badovinac, D., Gorièar, K., Zavrtanik, H., Petriè, M., Lavrin, T., Mavec, N., et al. (2021). Plasma extracellular vesicle characteristics correlate with tumor differentiation and predict overall survival in patients with pancreatic ductal adenocarcinoma undergoing surgery with curative intent. *J. Pers. Med.* 11:77. doi: 10.3390/jpm11020077

Bartsch, D. K., Gercke, N., Strauch, K., Wieboldt, R., Matthäi, E., Wagner, V., et al. (2018). The combination of MiRNA-196b, LCN2, and TIMP1 is a potential set of circulating biomarkers for screening individuals at risk for familial pancreatic cancer. *J. Clin. Med.* 7:295. doi: 10.3390/jcm7100295

Colombo, M., Raposo, G., and Théry, C. (2014). Biogenesis, secretion, and intercellular interactions of exosomes and other extracellular vesicles. *Annu. Rev. Cell Dev. Biol.* 30, 255–289. doi: 10.1146/annurev-cellbio-101512-122326

Cufaro, M. C., Pieragostino, D., Lanuti, P., Rossi, C., Cicalini, I., Federici, L., et al. (2019). Extracellular vesicles and their potential use in monitoring cancer progression and therapy: the contribution of proteomics. *J. Oncol.* 2019:1639854. doi: 10.1155/2019/1639854

Das, S. G., Romagnoli, M., Mineva, N. D., Barillé-Nion, S., Jézéquel, P., Campone, M., et al. (2016). miR-720 is a downstream target of an ADAM8-induced ERK signaling cascade that promotes the migratory and invasive phenotype of triple-negative breast cancer cells. *Breast Cancer Res.* 18:40. doi: 10.1186/s13058-016-0699-z

Gospodarowicz, M. K., and Brierley, J. D. (2017). *TNM Classification of Malignant Tumors*. Oxford: Wiley-Blackwell.

Guo, R., Gu, J., Zhang, Z., Wang, Y., and Gu, C. (2017). MiR-451 promotes cell proliferation and metastasis in pancreatic cancer through targeting CAB39. *Biomed. Res. Int.* 2017:2381482. doi: 10.1155/2017/2381482

Jaworek, C., Verel-Yilmaz, Y., Driesch, S., Ostgathe, S., Cook, L., Wagner, S., et al. (2021). Cohort analysis of ADAM8 expression in the PDAC tumor stroma. *J. Pers. Med.* 11:113. doi: 10.3390/jpm11020113

Keller, S., König, A.-K., Marmé, F., Runz, S., Wolterink, S., Koensgen, D., et al. (2009). Systemic presence and tumor-growth promoting effect of ovarian carcinoma released exosomes. *Cancer Lett.* 278, 73–81. doi: 10.1016/j.canlet.2008.12.028

Kowal, J., Arras, G., Colombo, M., Jouve, M., Morath, J. P., Primdal-Bengtson, B., et al. (2016). Proteomic comparison defines novel markers to characterize heterogeneous populations of extracellular vesicle subtypes. *Proc. Natl. Acad. Sci. U.S.A.* 113, E968–E977. doi: 10.1073/pnas.1521230113

Melo, S. A., Luecke, L. B., Kahlert, C., Fernandez, A. F., Gammon, S. T., Kaye, J., et al. (2015). Glypican-1 identifies cancer exosomes and detects early pancreatic cancer. *Nature* 523, 177–182. doi: 10.1038/nature14581

Minciacchi, V. R., You, S., Spinelli, C., Morley, S., Zandian, M., Aspuria, P. J., et al. (2015). Large oncosomes contain distinct protein cargo and represent a separate functional class of tumor-derived extracellular vesicles. *Oncotarget* 6, 11327–11341. doi: 10.18632/oncotarget.3598

Schlomann, U., Dorzweiler, K., Nuti, E., Tuccinardi, T., Rossello, A., and Bartsch, J. W. (2019). Metalloprotease inhibitor profiles of human ADAM8 in vitro and in cell-based assays. *Biol. Chem.* 400, 801–810. doi: 10.1515/hsz-2018-0396

Schlomann, U., Koller, G., Conrad, C., Ferdous, T., Golfi, P., Garcia, A. M., et al. (2015). ADAM8 as a drug target in pancreatic cancer. *Nat. Commun.* 6:6175. doi: 10.1038/ncomms7175

Shimoda, M., and Khokha, R. (2017). Metalloproteinases in extracellular vesicles. *Biochim. Biophys. Acta Mol. Cell Res.* 1864(11 Pt A), 1989–2000. doi: 10.1016/j.bbamcr.2017.05.027

Siegel, R. L., Miller, K. D., and Jemal, A. (2020). Cancer statistics, 2020. *CA Cancer J. Clin.* 70, 7–30. doi: 10.3322/caac.21590

Sperveslage, J., Hoffmeister, M., Henopp, T., Klöppel, G., and Sipos, B. (2014). Establishment of robust controls for the normalization of miRNA expression in neuroendocrine tumors of the ileum and pancreas. *Endocrine* 46, 226–230. doi: 10.1007/s12020-014-0202-

Su, M.-J., Aldawsari, H., and Amiji, M. (2016). Pancreatic cancer cell exosome-mediated macrophage reprogramming and the role of microRNAs 155 and 125b2 transfection using nanoparticle delivery systems. *Sci. Rep.* 6:30110. doi: 10.1038/srep30110

Sumrin, A., Moazzam, S., Khan, A. A., Ramzan, I., Batool, Z., Kaleem, S., et al. (2018). Exosomes as biomarker of cancer. *Braz. Arch. Biol. Technol.* 61. doi: 10.1590/1678-4324-2018160730

Théry, C., Amigorena, S., Raposo, G., and Clayton, A. (2006). Isolation and characterization of exosomes from cell culture supernatants and biological fluids. *Curr. Protoc. Cell Biol.* 30, 3.22.21–23.22.29.

Valkovskaya, N., Kayed, H., Felix, K., Hartmann, D., Giese, N. A., Osinsky, S. P., et al. (2007). ADAM8 expression is associated with increased invasiveness and reduced patient survival in pancreatic cancer. *J. Cell Mol. Med.* 11, 1162–1174. doi: 10.1111/j.1582-4934.2007.00082.x

Yee, N. S., Zhang, S., He, H.-Z., and Zheng, S.-Y. (2020). Extracellular vesicles as potential biomarkers for early detection and diagnosis of pancreatic cancer. *Biomedicines* 8:581. doi: 10.3390/biomedicines8120581

Zhang, Y., Su, Y., Zhao, Y., Lv, G., and Luo, Y. (2017). MicroRNA-720 inhibits pancreatic cancer cell proliferation and invasion by directly targeting cyclin D1. *Mol. Med. Rep.* 16, 9256–9262. doi: 10.3892/mmr.2017.7732

Zonari, E., Pucci, F., Saini, M., Mazzieri, R., Politi, L. S., Gentner, B., et al. (2013). A role for miR-155 in enabling tumor-infiltrating innate immune cells to mount effective antitumor responses in mice. *Blood* 122, 243–252. doi: 10.1182/blood-2012-08-449306

Conflict of Interest: The authors declare that the research was conducted in the absence of any commercial or financial relationships that could be construed as a potential conflict of interest.

Publisher's Note: All claims expressed in this article are solely those of the authors and do not necessarily represent those of their affiliated organizations, or those of the publisher, the editors and the reviewers. Any product that may be evaluated in this article, or claim that may be made by its manufacturer, is not guaranteed or endorsed by the publisher.

International Journal of
Molecular Sciences

MDPI

Article

ADAM8-Dependent Extracellular Signaling in the Tumor Microenvironment Involves Regulated Release of Lipocalin 2 and MMP-9

Lena Cook [1], Marie Sengelmann [1], Birte Winkler [1], Constanze Nagl [1], Sarah Koch [1], Uwe Schlomann [1,2], Emily P. Slater [2], Miles A. Miller [3], Elke Pogge von Strandmann [4], Bastian Dörsam [4], Christian Preußer [4] and Jörg W. Bartsch [1,*]

1 Department of Neurosurgery, Philipps University Marburg, Baldingerstr, 35033 Marburg, Germany; cookl@staff.uni-marburg.de (L.C.); sengelma@students.uni-marburg.de (M.S.); Winkler8@students.uni-marburg.de (B.W.); conni.nagl93@googlemail.com (C.N.); sarah.koch94@yahoo.de (S.K.); uweschlomann@hotmail.com (U.S.)
2 Department of Visceral Surgery, Philipps University Marburg, Baldingerstr, 35033 Marburg, Germany; slater@med.uni-marburg.de
3 Center for Systems Biology, Massachusetts General Hospital, 185 Cambridge Street, Boston, MA 02114, USA; Miles.Miller@mgh.harvard.edu
4 Department of Medicine, Institute for Tumor Immunology, Philipps University Marburg, 35043 Marburg, Germany; poggevon@staff.uni-marburg.de (E.P.v.S.); bastian_doersam@gmx.de (B.D.); preusserc@staff.uni-marburg.de (C.P.)
* Correspondence: jbartsch@med.uni-marburg.de; Tel.: +49-6421-58-61173

Citation: Cook, L.; Sengelmann, M.; Winkler, B.; Nagl, C.; Koch, S.; Schlomann, U.; Slater, E.P.; Miller, M.A.; von Strandmann, E.P.; Dörsam, B.; et al. ADAM8-Dependent Extracellular Signaling in the Tumor Microenvironment Involves Regulated Release of Lipocalin 2 and MMP-9. *Int. J. Mol. Sci.* **2022**, *23*, 1976. https://doi.org/10.3390/ijms23041976

Academic Editor: József Tőzsér

Received: 30 December 2021
Accepted: 8 February 2022
Published: 10 February 2022

Abstract: The metalloprotease-disintegrin ADAM8 is critically involved in the progression of pancreatic cancer. Under malignant conditions, ADAM8 is highly expressed and could play an important role in cell–cell communication as expression has been observed in tumor and immune cells of the tumor microenvironment (TME) such as macrophages. To analyze the potential role of ADAM8 in the TME, ADAM8 knockout PDAC tumor cells were generated, and their release of extracellular vesicles (EVs) was analyzed. In EVs, ADAM8 is present as an active protease and associated with lipocalin 2 (LCN2) and matrix metalloprotease 9 (MMP-9) in an ADAM8-dependent manner, as ADAM8 KO cells show a lower abundance of LCN2 and MMP-9. Sorting of ADAM8 occurs independent of TSG101, even though ADAM8 contains the recognition motif PTAP for the ESCRTI protein TSG101 within the cytoplasmic domain (CD). When tumor cells were co-cultured with macrophages (THP-1 cells), expression of LCN2 and MMP-9 in ADAM8 KO cells was induced, suggesting that macrophage signaling can overcome ADAM8-dependent intracellular signaling in PDAC cells. In co-culture with macrophages, regulation of MMP-9 is independent of the M1/M2 polarization state, whereas LCN2 expression is preferentially affected by M1-like macrophages. From these data, we conclude that ADAM8 has a systemic effect in the tumor microenvironment, and its expression in distinct cell types has to be considered for ADAM8 targeting in tumors.

Keywords: tumor microenvironment; extracellular vesicles; ADAM8; lipocalin 2; MMP-9; regulation; PDAC

1. Introduction

Extracellular proteolysis is a major process in tumor biology, thereby regulating the proliferation and invasion of tumor cells into the surrounding tissue, and recruitment of immune cells to the tumor site, eventually shaping a tumor-promoting tumor microenvironment [1]. In recent studies, A disintegrin and metalloprotease 8 (ADAM8) was identified as an extracellular metalloprotease-disintegrin important for tumor progression, invasion, and metastasis in pancreatic ductal adenocarcinoma (PDAC) [2]. PDAC is one of the most lethal solid tumors with a 5-year survival rate of less than 8%. In addition, the incidence

of PDAC is on the rise and could become a leading cause of cancer deaths by 2030 [3]. A strong desmoplastic stroma response to tumor growth is a hallmark of PDAC and, at least partially, a cause for the devastating patient prognosis [4]. In particular, the tumor microenvironment (TME) with its inflammatory nature activates several immune cell types and suppresses the immune competence of the TME, suggesting an intense communication between tumor and immune cells through the extracellular matrix (ECM). In this regard, ADAM proteases, as membrane-located shedding enzymes, are capable of creating these intercellular signals by the controlled release of membrane proteins involved in immune modulation. One such ADAM protease is ADAM8, a metalloprotease-disintegrin with a proven record of tumor-supporting effects when expressed in tumor cells, thereby facilitating tumor progression, invasion, and immune cell recruitment [2,5]. Recently, a systematic analysis of tumor-associated immune cells in tumor tissues of PDAC patients revealed the additional expression of ADAM8 in macrophages, neutrophils, and NK cells [6]. ADAM8$^+$ immune cells can transmigrate through endothelia and invade the ECM, as demonstrated in several inflammation models (e.g., [7,8]). These findings suggest that ADAM8 could also exert its function in immune cells of the TME. Given the strong endogenous expression of ADAM8 in macrophages, we hypothesized that ADAM8 serves important functions in tumor cell–macrophage interactions. These interactions could be mediated by extracellular vesicles (EVs), a defined type of lipid-enclosed particle ranging in size from 30 to 100 nm. ADAM8 was identified as an EV cargo and is of diagnostic value for the early detection of PDAC lesions [9]. In addition, cargo analyses of ADAM8-positive EVs isolated from PDAC patients revealed diagnostic miRNAs correlated with ADAM8 expression levels, such as miR-451 and miR-720. These miRNAs could play a role in regulating cellular functions in the TME as ADAM8-dependent miRNAs. In the current study, we analyzed EV release from PDAC cells and the cellular interactions between macrophages and PDAC tumor cells in an ADAM8-dependent manner. PDAC cell lines with endogenous expression of ADAM8 or a CRISPR/Cas9 knockout of the *ADAM8* gene were co-cultivated with macrophages, and the resulting changes in gene expression were analyzed.

2. Results

2.1. CRISPR/Cas 9 Knockout of ADAM8 in Tumor Cell Lines MDA MB-231 and Panc89

Initially, we used cell lines MDA MB-231 and Panc89 for knockout of the *ADAM8* gene, as these cell lines express high endogenous ADAM8 levels. After transfection and selection with puromycin, several representative cell clones were raised and analyzed further. As the effect of ADAM8 deficiency in MB-231 cells has been described extensively [10,11], these cells were only included in some experiments. For Panc89 cells, two representative ADAM8 knockout clones were chosen for the analysis of ADAM8-dependent effects (Figure 1). Loss of ADAM8 expression in Panc89 cells was confirmed in control ("WT") and KO cell clones by qPCR, Western blot, ELISA, and immunocytochemistry (Figure 1A–D). ADAM8 mRNA was hardly detectable in KO clones by qPCR, and no protein expression was measurable, even by the ELISA assay (Figure 1), where the sensitivity of the assay has a detection limit of 62 pg/mL.

Furthermore, migration was analyzed and showed a reduction for KO 1 (Figure 1E,F). More clones were tested for migration and showed similar results (Supplementary Figure S1A). Proliferation was not affected when comparing control with KO 1 cells (Figure 1H), whereas invasion was significantly reduced upon ADAM8 deficiency (Figure 1G), suggesting that, similar to previous results, ADAM8 has a strong effect on cellular motility in tumor cells. Additionally, another PDAC cell line called AsPC1 was used for CRISPR/Cas9 ADAM8 KO, and the results of AsPC1 and MB-231 ± ADAM8 applied to the here described experiments are shown in Supplementary Figure S2.

To further analyze the potential effect of ADAM8 deficiency on extracellular proteolysis, peptide cleavage assays using five distinct FRET-based peptides were utilized [12], allowing a comparative inference for the proteases MMP-2, MMP-9, ADAM8, and ADAM17 (Figure 1P,Q). Significant ADAM17 activity was not detectable in Panc89 control and

KO cells, whereas ADAM17 mRNA expression was detectable with Ct values of ~18 (Figure 1N,O) for both Panc89 control and KO cells. Activity levels of MMP-2 were low with no difference between Panc89 control and KO cells, but mRNA expression of MMP-2 was significantly downregulated in Panc89 KO cells (Figure 1N,O).

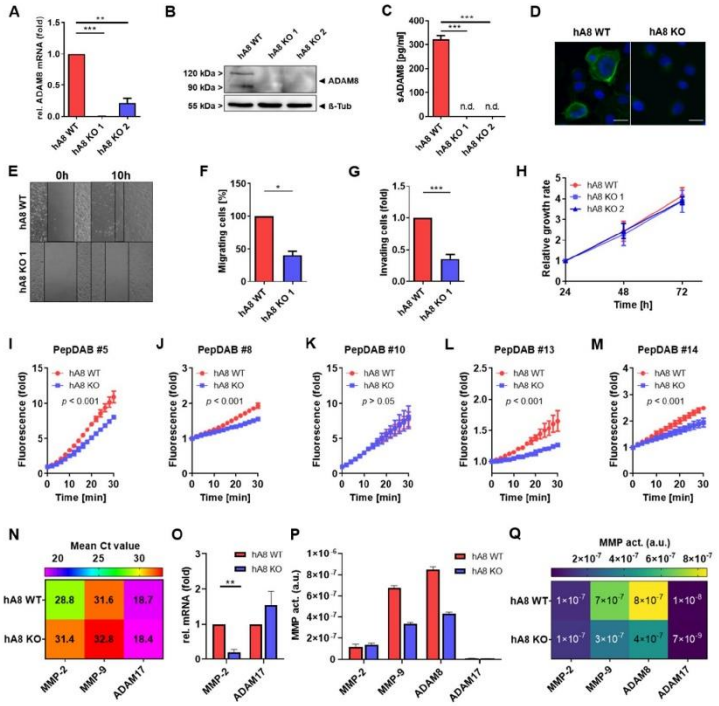

Figure 1. ADAM8 in Panc89 hA8 WT and KO cells. (**A**) mRNA expression, (**B**) Western blot, and (**C**) soluble ADAM8 levels ($n = 2$) in Panc89 hA8 WT and KO 1 and 2. (**D**) Representative immunofluorescence (green) of ADAM8 in Panc89 hA8 WT and KO cells; scale bar, 20 µm. (**A**–**D**) show the successful downregulation of ADAM8 in KO 1 and 2 cells. (**E**,**F**) display scratch assay of Panc89 hA8 WT and KO 1 cells. Images were acquired at 0 h and 10 h ($n = 2$). (**G**) Invasion assay of Panc89 hA8 WT and KO cells in Matrigel using transwell inserts (24 h) demonstrates a decreased invasive behavior in KO cells ($n = 3$). (**H**) Relative growth rates of Panc89 cells show no significant differences between hA8 WT, KO 1, and KO 2 cells ($n = 2$). MMP and ADAM activity assays of Panc89 hA8 WT- and KO cell-derived supernatants (SN) by using PepDAB# (**I**) 5, (**J**) 8, (**K**) 10, (**L**) 13, and (**M**) 14 are illustrated ($n = 2$). (**N**) Heat map of mean Ct values demonstrates the absolute gene expression of MMP-2, MMP-9, and ADAM17, and (**O**) diagram shows the relative mRNA expression of MMP-2 and ADAM17 in Panc89 hA8 WT and KO 1 cells ($n = 2$). (**P**,**Q**) show results of protease activities and cleavage rates of MMP-2, MMP-9, ADAM8, and ADAM17 calculated for hA8 WT and KO 1 cell-derived supernatants by PrAMA inference. Data are presented as mean values ± S.D. * $p < 0.05$, ** $p < 0.01$, *** $p < 0.001$.

In contrast, for MMP-9 and ADAM8, activity levels were reduced in Panc89 KO cells compared to control cells, suggesting that ADAM8 and MMP-9 activities are associated, even though there are very low levels of MMP-9 mRNA (Figure 1N) and protein (Supplementary Figure S1A) detectable in Panc89 cells.

2.2. ADAM8 Regulates Intracellular and Extracellular LCN2 Levels in Panc89 Cells

The data shown in Figure 1 suggest that the presence of ADAM8 regulates extracellular proteolytic activity. Thus, we attempted to identify the impact of ADAM8 on the extracellular abundance of other proteases such as MMP family members and potential inhibitors and modulators of protease activity by an antibody-based array screen using MB-231 cells deficient in *ADAM8* (Supplementary Figures S3 and S4). Notably, the strongest effects of the ADAM8 knockout were observed, in addition to ADAM8 itself, for MMP-9 and lipocalin 2 (LCN2, Figure 2A–C). mRNA expression levels of LCN2 were quantified in MB-231 cells by qPCR, showing that the observed downregulation of LCN2 occurs at the protein and, less pronounced, at the mRNA level (Figure 2D). The results obtained for MB-231 cells were confirmed for Panc89 cells (Figure 2F,G), demonstrating decreased relative LCN2 mRNA (Figure 2F). In accordance, the protein expression of LCN2 was decreased in Panc89 hA8 KO cell clones 1 and 2 compared to control cells. More Panc89 hA8 KO clones that were tested for LCN2 at the protein level showed a decrease in protein expression (Supplementary Figure S1B). From these results, we conclude that ADAM8 regulates levels of MMP-9 in MB-231 cells and LCN2 in MB-231 and Panc89 cells. The correlation between ADAM8 and LCN2 levels raised the hypothesis that LCN2 might regulate ADAM8 activity itself. To address this, we performed a peptide cleavage assay using the peptide PepDAB#13 in conjunction with recombinant ADAM8 (50 ng) and recombinant LCN2 at concentrations of 1, 10, and 100 ng and determined ADAM8 activity (Figure 2H). After pre-incubation with recombinant LCN2 for 30 min, we did not find that ADAM8 activity in vitro is affected by LCN2, suggesting that lipocalin 2 is not a physiological inhibitor of ADAM8 activity.

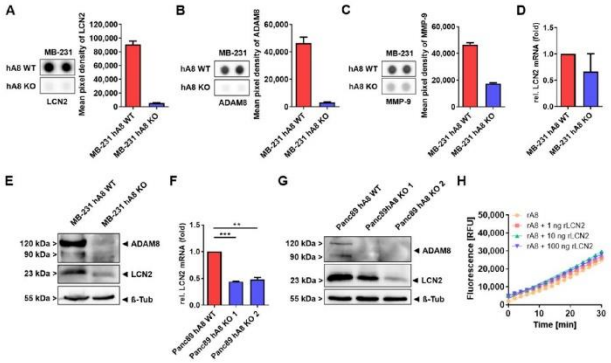

Figure 2. ADAM8 regulates LCN2 levels in tumor cell lines MB-231 and Panc89. The Human Protease/Protease Inhibitory Array demonstrates downregulation of ADAM8 (**A**), MMP-9 (**B**), and LCN2 (**C**) in supernatants derived from MB-231 hA8 KO cells. (**D**) mRNA expression and (**E**) representative Western blot of LCN2 in MB-231 hA8 WT and hA8 KO cells confirm results from (**C**) ($n = 2$). (**F**) mRNA expression and (**G**) representative Western blot of LCN2 in Panc89 hA8 WT, KO 1, and KO 2 cells demonstrate decreased LCN2 expression in hA8 KO cells ($n = 2$). Data are presented as mean values ± S.D., ** $p < 0.01$, *** $p < 0.001$. (**H**) Recombinant LCN2 (1 ng, 10 ng, 100 ng) does not affect protease activity of recombinant ADAM8 using a CD23 substrate (PepDAB# 13).

2.3. ADAM8 Is Present in EVs as an Active Protease

We further analyzed a possible localization of ADAM8 in extracellular vesicles (EVs). EVs were isolated according to a protocol recommended by the German Society for Extracellular Vesicles (GSEV [13]), using ultracentrifugation and subsequent validation of EV preparations (Figure 3). At first, successful isolation of EVs from Panc89 cells was confirmed by NanoFCM (Figure 3A) and revealed particle sizes of 40–120 nm. Furthermore, electron microscopy was employed to visualize EVs with their membrane composition (Figure 3B).

Western blots were performed to detect EV markers Flotillin-1, the ESCRT I protein TSG101, and CD81. All proteins were also tested in whole-cell lysates and demonstrated accumulation of these proteins in EVs from control and ADAM8 KO cells (Figure 3C). Next, we detected the presence of ADAM8 in EVs by Western blots (Figure 3C). In whole-cell lysates of Panc89 control cells, ADAM8 expression was detectable with a strong signal for pro-ADAM8 and the active, mature form. When compared to ADAM8 expression in EVs, mainly the mature form and some lower-molecular weight forms were detected, suggesting that the ADAM8 protein is enriched in EVs as an active protease. In agreement, protease activities were determined for EVs isolated from either control or ADAM8 KO cells (Figure 3D). To investigate the sorting of ADAM8 into EVs, we looked at TSG101, a protein that is part of the ESCRT machinery. TSG101 has been described to recognize PS/TAP motifs at the C-terminus of proteins [14], which can be found at the C-terminal end of the ADAM8 amino acid sequence. Therefore, for that, we checked a possible co-localization of TSG101 (green) and ADAM8 (red) in Panc89 cells (Figure 3E). Therefore, Panc89 hA8 KO cells were used to insert stable full-length ADAM8 ("hA8 rescue") into the AAVS1 locus. Barely any or no co-localization of ADAM8 and TSG101 was evident in the immunofluorescent staining of Panc89 hA8 rescue cells (Figure 3E, lower right). We also wanted to see whether ADAM8 lacking the PTAP motif would still be packaged into EVs. EVs were isolated from Panc89 hA8 rescue (described in Figure 3E), Panc89 hA8 ΔCD rescue (insertion of ADAM8 without the C-terminal domain), and Panc89 hA8 KO cells. The immunodetection in Figure 3F shows a positive signal for ADAM8 in EVs derived from Panc89 hA8 rescue and Panc89 hA8 ΔCD rescue cells.

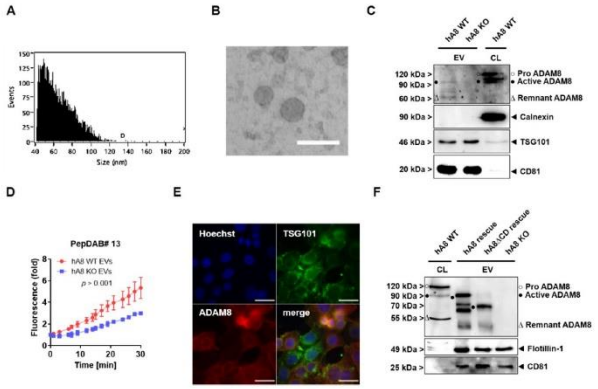

Figure 3. ADAM8 is secreted by Panc89 hA8 WT-derived extracellular vesicles (EV). (**A**) The histogram shows the particle size distribution of EVs isolated from Panc89 cells (analyzed by NanoFCM). (**B**) Electron microscopy of Panc89 hA8 WT-derived EVs demonstrates the successful isolation of EVs; scale bar, 100 nm. Representative Western blot of EVs derived either from Panc89 hA8 WT or KO cells, and cell lysate (CL) of Panc89 hA8 WT cells is shown in (**C**). ADAM8 can be detected as active and remnant ADAM8 in EVs. The negative control Calnexin was not detectable in isolated EVs. The measured activity of Panc89 hA8 WT- and KO-derived EVs on PepDAB #13 is displayed in (**D**) and is upregulated in Panc89 hA8 WT-derived EVs (n = 2). (**E**) Representative images of immunofluorescence staining of Panc89 hA8 rescue cells with Hoechst dye (upper left), TSG101 (green; upper right), and ADAM8 (red; lower left). Merged images are displayed in the lower right and show that TSG101 shows little or no co-localization with ADAM8. Scale bar, 50 µm. (**F**) shows the detection of ADAM8, Flotillin-1, and CD81 via Western blot of Panc89 hA8 WT CL and EV preparations isolated from Panc89 hA8 WT, Panc89 hA8 rescue, Panc89 hA8 ΔCD rescue, and Panc89 hA8 KO cells. ADAM8 is detectable in all EV preparations except in EVs isolated from hA8 KO cells. Data are presented as mean values ± S.D.

2.4. ADAM8 Protein Content Correlates with LCN2 Concentration in EVs Derived from Panc89 and MB-231 Cells and MMP-9 Concentration in EVs from MB-231 Cells

Given the correlation of ADAM8 with the extracellular presence of LCN2 and MMP-9, we next investigated whether EVs containing ADAM8 are composed similarly in Panc89 and MB-231 cells (Figure 4A,B). EVs were isolated from MB-231 and Panc89 tumor cells ± ADAM8, and their protein cargo was analyzed by Western blot. Notably, EVs from ADAM8-deficient MB-231 and Panc89 cells were very low in LCN2. However, in the case of EVs derived from MB-231 cells, the secretion of MMP-9 was lower, whereas in Panc89, MMP-9 was not detectable (Figure 4A).

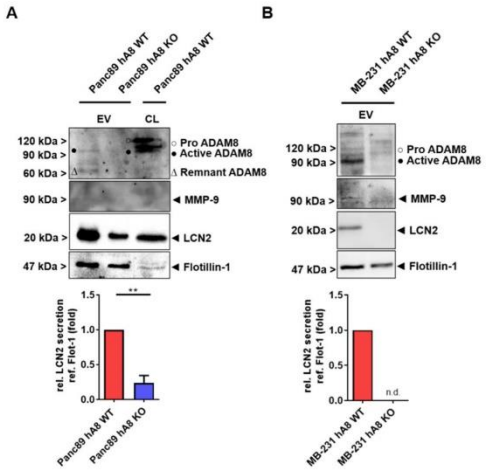

Figure 4. ADAM8 and LCN2 levels correlate in Panc89- and MB-231-derived extracellular vesicles (EV). Representative Western blots (**A**) of EVs derived from either Panc89 hA8 WT or KO cells, and cell lysate (CL) of Panc89 hA8 WT cells, and (**B**) of EVs derived from either MB-231 hA8 WT or MB-231 KO cells show the detection of ADAM8, MMP-9, LCN2, and Flotillin-1 in the upper part. Diagrams below illustrate the quantification and downregulation of LCN2 secretion (relative to Flotillin-1 secretion) in EVs isolated from Panc89 (hA8 WT or hA8 KO 1) or MB-231 (hA8 WT or hA8 KO) cells ($n = 3$). Data are presented as mean values ± S.D. ** $p < 0.01$.

2.5. LCN2 Effect on Downstream Signaling of EGFR in PDAC Cells

The controlled release of LCN2 into the tumor microenvironment could cause effects on EGFR shuttling and on activation of EGFR by phosphorylation, as reported in a recent study [15]. Therefore, we tested the EGFR activation status in Panc89 cells in the absence or presence of ADAM8. In addition, we used exogenous LCN2 in an attempt to compensate for effects caused by downregulation of LCN2 in ADAM8 knockout cells (Figure 5). As a positive control for EGFR activation, TGF-α was used. Figure 5A illustrates the downregulation of LCN2 in Panc89 hA8 KO cells. Apparently, the addition of recombinant LCN2 could not induce endogenous LCN2 expression in KO cells, whereas the application of TGF-α increased LCN2 expression to Panc89 hA8 WT levels (Figure 5B). After quantifying the extent of EGFR activation, no EGFR phosphorylation could be detected in this experiment (Figure 5C). However, lower activation of MAPK could be observed in Panc89 hA8 KO, further enhanced by the addition of TGF-α in WT and KO cells (Figure 5D). Total EGFR and MAPK protein expression was not affected by ADAM8 KO in Panc89 cells (Supplementary Figure S5).

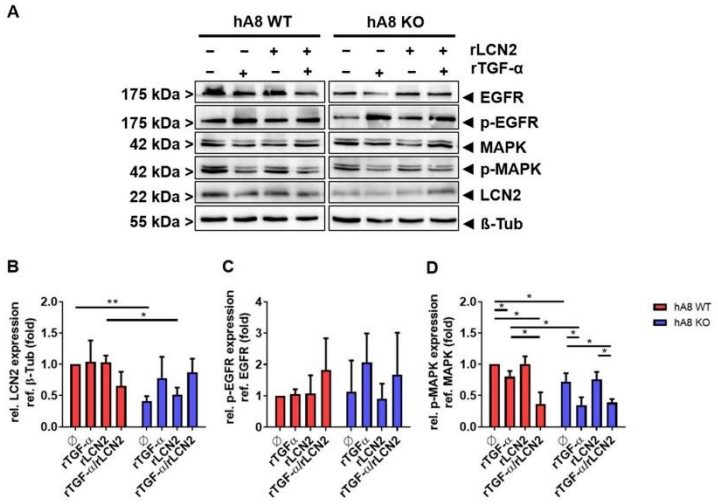

Figure 5. Downstream signaling of EGFR is affected by ADAM8 KO in Panc89 cells. (**A**) Representative immunoblot of EGFR and MAPK phosphorylation, and LCN2 expression after treatment with recombinant LCN2 (rLCN2) and recombinant transforming growth factor-alpha (rTGF-α) for 1 h. (**B**) Quantification of LCN2 shows the downregulation of LCN2 expression in Panc89 hA8 KO cells. The addition of rLCN2 does not increase LCN2 expression in Panc89 hA8 KO cells, whereas rTGF-α alone or combined with rLCN2 adjusts LCN2 expression to Panc89 hA8 WT levels. (**C**) Quantification of p-EGFR illustrates no significant changes in EGFR phosphorylation of Panc89 hA8 KO compared to Panc89 hA8 WT cells. (**D**) The diagram displays the quantification of p-MAPK. The phosphorylation of MAPK is significantly downregulated in Panc89 hA8 KO cells. rTGF-α stimulation decreases MAPK phosphorylation in both Panc89 hA WT and KO cells. Data are presented as mean values ± S.D. * $p < 0.05$, ** $p < 0.01$ ($n = 2$).

2.6. Regulation of LCN2 and MMP-9 in Panc89 Cells after Macrophage Co-Culture

An earlier report found a correlation between ADAM8 and MMP-9 when PDAC cells were co-cultivated with macrophages [16]. We investigated this further by addressing whether this effect is ADAM8-dependent and if LCN2 expression is also affected by co-culture with macrophages (Figure 6). In a pre-experiment, we checked ADAM8 mRNA expression and the successful differentiation of THP-1 cells into M0 macrophages (CD68 mRNA expression), as well as the subsequent polarization into M1 (CCL2 mRNA expression) and M2 (CD206 mRNA expression) macrophages. ADAM8 mRNA expression was upregulated in M0, M1, and M2 macrophages. CD68 mRNA expression was significantly increased in M0, M1, and M2, CCL2 mRNA expression in M1, and CD206 mRNA expression in M2 macrophages (Supplementary Figure S6). For the actual co-culture procedure, THP-1 cells were differentiated (M0) for 48 h and then co-cultured with Panc89 cells by inserts of 0.4 µm pore size. Effects on the gene expression of ADAM8 and macrophage-specific genes were determined in M0 macrophages 48 h after starting the co-culture with either Panc89 hA8 WT or KO cells and revealed some expression changes (Supplementary Figure S7). For instance, ADAM8 expression was significantly downregulated in macrophages co-cultivated with Panc89 hA8 WT cells. In addition, the relative expression of the macrophage-specific marker CD68 increased in macrophages co-cultivated with Panc89 hA8 WT cells. With regard to macrophage polarization, CCL2 mRNA expression as an M1 marker was upregulated after co-culture with Panc89 cells and was dependent on ADAM8. In contrast, expression of CD206 as an M2 marker was downregulated after co-

culture with Panc89 cells and even less in co-cultures with Panc89 KO cells (Supplementary Figure S7).

These results suggest a subtle effect of tumor cell-derived ADAM8 and signaling on macrophage differentiation in accordance with earlier observations that ADAM8 in macrophages does not affect their differentiation in the TME [17].

We next investigated the effect of THP-1 macrophages on Panc89 cells (Figure 6A). In this experimental setting, ADAM8 expression did not change in Panc89 cells after co-culture in both hA8 WT and KO cells (Figure 6B).

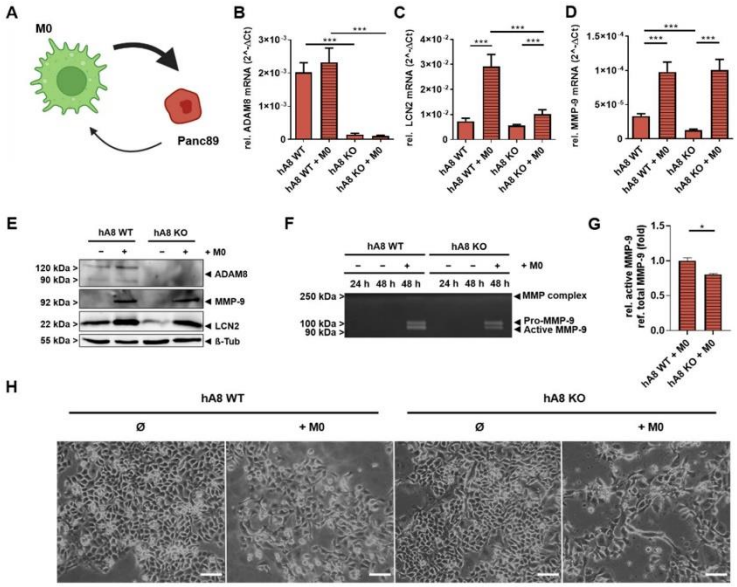

Figure 6. Co-culture of THP1-derived macrophages with Panc89 hA8 WT and KO cells. (**A**) The schematic model depicts the interactions of THP1-derived macrophages (green, M0) and Panc89 cells with or without ADAM8 (red). Created with BioRender.com. (**B**) ADAM8 mRNA expression in both Panc89 hA8 WT and KO is not affected by M0, whereas LCN2 mRNA expression. Data are presented as mean values ± S.D. *** $p < 0.001$. (**C**) is upregulated after co-culture in an ADAM8-dependent manner. Data are presented as mean values ± S.D. *** $p < 0.001$. (**D**) The graph illustrates the upregulation of MMP-9 mRNA expression in both Panc89 hA8 WT and KO after co-culture ($n = 2$). Data are presented as mean values ± S.D. *** $p < 0.001$. (**E**) Representative immunoblot shows the detection of ADAM8, MMP-9, and LCN2 with or without co-culture. In addition to the qPCR results, MMP-9 and LCN2 are upregulated after co-culture at the protein level ($n = 2$). (**F**) Representative zymography of Panc89 hA8 WT and KO cells with or without co-culture demonstrates less active MMP-9 in Panc89 hA8 KO cells than in Panc89 hA8 WT cells after co-culture. (**G**) Quantification of active MMP-9 refers to total MMP-9 in zymography of Panc89 hA8 WT and KO cells after co-culture ($n = 2$). Data are presented as mean values ± S.D. * $p < 0.05$. Representative images of Panc89 cells before and after co-culture are shown in (**H**); scale bar, 100 µm. After co-culture, morphological changes are visible in both Panc89 hA8 WT and KO cells.

Relative LCN2 mRNA expression levels increased in Panc89 hA8 WT cells after co-culture. As a slight increase in LCN2 mRNA expression was observed in Panc89 KO cells, we conclude that regulation of LCN2 in Panc89 cells is dependent on ADAM8, primarily

at the protein level (Figure 6C). Notably, the relative MMP-9 mRNA expression levels were significantly higher in Panc89 cells after co-cultivation with M0 and independent of ADAM8 (Figure 6D). In Western blots, we confirmed the induction of LCN2 and MMP-9 in co-cultured Panc89 cells (Figure 6E). It is interesting to note that expression levels of MMP-9 in Panc89 cells were very low and hardly detectable, and they increased significantly when cells were co-cultured with macrophages. MMP-9 activities released from Panc89 cells after co-culture were assessed by gelatin zymography (Figure 6F,G). MMP-9 activities were significantly increased and suggest that Panc89 cells lacking ADAM8 release lower MMP-9 activities in the TME than Panc89 cells expressing ADAM8 since the amount of pro-MMP-9 is similar in both Panc89 cells lines after 48 h, whereas the amount of active MMP-9 is reduced in Panc89 KO cells (Figure 6F,G). We also checked whether MMP-9 activity could be affected by extrinsic LCN2 by adding recombinant LCN2 to either supernatant derived from co-cultured Panc89 cells for zymography or recombinant MMP-9 for PrAMA analysis (Supplementary Figure S8). It could be determined that recombinant LCN2 had no impact on MMP-9 activity in both experiments. Additionally, co-culture experiments were simulated by adding macrophage-derived supernatants (SN) to Panc89 hA8 WT and KO cells. Subsequently, LCN2 and MMP-9 expression was checked at the mRNA and protein levels (Supplementary Figure S9). Whereas, in this setup, LCN2 expression in Panc89 was not affected by treatment with macrophage-derived SNs, MMP-9 expression was upregulated after the addition of SNs and was dependent on ADAM8. Moreover, the morphology of Panc89 cells dependent on the co-culture with macrophages looked distinct from that of individual Panc89 cells and tended to develop a more mesenchymal character. However, we did not find indications for a "classical" EMT activation, as judged by qPCR analyses for the mRNA expression of N-cadherin, E-cadherin, and the transcription factor ZEB-1 (Figure 6H and data not shown). From these experiments, we conclude that MMP-9 is upregulated after co-culture but independent of ADAM8. However, MMP-9 activation is affected by the presence of ADAM8, which might be related to the regulation of LCN2, which is even more upregulated after co-culture in Panc89 hA8 WT cells than in Panc89 hA8 KO cells. Thus, ADAM8 regulates LCN2 levels and could, thereby, indirectly affect MMP-9 activity.

2.7. ADAM8-Dependent Regulation of LCN2 and MMP-9 in Panc89 Cells after Macrophage Polarization

Given the strong effect of macrophage co-culture on MMP-9 expression and activity, we next investigated the effect of macrophage polarization on MMP-9 expression in PDAC cells (Figure 7). THP-1 macrophages were differentiated (M0) and polarized (M1, M2) using protocols as previously described [17]. Afterward, co-culture of M0, M1, and M2 macrophages with Panc89 cells was performed for 48 h, and expression levels of ADAM8, LCN2, and MMP-9 in Panc89 cells were determined using Western blot (Figure 7A) and ELISA (Figure 7B–D). Whereas ADAM8 levels in Panc89 cells are strongly induced particularly by M2-polarized macrophages, the increase in MMP-9 levels in Panc89 cells seems not to be dependent on macrophage polarization. For instance, the MMP-9 ELISA results show that Panc89 cells co-cultivated with M0 macrophages had the highest MMP-9 secretion (Figure 7C). For LCN2, Panc89 cells co-cultivated with macrophages of the M1-like polarization type expressed more elevated levels of LCN2 than M2-like macrophages (Figure 7D). Except for co-culture with M1-like macrophages, LCN2 is upregulated in Panc89 cells in an ADAM8-dependent manner. The ADAM8-dependent LCN2 expression in Panc89 cells can be enhanced by co-culture of Panc89 cells with M0 macrophages, as described in Section 2.6.

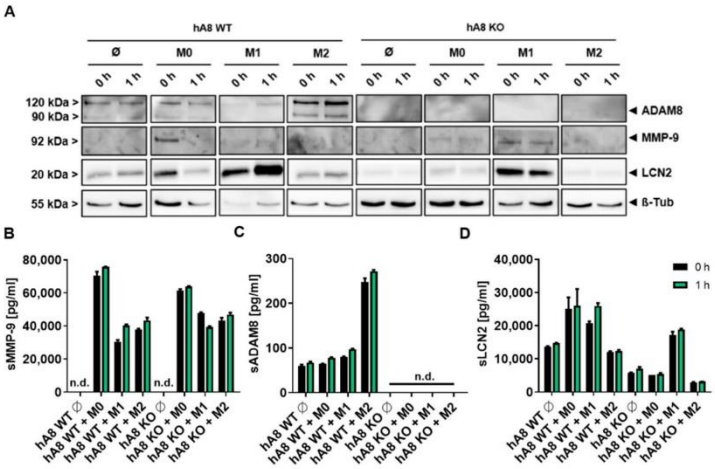

Figure 7. Co-culture of THP1-derived and polarized macrophages with Panc89 hA8 WT and KO cells. (**A**) Western blot illustrates the detection of ADAM8, MMP-9, and LCN2 in Panc89 hA8 WT and KO control cells (*Ø*) and after co-culture with M0, M1, and M2 macrophages (two time points: 0 h and 1 h). ADAM8 is upregulated in Panc89 hA8 WT cells after co-culture with M2-polarized macrophages. Panc89 cells show the highest MMP-9 expression after co-culture with M0, but M1 macrophages also upregulate MMP-9. LCN2 is dependent on ADAM8 when upregulated in Panc89 cells after co-culture with M0 and M2 macrophages but independent of ADAM8 in Panc89 cells co-cultured with M1 macrophages. (**B**) ADAM8, (**C**) MMP-9, and (**D**) LCN2 ELISA of Panc89 hA8 WT and KO cell-derived supernatants of control cells and after co-culture with M0, M1, and M2 (two time points: 0 h and 1 h). In accordance with the immunoblot results of (**A**), ADAM8 is upregulated in supernatants derived from Panc89 hA8 WT cells after co-culture with M2 macrophages (**B**). At the same time, macrophages increase MMP-9 secretion from an undetectable level to almost 80,000 pg/mL in Panc89 hA8 WT and 60,000 pg/mL in Panc89 hA8 KO cells. M1 and M2 macrophages increase MMP-9 secretion of Panc89 independent of ADAM8, but not as high as in Panc89 cells co-cultured with M0. In contrast, LCN2 is upregulated in Panc89 hA8 WT cells by M0 and M1, but not by M2 macrophages. In the absence of ADAM8, Panc89 hA8 KO cells show low LCN2 secretion in control cells and after co-culture with M0 and M2 macrophages. Only after co-culture with M1 macrophages is the LCN2 secretion level increased ($n = 1$). Data are presented as mean values ± S.D.

3. Discussion

In this study, we provide insights into the protease-dependent mechanisms underlying the progression of PDAC as a highly invasive tumor entity. First, we demonstrate the essential function of ADAM8 in the extracellular release of MMP-9 and LCN2, two important mediators of cancer progression in PDAC. For instance, a recent report demonstrated that MMP-9, when derived from macrophages, is essential for EMT in tumor cells via activation of protease-activated receptor (PAR-1, [18]). Here, we report on the activation of MMP-9 in tumor cells by macrophages and demonstrate that the communication between macrophages and tumor cells can likely cause MMP-9-dependent effects in an autocrine manner, i.e., by self-induction of MMP-9 in tumor cells when associated with macrophages, as our co-culture experiments suggest. Notably, this effect is not dependent on the polarization state of macrophages, as M1- and M2-like macrophages have similar effects on MMP-9 expression in Panc89 cells. Another strong correlation with ADAM8 expression is reported here for LCN2, a siderophore protein involved in pathogen defense and covalent stabilization of MMP-9. From our data, there are some indications that LCN2 can lead

to enhanced activation of pro-MMP-9, thereby causing a higher degree of extracellular proteolysis, leading to the tumor-promoting effect of positive co-regulation of MMP-9 and LCN2 by ADAM8. More directly, LCN2 was recently investigated in a mouse model of PDAC. LCN2-deficient mice were crossed with transgenic mice expressing $Kras^{G12D}$ in acinar cells [19]. In these mice, the lack of LCN2 caused a significant reduction in immune cell infiltration, PanIN, and tumor growth, suggesting that LCN2 in the TME is an important determinant for PDAC progression and patient prognosis, similar to MMP-9. Thus, ADAM8 could amplify its detrimental function in PDAC by simultaneously affecting MMP-9 and LCN-2 expression. Given the finding that LCN2 can determine MMP-9 activity in vivo, it can be hypothesized that MMP-9 activity in the TME is directly affected. However, in contrast to the regulation of MMP-9, LCN2 is differentially regulated by co-culturing PDAC cells with macrophages. Undifferentiated as well as M1-polarized macrophages cause increased LCN2 release, whereas M2-polarized macrophages suppress LCN2 secretion. Thus, a distinct regulation of MMP-9 and LCN2 expression by macrophages could imply that both proteins serve functions distinct from the regulation of net protease activity in the TME. A limitation of this study is the sole use of THP-1 cells rather than primary macrophages derived from PBMCs. To address this issue, we tried to include these cell sources in our analysis; however, we obtained heterogeneous results that prevent a conclusive interpretation. A further limitation is the analysis of 2D co-cultures that might not reflect the interaction of tumor cells with macrophages **in vivo.** In this regard, a 3D model using organoid co-cultures will be required to get closer to a more authentic tumor microenvironment. Since we could demonstrate that only MMP-9 and not LCN2 expression is affected in Panc89 cells after treatment with M0-derived supernatants, another limitation of this study is the treatment of Panc89 cells with THP-1 macrophage-derived EVs. As EVs can function as a carrier of signaling molecules, we hypothesize that EV treatment could induce LCN2 expression and therefore MMP-9 activity, which is a matter of further studies.

Other important findings in this study are that ADAM8 is sorted into EVs, and the ADAM8 dependence of MMP-9 and LCN2 is found, in addition to lysates, in the EV cargo; thus, we can conclude that ADAM8 is a key regulator of MMP-9 and LCN2 release in the TME. However, the mechanism by which ADAM8 is sorted into EVs remains unclear. Besides the most described ESCRT machinery, many ESCRT-independent cargo and biomolecule sorting pathways in EVs have been reported [20]. TSG101, as part of the ESCRT complex, can recognize the tetrapeptide protein motif PS/TAP [14]. The amino acid motif PTAP is found in ADAM8 at the very C-terminus (aa residues 821–824). To demonstrate the function of this motif, we established a Panc89 cell line lacking the C-terminal domain of ADAM8, thereby deleting the PTAP motif of ADAM8, and expected this form of ADAM8 not to be present in EVs. Unexpectedly, the C-terminal mutant form of ADAM8 is still capable of being secreted in EVs. Furthermore, the lack of co-localization of TSG101 with ADAM8 supports the hypothesis that the internalization of ADAM8 in EVs occurs independently of the ESCRT-I protein TSG101. ESCRT-independent pathways such as lipid raft-, tetraspanin-, and ceramide-mediated mechanisms could exhibit potential ADAM8 EV cargo loading alternatives that must be investigated [21]. Tan et al. [22] demonstrated that lipid rafts could conduce to a platform for exosomal biogenesis in mesenchymal stem cells. ADAM17 has been described as an active protease associated with lipid rafts [23] and could indicate a possible mechanism for ADAM17 EV encapsulation, and thus for ADAM8. In addition, the release of ADAM10 in EVs by melanoma cells was shown to be linked to a paxillin/integrin interaction and a subsequent shift to lipid rafts [24], supporting the suggested mechanism for ADAM8 exosomal release. In EVs, ADAM8 can be detected as an active protease, as peptide cleavage assays with WT and KO cells demonstrate. Thus, the topological orientation of ADAM8 in EVs is likely to be directed to the extracellular compartment where ADAM8-dependent cleavage can occur. In some reports, ADAM8 was also discussed as a membrane protein mediating cell–cell fusion, where ADAM8 on the surface of EVs could potentially contribute to the fusion of EVs with adjacent cells to release their cargo [25]. In addition, as ADAM8 can regulate

miRNA expression in tumor cells (Schäfer et al., manuscript submitted), it is likely that ADAM8–ADAM8 interactions between EVs and ADAM8-expressing cells could lead to fusion events and facilitate the transfer of miRNAs into cells to regulate gene expression. In the case of ADAM8-positive EVs in PDAC, such miRNAs were reported to be miRNAs 720 and 451 [9]. Concomitant with the ADAM8 content in EVs, MMP-9 and LCN2 are affected, suggesting that ADAM8 regulates the amount of these proteins in the TME. A cell-autonomous effect of ADAM8 in tumor cells was extensively described in numerous studies. However, the function of ADAM8 in the TME, given the localization in EVs, is worth further studies involving other immune cell types such as neutrophils and natural killer cells in which ADAM8 is also highly expressed.

4. Materials and Methods

4.1. Cell Culture

Panc89 cells were kindly provided by Prof. Anna Trauzold, Kiel University, and were cultivated in RPMI (Gibco™, Life Technologies, Carlsbad, CA, USA) supplemented with 10% (*v*/*v*) Fetal Bovine Serum (FBS; Sigma-Aldrich, Munich, Germany), 0.1 mg/mL Penicillin-Streptomycin (Gibco™, Life Technologies, Carlsbad, CA, USA), and 1 mM Sodium Pyruvate (Gibco™, Life Technologies, Carlsbad, CA, USA) in a humidified atmosphere at 37 °C and 5% CO_2. MB-231 cells were purchased from American Type Culture Collection (ATCC, Manassas, VA, USA) and were cultivated in DMEM (Gibco™, Life Technologies, Carlsbad, CA, USA) with the same additives as described for Panc89 cells.

4.2. Generation of Stable Panc89 and MB-231 ADAM8 Knockout Cells

To generate a genomic ADAM8 knockout in Panc89 and MB-231 cells, the ADAM8 Human Gene Knockout Kit (CRISPR) from OriGene (CAT#: KN213386, Rockville, ML, USA) was used. The transfection of the cells and further necessary steps were performed as previously described [11]. Single-cell clones were obtained after the selection with 1 µg/mL Puromycin (InvivoGen, San Diego, CA, USA).

4.3. Generation of Stable Panc89 ADAM8 Rescue Cells

For a genomic knock-in of the full-length ADAM8 or an ADAM8 lacking the C-terminal domain in Panc89 hA8 KO cells, the ADAM8 AAVS1 Transgene Kockin kit (BSD) from OriGene (CAT#: GE100036, Rockville, ML, USA) was used. The transfection of the cells and further necessary steps were performed as described in Section 4.2. Single-cell clones were obtained after the selection with 10 µg/mL Blasticidin (InvivoGen, San Diego, CA, USA).

4.4. THP-1 Cell Differentiation and Polarization

For macrophage differentiation, THP-1 cells were seeded at a density of 500,000 cells per well of a 6-well plate and treated with 10 ng/mL phorbol 12-myristate 13-acetate (PMA, Sigma-Aldrich, Munich, Germany). After 48 h, differentiated THP-1 cells were exposed for another 6 h to either 50 ng/mL LPS (Sigma-Aldrich, Munich, Germany) and 20 ng/mL IFN-γ (PeproTech, Hamburg, Germany) for M1 polarization or 20 ng/mL IL-4 (PeproTech, Hamburg, Germany) for M2 polarization.

4.5. Co-Culture of Panc89 with THP-1

At a density of 500,000 cells per approach, THP-1 cells were seeded in the upper part of ThinCert™ Cell Culture Insert with a 0.4 µm diameter (Greiner Bio-One GmbH, Frickenhausen, Germany). After 48 h of differentiation, 500,000 Panc89 cells were seeded in the lower compartment (well) and left in co-culture for another 48 h. Cells were either harvested for RNA isolation or protein extraction and subsequent Western blot analysis. For M1 and M2 co-culture, THP-1 cells were treated with 50 ng/mL LPS (Sigma-Aldrich, Munich, Germany) and 20 ng/mL IFN-γ (PeproTech, Hamburg, Germany) for M1 polarization or 20 ng/mL IL-4 (PeproTech, Hamburg, Germany) for M2 polarization 6 h after

differentiation and before co-culture. The described co-culture procedure was performed considering different established protocols, as described, for example, in Landmann and Buchholz, Department of Gastroenterology, Endocrinology, Metabolism, and Infectiology, Philipps University Marburg https://archiv.ub.uni-marburg.de/ubfind/Record/urn:nbn:de:hebis:04-z2019-0310 (accessed on 29 December 2021) and [26,27].

4.6. EV Isolation and Characterization by NanoFCM and Electron Microscopy

After the tumor cells reached 80% confluency, the medium was changed to RPMI medium without Phenol Red (Gibco™, Life Technologies, Carlsbad, CA, USA) but supplemented with 1% (*v*/*v*) Insulin-Transferrin-Selenium (Gibco™, Life Technologies, Carlsbad, CA, USA). After 72 h, the supernatants were centrifuged at 300× *g* for 10 min followed by an additional centrifugation step at 3000× *g* for 10 min. The resulting supernatant was filtered (0.2 µm) and subsequently centrifuged at 10,000× *g* for 1 h at 4 °C. EVs were pelleted at 100,000× *g* for 90 min at 4 °C in an Optima XPN-80 ultracentrifuge (Beckman Coulter, Krefeld, Germany) with an SW32Ti swing-out rotor, resuspended in 700 µm HBSS (Gibco™, Life Technologies, Carlsbad, CA, USA), and again centrifuged at 100,000× *g* for 90 min at 4 °C in an Optima MAX-XP (Beckman Coulter, Krefeld, Germany) ultracentrifuge with a TLA-55 fixed angle rotor. Finally, the EVs were resuspended in 50 µL HBSS (Gibco™, Life Technologies, Carlsbad, CA, USA). For particle size and quantity determination, EVs were applied to a flow nano analyzer (NanoFCM Co. Ltd., Nottingham, UK). Electron microscopy was conducted as previously described [9].

4.7. RNA Isolation and Quantitative Real-Time PCR

For total RNA isolation, cells were resuspended in 1 mL Qiazol (Qiagen, Hilden, Germany) and 200 µL Chloroform was added. After mixing the samples, the lysed cells were incubated at RT for 5 min and subsequently centrifuged at 12,000× *g* for 15 min at 4 °C. The RNA in the upper aqueous phase was then precipitated by adding 500 µL Isopropanol. After repeated centrifugation, the RNA was washed with 75% (*v*/*v*) Ethanol, dried, and dissolved in 10–30 µL RNase-Free Water. The resulting concentration of the isolated RNA was determined by NanoPhotometer® NP80 (Implen, Munich, Germany). An amount of 2 µg of isolated RNA was applied to RNA to cDNA EcoDry™ kit (Takara Bio Inc., Kusatsu, Japan) for reverse transcription. The procedure was conducted according to the manufacturer's instructions. Quantitative real-time PCR was performed using iTaq™ Universal SYBR® Green Supermix (Bio-Rad Laboratories GmbH, Feldkirchen, Germany), cDNA equivalent of 20 ng total RNA, and either forward and reverse primers or QuantiTect Primer Assay (Qiagen, Hilden, Germany) in a 20 µL total PCR reaction volume in a StepOnePlusTM Real-Time PCR System (Thermo Fisher Scientific, Waltham, MA, USA). Relative changes in mRNA expression were calculated using the ΔCt method using XS13 as a housekeeping gene (the sequence was described elsewhere) [2].

4.8. rLCN2 and rTGF-α Stimulation of Panc89 Cells

A total of 500,000 cells were seeded in each well of a 6-well plate. After 48 h, the medium was changed to RPMI (Gibco™, Life Technologies, Carlsbad, CA, USA) Medium supplemented with 0.5% (*v*/*v*) FBS (Sigma-Aldrich, Munich, Germany) and cultivated for another 6 h. Starved cells were then treated with either rTGF-α (PeproTech, Hamburg, Germany), rLCN2 (R&D Systems, Minneapolis, MN, USA), or their combination for 1 h. Stimulated cells were then applied to total protein extraction and Western blot analysis.

4.9. Protein Extraction and Western Blot Analysis

Total protein extraction was performed by detaching the cells with a cell scraper. Cells were washed with PBS, resuspended in 50 µL RIPA (50 mM HEPES pH 7.4; 150 mM NaCl; 1% (*v*/*v*) NP-40; 0.5% (*w*/*v*) Natriumdeoxycholate; 0.1% (*w*/*v*) SDS; 10 mM Phenantrolin; 10 mM EDTA; Pierce™ Protease Inhibitor Mini Tablets, EDTA-free, Thermo Scientific, Waltham, MA, USA; Pierce™ Phosphatase Inhibitor Mini Tablets, Thermo Scientific,

Waltham, MA, USA) and incubated for 30 min on ice. After centrifugation at 12,000× *g* for 5 min at 4 °C, the protein concentration of the supernatant containing the total protein was determined by Pierce™ BCA Protein Assay Kit (Thermo Scientific, Waltham, MA, USA). Proteins from equal amounts of lysate were then boiled in 1× loading buffer (5× loading buffer: 60 mM Tris-HCl pH 6.8; 2% (*w/v*) SDS; 10% (*w/v*) Glycerol; 5% (*v/v*) ß-Mercaptoethanol; 0.01% (*w/v*) Bromphenol-Blue) for 5 min. The proteins were separated by 10% SDS-PAGE and subsequently transferred to a nitrocellulose membrane (GE Healthcare, Chicago, IL, USA). The membrane was then blocked with 5% (*w/v*) milk powder (MP) in TBST (50 mM Tris, pH 7.5; 150 mM NaCl; 0.1% (*w/v*) Tween-20) for 1 h and probed with the following primary antibodies: anti-ADAM8 (PA5-47047, Thermo Fisher Scientific, Waltham, MA, USA; 1:1000 in 5% MP in TBST), anti-beta Tubulin (NB600-936, Novus Biological, Littleton, CO, USA; 1:2000), anti-LCN2 (AF1757, R&D Systems, Minneapolis, MN, USA; 1:1000), anti-EGFR (4267, Cell Signaling Technology, Danvers, MA, USA; 1:1000), anti-pEGFR (3777, Cell Signaling Technology, Danvers, MA, USA; 1:1000), anti-MAPK (4696, Cell Signaling Technology, Danvers, MA, USA; 1:2000), anti-pMAPK (4370, Cell Signaling Technology, Danvers, MA, USA; 1:2000), Calnexin (2679, Cell Signaling Technology, Danvers, MA, USA; 1:1000), anti-Flotillin-1 (PA5-18053, Thermo Scientific, Waltham, MA, USA; 1:2000), anti-TSG101 (ab83, Abcam, Cambridge, UK; 1:1000), MMP-9 (AF911, R&D Systems, Minneapolis, MN, USA; 1:2000), and anti-CD81 (sc166029, Santa Cruz Biotechnology, Dallas, TX, USA; 1:500), at 4 °C overnight. After washing 3 times with TBST, the membrane was incubated with horseradish peroxidase-conjugated secondary antibodies for 1 h (Abcam, Cambridge, UK; 1:5000) followed by a repeated washing step. Detection was performed by using Chemiluminescent HRP Substrate, Western Bright Sirius (Advansta Inc., San Jose, CA, USA).

4.10. Human Protease/Protease Inhibitor Array

For the Proteome Profiler Human Protease/Protease Inhibitor Array (ARY025, R&D Systems, Minneapolis, MN, USA), 500,000 MB-231 cells were seeded in each well of a 6-well plate overnight. The next day, the medium was changed to Gibco™, Life Technologies, Carlsbad, CA, USA) supplemented with 2% (*v/v*) FBS (Sigma-Aldrich, Munich, Germany) for 48 h. The supernatants were collected, and protein concentration was determined by NanoPhotometer® NP80 (Implen, Munich, Germany). Concentrations were adjusted, and the array was carried out according to the manufacturer's protocol.

4.11. Immunofluorescence Staining

Before the procedure, coverslips were coated with 50 µg/mL Collagen Type I from rat tail (Sigma-Aldrich, Munich, Germany) and incubated for 1 h at 37 °C. The coating was then washed 2 times with PBS, and subsequently, Panc89 cells were seeded at a density of 100,000 cells per 0.5 mL on the coated coverslips. After 24 h, cells were washed 3 times with PBS and then fixed with 4% (*w/v*) PFA for 15 min followed by 1 h blocking with 5% (*w/v*) BSA in PBS. Primary ADAM8 (PA5-47047, Thermo Fisher Scientific, Waltham, MA, USA; 1:100) or TSG101 (ab83, Abcam, Cambridge, UK; 1:100) antibody was added for overnight incubation at 4 °C. The next day, cells were washed 3 times with PBS and incubated with secondary antibody Alexa Fluor 488 (A-11055, Thermo Fisher Scientific, Waltham, MA, USA; 1:500), Alexa Fluor 488 (ab150105, Abcam, Cambridge, UK; 1:500), or Texas Red (PA1-28662, Thermo Fisher Scientific, Waltham, MA, USA; 1:1000) for 1 h at RT. After another washing step, cells were incubated with Hoechst 33,342 dye (Sigma-Aldrich, Munich, Germany) for counterstaining for 20 min. Images were obtained using a Leica DM 5500 microscope (Leica Microsystems, Wetzlar, Germany).

4.12. Gelatin Zymography

After 48 h of co-culture, cells were cultivated in monoculture for another 24 h with 1 mL RPMI (Gibco™, Life Technologies, Carlsbad, CA, USA) without phenol red and FBS, but supplemented with 1% (*v/v*) Insulin-Transferrin-Selenium (Gibco™, Life Tech-

nologies, Carlsbad, CA, USA). The supernatants were collected, centrifuged at 4000× *g* for 10 min, and concentrated with Vivaspin (Sartorius AG, Göttingen, Germany). Protein concentration determination was performed as described above. Before the electrophoresis, the samples were either treated with 0.6 mM APMA (Sigma-Aldrich, Munich, Germany), with recombinant LCN2 (R&D Systems, Minneapolis, MN, USA), or with both for 1 h at 37 °C. The samples were then diluted with 2x non-reducing loading dye (1 M Tris-HCl, pH 6.8; 20% (*w/v*) Glycerol; 10% SDS (*w/v*); 0.1% (*w/v*) Bromphenol-Blue) and loaded on a gel containing 0.1% (*w/v*) Gelatin in the separating gel. After the run, the gel was initially washed 2 times with renaturation buffer (2.5% (*v/v*) Triton-X-100) for 30 min each, followed by equilibration with developing buffer (1 M Tris-HCl, pH 7.5; 200 mM NaCl; 4 mM $CaCl_2$; 0.02% (*v/v*) Brij-35) for 30 min and subsequent incubation in a fresh developing buffer for 16 h at 37 °C. The next day, the gel was stained with Coomassie staining solution (50% (*v/v*) Methanol, 10% (*v/v*) Acetic acid, 0.5% (*w/v*) Coomassie Brilliant Blue G250) for 1 h and destained with destaining solution (50% (*v/v*) Methanol, 10% (*v/v*) Acetic acid) until the bands of the active enzyme were visible.

4.13. Protease Activity Assay in Panc89-Derived Supernatants or EVs

Both supernatants and EVs derived from Panc89 cells were tested for ADAM and MMP activities by determining the cleavage of FRET-based polypeptide substrates with a high Kcat/Km for different proteases (PEPDab5, PEPDab8, PEPDab10, PEPDab13, PEPDab14, BioZyme, Inc., Apex, NC, USA), as previously described [28]. For the conditioned supernatants, 500,000 cells were seeded in each well of a 6-well plate. After 24 h, the medium was changed to 1 mL RPMI (Gibco™, Life Technologies, Carlsbad, CA, USA)without phenol red and FBS, but supplemented with 1% (*v/v*) Insulin-Transferrin-Selenium (Gibco™, Life Technologies, Carlsbad, CA, USA) for another 24 h. After the incubation, the supernatants were centrifuged at 4000× *g* for 10 min. Briefly, 10 µM of each PEPDab in 50 µL assay buffer (1 mM ZnCl2, 20 mM Tris-HCl pH 8.0, 10 mM CaCl2, 150 mM NaCl, 0.0006% Brij-35) was incubated with either 50 µL conditioned supernatant or 5×10^9 EVs in a total volume of 100 µL. The resulting fluorescence was monitored every 2 min for 6 h at 37 °C with a multiwell plate reader (FLUOstar OPTIMA, BMG Labtech, Offenburg, Germany) using a λex of 485 nm and a λem of 530 nm.

4.14. ELISA

Soluble ADAM8 (DY1031, R&D Systems, Minneapolis, MN, USA), LCN2 (DY1737, R&D Systems, Minneapolis, MN, USA), and MMP-9 (DY911, R&D Systems, Minneapolis, MN, USA) levels in Panc89-derived supernatants were determined by using DuoSet ELISA kits. A total of 500,000 cells were incubated in a normal growth medium (as described above) in each well of a 6-well plate for 48 h. Before the procedure, the collected supernatants were centrifuged at 4000× *g* for 10 min and subjected to ELISA according to the manufacturer's protocol.

4.15. Proliferation Assay

A total of 5000 cells per well were seeded in triplicates in a 96-well plate. After 24 h, 48 h, and 72 h, viability was determined by adding 50 µL CellTiter-Glo® 3D Cell Viability Assay (Promega, Walldorf, Germany), followed by a shaking step for 15 min and subsequent incubation for 15 min at RT in the dark. The resulting luminescence was measured using a multiwell plate reader (FLUOstar OPTIMA, BMG Labtech, Offenburg, Germany).

4.16. Scratch Assay

The scratch assay was performed by seeding 30,000 cells per well of a Culture-Insert 2 Well (ibidi GmbH, Gräfelfing, Germany) inserted in a 24-well plate. After 6 h and allowing the cells to attach, the normal growth medium was changed to RPMI Medium (Gibco™, Life Technologies, Carlsbad, CA, USA) supplemented with 0.5% (*v/v*) FBS

(Sigma-Aldrich, Munich, Germany) for overnight starvation. The Culture-Insert 2 Well was removed, and cells were washed with a fresh normal growth medium to remove non-adherent cells. From this moment, images at each edge of the gap were taken at time points 0 h and 10 h. The images were analyzed using the Image J software plugin "Wound_healing_size_tool_updated" published by [29].

4.17. Invasion Assay

To examine the cells' invasive behavior, an invasion assay was performed using ThinCert™ Cell Culture Inserts with an 8 µm pore diameter (Greiner Bio-One GmbH, Frickenhausen, Germany). Before seeding the cells, the upper side of the Thincert was coated with 50 µL Basement Membrane Matrix Growth Factor Reduced Matrigel (Corning®, Corning, NY, USA). After 1 h incubation at 37 °C, 25,000 cells were seeded in 50 µL RPMI Medium (Gibco™, Life Technologies, Carlsbad, CA, USA) supplemented with 0.5% (*v*/*v*) FBS (Sigma-Aldrich, Munich, Germany) at the lower side of the Thincert. Cells were allowed to attach to the membrane for a maximum of 4 h. Subsequently, 250 µL RPMI Medium (Gibco™, Life Technologies, Carlsbad, CA, USA) supplemented with 20% (*v*/*v*) FBS (Sigma-Aldrich, Munich, Germany) was added to the upper part of the Thincert and 750 µL RPMI Medium (Gibco™, Life Technologies, Carlsbad, CA, USA) supplemented with 0.5% (*v*/*v*) FBS (Sigma-Aldrich, Munich, Germany) to the well. Cells were then allowed to invade the Matrigel due to an FBS gradient. After 24 h, the Thincerts were treated with 4% (*w*/*v*) PFA for 30 min, and subsequently, cells were permeabilized with 0.3% (*v*/*v*) Triton-X for another 30 min. For counting and quantification, cells were stained with Hoechst 33,342 (Thermo Scientific, Waltham, MA, USA) dye overnight. Z-Stacks of five random viewing fields were recorded, and cells on the lower part of the Thincert (non-invasive) and cells in the matrigel (invasive) were counted.

4.18. Statistical Analysis

Student's *t*-test or two-way ANOVA was applied for statistical analysis. Data were considered not significant ($p > 0.05$, no asterisk), significant * ($p < 0.05$), highly significant ** ($p < 0.01$), or very highly significant *** ($p < 0.001$) and are expressed as the mean ± S.D.

5. Conclusions

Taken together, our study sheds more light on the role of ADAM8 in the TME by providing evidence that effects observed for ADAM8 in a cell-autonomous manner can be overcome by co-culture with macrophages in a "systemic" mode, i.e., by intense communication between tumor and immune cells that could be mediated by EVs. When considering ADAM8 as a potential drug target in PDAC, these findings have to be taken into account.

Supplementary Materials: The following supporting information can be downloaded at: https://www.mdpi.com/article/10.3390/ijms23041976/s1.

Author Contributions: Conceptualization, L.C., E.P.S., E.P.v.S., J.W.B.; methodology, L.C., M.S., B.W., C.N., U.S., C.P., B.D., M.A.M.; formal analysis, L.C., J.W.B.; investigation, L.C., M.S., B.W., C.N., S.K., U.S., C.P., B.D., M.A.M.; data curation, L.C., M.S., J.W.B.; writing—original draft preparation, L.C., J.W.B.; writing—review and editing, L.C., M.S., E.P.S., M.A.M., J.W.B.; visualization, L.C.; supervision, E.P.S., E.P.v.S., J.W.B.; project administration, J.W.B., E.P.S.; funding acquisition, J.W.B., E.P.S., E.P.v.S. All authors have read and agreed to the published version of the manuscript.

Funding: This work was supported by the Deutsche Forschungsgemeinschaft (DFG) with a Clinical Research Unit grant (CRU 325) and grants to J.W.B. (BA-1606/4-1 and BA-1606/3-1), E.P.S. (SL-17/5-1), and E.P.v.S. (GRK2573/1). The APC was funded by the University of Marburg.

Institutional Review Board Statement: Not applicable.

Informed Consent Statement: Not applicable.

Data Availability Statement: All data presented here are available on request to the corresponding author.

Acknowledgments: The authors thank the Marburg University Core Facility "Mouse Pathology" Axel Pagenstecher and Frederik Helmprobst for EM imaging, and Susanne Stei for excellent technical assistance.

Conflicts of Interest: The authors declare no conflict of interest.

References

1. Mohan, S.P.; Bhaskaran, M.K.; George, A.L.; Thirutheri, A.; Somasundaran, M.; Pavithran, A. Immunotherapy in Oral Cancer. *J. Pharm. Bioallied Sci.* **2019**, *11*, S107–S111. [CrossRef] [PubMed]
2. Schlomann, U.; Koller, G.; Conrad, C.; Ferdous, T.; Golfi, P.; Garcia, A.M.; Höfling, S.; Parsons, M.; Costa, P.; Soper, R.; et al. ADAM8 as a Drug Target in Pancreatic Cancer. *Nat. Commun.* **2015**, *6*, 6175. [CrossRef] [PubMed]
3. Siegel, R.L.; Miller, K.D.; Jemal, A. Cancer Statistics, 2020. *Cancer J. Clin.* **2020**, *70*, 7–30. [CrossRef] [PubMed]
4. Huber, M.; Brehm, C.U.; Gress, T.M.; Buchholz, M.; Alashkar Alhamwe, B.; Strandmann, E.P.; Slater, E.P.; Bartsch, J.W.; Bauer, C.; Lauth, M. The Immune Microenvironment in Pancreatic Cancer. *Int. J. Mol. Sci.* **2020**, *21*, 7307. [CrossRef] [PubMed]
5. Valkovskaya, N.; Kayed, H.; Felix, K.; Hartmann, D.; Giese, N.A.; Osinsky, S.P.; Friess, H.; Kleeff, J. ADAM8 Expression Is Associated with Increased Invasiveness and Reduced Patient Survival in Pancreatic Cancer. *J. Cell. Mol. Med.* **2007**, *11*, 1162–1174. [CrossRef] [PubMed]
6. Jaworek, C.; Verel-Yilmaz, Y.; Driesch, S.; Ostgathe, S.; Cook, L.; Wagner, S.; Bartsch, D.K.; Slater, E.P.; Bartsch, J.W. Cohort Analysis of ADAM8 Expression in the PDAC Tumor Stroma. *J. Pers. Med.* **2021**, *11*, 113. [CrossRef] [PubMed]
7. Naus, S.; Blanchet, M.-R.; Gossens, K.; Zaph, C.; Bartsch, J.W.; McNagny, K.M.; Ziltener, H.J. The Metalloprotease-Disintegrin ADAM8 Is Essential for the Development of Experimental Asthma. *Am. J. Respir. Crit. Care Med.* **2010**, *181*, 1318–1328. [CrossRef]
8. Schick, D.; Babendreyer, A.; Wozniak, J.; Awan, T.; Noels, H.; Liehn, E.; Bartsch, J.-W.; Vlacil, A.-K.; Grote, K.; Zayat, R.; et al. Elevated Expression of the Metalloproteinase ADAM8 Associates with Vascular Diseases in Mice and Humans. *Atherosclerosis* **2019**, *286*, 163–171. [CrossRef]
9. Verel-Yilmaz, Y.; Fernández, J.P.; Schäfer, A.; Nevermann, S.; Cook, L.; Gercke, N.; Helmprobst, F.; Jaworek, C.; Pogge von Strandmann, E.; Pagenstecher, A.; et al. Extracellular Vesicle-Based Detection of Pancreatic Cancer. *Front. Cell Dev. Biol.* **2021**, *9*, 697939. [CrossRef]
10. Romagnoli, M.; Mineva, N.D.; Polmear, M.; Conrad, C.; Srinivasan, S.; Loussouarn, D.; Barillé-Nion, S.; Georgakoudi, I.; Dagg, Á.; McDermott, E.W.; et al. ADAM8 Expression in Invasive Breast Cancer Promotes Tumor Dissemination and Metastasis. *EMBO Mol. Med.* **2014**, *6*, 278–294. [CrossRef]
11. Scharfenberg, F.; Helbig, A.; Sammel, M.; Benzel, J.; Schlomann, U.; Peters, F.; Wichert, R.; Bettendorff, M.; Schmidt-Arras, D.; Rose-John, S.; et al. Degradome of Soluble ADAM10 and ADAM17 Metalloproteases. *Cell. Mol. Life Sci.* **2020**, *77*, 331–350. [CrossRef]
12. Miller, M.A.; Barkal, L.; Jeng, K.; Herrlich, A.; Moss, M.; Griffith, L.G.; Lauffenburger, D.A. Proteolytic Activity Matrix Analysis (PrAMA) for Simultaneous Determination of Multiple Protease Activities. *Integr. Biol. Quant. Biosci. Nano Macro* **2011**, *3*, 422–438. [CrossRef]
13. Théry, C.; Witwer, K.W.; Aikawa, E.; Alcaraz, M.J.; Anderson, J.D.; Andriantsitohaina, R.; Antoniou, A.; Arab, T.; Archer, F.; Atkin-Smith, G.K.; et al. Minimal Information for Studies of Extracellular Vesicles 2018 (MISEV2018): A Position Statement of the International Society for Extracellular Vesicles and Update of the MISEV2014 Guidelines. *J. Extracell. Vesicles* **2018**, *7*, 1535750. [CrossRef] [PubMed]
14. Nabhan, J.F.; Hu, R.; Oh, R.S.; Cohen, S.N.; Lu, Q. Formation and Release of Arrestin Domain-Containing Protein 1-Mediated Microvesicles (ARMMs) at Plasma Membrane by Recruitment of TSG101 Protein. *Proc. Natl. Acad. Sci. USA* **2012**, *109*, 4146–4151. [CrossRef]
15. Yammine, L.; Zablocki, A.; Baron, W.; Terzi, F.; Gallazzini, M. Lipocalin-2 Regulates Epidermal Growth Factor Receptor Intracellular Trafficking. *Cell Rep.* **2019**, *29*, 2067–2077.e6. [CrossRef] [PubMed]
16. Puolakkainen, P.; Koski, A.; Vainionpää, S.; Shen, Z.; Repo, H.; Kemppainen, E.; Mustonen, H.; Seppänen, H. Anti-Inflammatory Macrophages Activate Invasion in Pancreatic Adenocarcinoma by Increasing the MMP9 and ADAM8 Expression. *Med. Oncol. Northwood Lond. Engl.* **2014**, *31*, 884. [CrossRef]
17. Gjorgjevski, M.; Hannen, R.; Carl, B.; Li, Y.; Landmann, E.; Buchholz, M.; Bartsch, J.W.; Nimsky, C. Molecular Profiling of the Tumor Microenvironment in Glioblastoma Patients: Correlation of Microglia/Macrophage Polarization State with Metalloprotease Expression Profiles and Survival. *Biosci. Rep.* **2019**, *39*, BSR20182361. [CrossRef] [PubMed]
18. Tekin, C.; Aberson, H.L.; Waasdorp, C.; Hooijer, G.K.J.; Boer, O.J.; Dijk, F.; Bijlsma, M.F.; Spek, C.A. Macrophage-Secreted MMP9 Induces Mesenchymal Transition in Pancreatic Cancer Cells via PAR1 Activation. *Cell. Oncol. Dordr.* **2020**, *43*, 1161–1174. [CrossRef]
19. Gomez-Chou, S.B.; Swidnicka-Siergiejko, A.K.; Badi, N.; Chavez-Tomar, M.; Lesinski, G.B.; Bekaii-Saab, T.; Farren, M.R.; Mace, T.A.; Schmidt, C.; Liu, Y.; et al. Lipocalin-2 Promotes Pancreatic Ductal Adenocarcinoma by Regulating Inflammation in the Tumor Microenvironment. *Cancer Res.* **2017**, *77*, 2647–2660. [CrossRef]
20. Mir, B.; Goettsch, C. Extracellular Vesicles as Delivery Vehicles of Specific Cellular Cargo. *Cells* **2020**, *9*, 1601. [CrossRef]

21. Wei, H.; Chen, Q.; Lin, L.; Sha, C.; Li, T.; Liu, Y.; Yin, X.; Xu, Y.; Chen, L.; Gao, W.; et al. Regulation of Exosome Production and Cargo Sorting. *Int. J. Biol. Sci.* **2021**, *17*, 163–177. [CrossRef] [PubMed]
22. Tan, S.S.; Yin, Y.; Lee, T.; Lai, R.C.; Yeo, R.W.Y.; Zhang, B.; Choo, A.; Lim, S.K. Therapeutic MSC Exosomes Are Derived from Lipid Raft Microdomains in the Plasma Membrane. *J. Extracell. Vesicles* **2013**, *2*, 22614. [CrossRef]
23. Tellier, E.; Canault, M.; Rebsomen, L.; Bonardo, B.; Juhan-Vague, I.; Nalbone, G.; Peiretti, F. The Shedding Activity of ADAM17 Is Sequestered in Lipid Rafts. *Exp. Cell Res.* **2006**, *312*, 3969–3980. [CrossRef]
24. Lee, J.-H.; Wittki, S.; Bräu, T.; Dreyer, F.S.; Krätzel, K.; Dindorf, J.; Johnston, I.C.D.; Gross, S.; Kremmer, E.; Zeidler, R.; et al. HIV Nef, Paxillin, and Pak1/2 Regulate Activation and Secretion of TACE/ADAM10 Proteases. *Mol. Cell* **2013**, *49*, 668–679. [CrossRef] [PubMed]
25. Ma, G.-F.; Miettinen, S.; Porola, P.; Hedman, K.; Salo, J.; Konttinen, Y.T. Human Parainfluenza Virus Type 2 (HPIV2) Induced Host ADAM8 Expression in Human Salivary Adenocarcinoma Cell Line (HSY) during Cell Fusion. *BMC Microbiol.* **2009**, *9*, 55. [CrossRef]
26. Smith, M.P.; Young, H.; Hurlstone, A.; Wellbrock, C. Differentiation of THP1 Cells into Macrophages for Transwell Co-Culture Assay with Melanoma Cells. *Bio-Protoc.* **2015**, *5*, e1638. [CrossRef] [PubMed]
27. Zhang, X.; Zhu, M.; Hong, Z.; Chen, C. Co-Culturing Polarized M2 Thp-1-Derived Macrophages Enhance Stemness of Lung Adenocarcinoma A549 Cells. *Ann. Transl. Med.* **2021**, *9*, 709. [CrossRef] [PubMed]
28. Schlomann, U.; Dorzweiler, K.; Nuti, E.; Tuccinardi, T.; Rossello, A.; Bartsch, J.W. Metalloprotease Inhibitor Profiles of Human ADAM8 in Vitro and in Cell-Based Assays. *Biol. Chem.* **2019**, *400*, 801–810. [CrossRef] [PubMed]
29. Suarez-Arnedo, A.; Torres Figueroa, F.; Clavijo, C.; Arbeláez, P.; Cruz, J.C.; Muñoz-Camargo, C. An Image J Plugin for the High Throughput Image Analysis of in Vitro Scratch Wound Healing Assays. *PLoS ONE* **2020**, *15*, e0232565. [CrossRef]

8 Appendix

8.1 Curriculum Vitae

8.2 Verzeichnis akademischer Lehrer

Meine akademischen Lehrer waren die Damen und Herren in Marburg und Regensburg Barbey, Bartsch, Deutzmann, Díaz Díaz, Dick, Dörsam, Dresselhaus, Durchschlag, Flor, Grasser, Griesenbeck, Gschwind, Hammes, Heinze, Kalbitzer, König, Kurtz, Lang, Längst, Mages, Matysik, Meister, Merkl, Milkereit, Müller, Neumann, Nimsky, Pfitzner, Pogge von Strandmann, Poschlod, Reiser, Roth, Schlomann, Seufert, Slater, Slenczka, Spörner, Sprunck, Sterner, Thomm, Tschochner, Walter, Wagner, Wenzl, Wegener, Wirth, Wolf.

8.3 Danksagung

Ich möchte mich hiermit bei allen Menschen bedanken, ohne die diese Arbeit nicht möglich gewesen wäre. An erster Stelle möchte ich mich bei meinem Doktorvater, Prof. Dr. Jörg-Walter Bartsch bedanken. Ich bin dir zutiefst dankbar für all deine Unterstützung vor allem bei den unzähligen wissenschaftlichen Fragestellungen und für die vielen konstruktiven Diskussionen. Du hast mich während meiner Zeit als Doktorandin immer motiviert und mir gezeigt, was es bedeutet als Wissenschaftler/in erfolgreich zu sein.

Liebe Suse, ich danke dir von Herzen, dass du mich in den letzten vier Jahren immer, egal womit, unterstützt hast. Ich konnte so viele Sachen von dir lernen. Du hast mich immer aufgebaut und motiviert, vor allem wenn der Laboralltag mir über den Kopf gewachsen ist. Ich bin dir so dankbar für all die gute Laune und Ratschläge, die du jeden Tag mitgebracht hast. Liebe Agnes, auch dir möchte ich für die unglaublich tolle Zeit bedanken. Vielen, vielen Dank für jeden lustigen Moment, für jedes aufbauende Wort und die vielen intensiven Diskussionen und Gespräche. Ich freue mich darüber, dass wir während dieser Zeit wirklich Freunde geworden sind.

Ich möchte mich auch bei Marie Sengelmann bedanken, die mich bei meinen Laborarbeiten während ihrer Masterarbeit tatkräftig unterstützt hat und dass aus dieser Zeit eine Freundschaft entstanden ist. Vielen herzlichen Dank auch an Uwe Schlomann, Emily P. Slater und Ricarda Hannen für die uneingeschränkte Hilfe und den wissenschaftlichen Austausch. Ich bedanke mich bei Kai Zhao, Constanze Nagl, Birte Winkler, Johanna Graß, Sina Wagner, Bastian Dörsam, Christian Preußer, Frederik Helmprobst, Katrin Roth und Vivian Ponath für die Hilfe im Labor und die unkomplizierte Zusammenarbeit.

Als nächstes möchte ich meinen Freunden danken, die mich während meiner Doktorarbeit immer unterstützt, aufgebaut, abgelenkt und motiviert haben. Ich freue mich darüber, so viele tolle Menschen um mich herum zu wissen. Danke an Lena und Anja, ihr habt mich während des düsteren Corona-Alltags immer unterstützt und immer Verständnis gehabt, wenn der Laboralltag den Großteil meiner Zeit beansprucht hat. Vielen Dank auch an Laura und Annika, die mich sowohl wissenschaftlich als auch sonst immer unterstützt haben. Unbedingt möchte ich auch Jenny danken. Ich freue mich, dass du zu unserer Familie gehörst und wir mittlerweile richtige Freunde geworden sind. Danke, dass du mich bei meinen Englischen Hürden unterstützt hast. Ich danke dir für deine Hilfe.

Lieber Patrick, ich kann dir garnicht genug danken. Ich bin so unglaublich froh, dass wir uns kennengelernt haben. Du hast immer an mich geglaubt und immer Verständnis

gehabt, wenn ich nicht die beste Laune an den Tag gelegt habe. Du bringst das Beste in mir zum Vorschein. Ich danke dir für alles.

Meinen Großeltern danke ich für Ihre bedingungslose Liebe, Hilfe und Unterstützung. Ohne euch wäre ich nicht da, wo ich heute bin. Ihr habt mir immer den Rücken gestärkt und mich immer wieder motiviert, durchzuhalten. Ich bin froh, dass ich euch habe.

Mein allergrößter Dank gilt meiner Schwester, welche mich bis heute durch jede Lebenslage begleitet hat. Du hast immer an mich geglaubt, egal wie groß die Hürde war. Ich danke dir für all die Kraft, die du mir während meiner Doktorarbeit gegeben hast. Durch dich bin ich die Person geworden, die ich heute bin. Ich danke dir für alles. Wir beide.

8.4 Ehrenwörtliche Erklärung